



FINAL REPORT 2012/054

Determine the optimum tube dimensions for Robert evaporators through experimental investigations and CFD modelling

Date of public access: 1/11/2017

Final report prepared by:	Dr Ross Broadfoot
Chief Investigator(s):	Dr Ross Broadfoot
Research organisation(s):	Queensland University of Technology
Co-funder(s):	Sugar Research Limited; QUT
Date:	1 October 2017
Key Focus Area (KFA):	KFA5



© Sugar Research Australia Limited 2017

Copyright in this document is owned by Sugar Research Australia Limited (SRA) or by one or more other parties which have provided it to SRA, as indicated in the document. With the exception of any material protected by a trade mark, this document is licensed under a [Creative Commons Attribution-NonCommercial 4.0 International](#) licence (as described through this link). Any use of this publication, other than as authorised under this licence or copyright law, is prohibited.



<http://creativecommons.org/licenses/by-nc/4.0/legalcode> - This link takes you to the relevant licence conditions, including the full legal code.

In referencing this document, please use the citation identified in the document.

Disclaimer:

In this disclaimer a reference to "SRA" means Sugar Research Australia Ltd and its directors, officers, employees, contractors and agents.

This document has been prepared in good faith by the organisation or individual named in the document on the basis of information available to them at the date of publication without any independent verification. Although SRA does its best to present information that is correct and accurate, to the full extent permitted by law SRA makes no warranties, guarantees or representations about the suitability, reliability, currency or accuracy of the information in this document, for any purposes.

The information contained in this document (including tests, inspections and recommendations) is produced for general information only. It is not intended as professional advice on any particular matter. No person should act or fail to act on the basis of any information contained in this document without first conducting independent inquiries and obtaining specific and independent professional advice as appropriate.

To the full extent permitted by law, SRA expressly disclaims all and any liability to any persons in respect of anything done by any such person in reliance (whether in whole or in part) on any information contained in this document, including any loss, damage, cost or expense incurred by any such persons as a result of the use of, or reliance on, any information in this document.

The views expressed in this publication are not necessarily those of SRA.

Any copies made of this document or any part of it must incorporate this disclaimer.

Please cite as: Thaval, OP, Broadfoot, R & Kent, GA 2017. Determine the optimum tube dimensions for Robert evaporators through experimental investigations and CFD modelling. Final Report 2012/054. Sugar Research Australia Limited, Brisbane.

ABSTRACT

Experimental investigations were undertaken in a single tube pilot evaporator for nine tubes of three different lengths and three different diameters to determine the optimum tube dimensions for Robert evaporators. Heat transfer performance was determined at operating conditions typically encountered in sugar factory evaporators. Juice of three brix levels were selected to mimic conditions for the 1st, 3rd and 5th effects in a quintuple evaporator set. For each brix, the heat transfer coefficient (HTC) was calculated at four juice levels, two headspace pressures and two pressure differences between the steam chest and the headspace. Of the four juice levels, one juice level was identified as the optimum juice level corresponding to the maximum HTC. In total, 432 tests were undertaken with nine tubes and a further 128 tests were replicated with four tubes. The maximum HTC and optimum juice level results, linked together with a capital cost analysis and sucrose loss considerations, determined the preferred tube dimensions for Robert evaporators in a quintuple evaporator set.

Tubes of 3 m length and either 44.45 mm or 38.1 mm outside diameter are preferred for the 1st, 2nd and 3rd effects instead of the traditionally used tube of 2 m length and 44.45 mm outside diameter. The tube of 2 m length and 44.45 mm outside diameter is recommended for the 4th and 5th effects.

The investigations in this project were undertaken by Omkar Thaval for his PhD thesis at QUT “Investigating the effect of tube dimensions and operating conditions on heat transfer performance in a rising film vertical tube evaporator”.

EXECUTIVE SUMMARY

The juice evaporation stations in Australian sugar factories mostly comprise Robert (rising film tube) evaporators. Many of the currently installed evaporators are nearing the ends of their service lives and replacement evaporators, together with additional evaporator area to suit more steam efficient operation, are required in the coming years. Replacement of evaporator vessels for a 500 t/h factory would cost in excess of \$20 m. The calandrias in the existing vessels mostly use tubes of 2 m length and 44.45 mm outside diameter.

The project investigated whether tubes of different dimensions are preferred by considering the capital cost, heat transfer performance and operating costs resulting from sucrose hydrolysis and entrainment.

A capital cost model for the Robert evaporator was developed for 2000, 3000, 4000 and 5000 m² vessels with 2, 3, and 4 m tube lengths and 38.10, 44.45, and 50.80 mm tube outside diameters.

The designation for the diameters of the tubes was S (Small), M (Medium) and L (Large) being for 38.1, 44.45 and 50.8 mm outside diameters (OD) respectively. The tube lengths were 2, 3 and 4 m. Thus code M2 was for the tube traditionally used in evaporators in Australian factories of 2 m length and 44.45 mm outside diameter.

The results showed that the conventional evaporator with M2 tubes is more expensive than using the other tubes except for evaporators with 2 m tubes of 50.8 mm outside diameter. Longer tubes and tubes of smaller diameter provide substantial cost savings.

Heat transfer measurements were undertaken in a single tube evaporator rig for nine stainless steel tubes of the same dimensions as considered in the cost analysis for operating conditions corresponding to the conditions at the 1st, 3rd and 5th effects. The measurements were undertaken at three brix values, two headspace pressures, two pressure differences and four juice levels within the heating tube. The selection of two headspace pressures and two pressure differences for each set of test conditions provided heat transfer data for four temperature differences between the vapour in the steam chest and the boiling juice. Replicate tests demonstrated a high level of consistency with the heat transfer results of the original test program.

Each of the heating tubes was fitted with four gutters spaced equidistantly along the outside of the tube to collect and drain condensate to an external container. This arrangement allowed the HTC for each of the four sections of tube to be calculated and so provide information on the boiling behaviour within the different sections of the tube.

For each tube at each set of processing conditions (juice brix, headspace pressure and pressure difference) HTC measurements were undertaken at four juice levels. In all cases a particular juice level provided a maximum HTC value (HTC_{max}) for those conditions. An analysis of variance determined that tube diameter is more important than tube length in affecting HTC_{max}.

The experimental program showed that the traditional M2 tube provides good heat transfer performance across the full set of processing conditions typically found in a quintuple evaporation station. Tubes of 38.1 mm OD and/or longer tubes (3 or 4 m length) provided comparable (or perhaps slightly inferior) heat transfer performance to the traditional tube at the 1st effect position, and superior heat transfer performance at the 3rd effect position.

The experimental program, cost analysis for fabricating Robert evaporators and consideration of operating costs concluded that tubes of 3 m length and either 44.45 mm or 38.1 mm outside diameter are preferred for the 1st, 2nd and 3rd effects instead of the traditional M2 tube. Cost savings of ~20% should be achievable. The M2 tube is recommended for the 4th and 5th effects.

An important benefit from using smaller diameter and longer tubes is that the juice volume is smaller than in an evaporator with traditional tube dimensions. For a 1st effect evaporator operating in a high steam efficiency configuration (typically at high boiling temperature and with large heating surface area at the 1st effect), the smaller juice volume and shorter residence time would result in reduced sucrose losses through hydrolysis and hence provide increased revenue for the factory.

The use of S3 or M3 tubes to replace a calandria of M2 tubes in an existing evaporator increases the heating surface area of the vessel by 75% and 50% respectively, and so provides a more economical way to refurbish an existing evaporator when additional heating area is required.

The investigations in this project were undertaken by Omkar Thaval for his PhD thesis "Investigating the effect of tube dimensions and operating conditions on heat transfer performance in a rising film vertical tube evaporator". This thesis was undertaken at the Queensland University of Technology, Brisbane. Omkar is thanked for his effort and commitment to undertaking this study and completing the onerous experimental program. The management and staff at Rocky Point Mill are thanked for hosting Omkar and the evaporator rig for the experimental trials.

Only limited CFD modelling was undertaken in the project.

TECHNICAL SUMMARY

Aim of the Research Program

The research project aimed to investigate the effect of tube dimensions and operating conditions on the heat transfer coefficient (HTC) of a rising film vertical tube evaporator (Robert evaporator) and, when combined with a cost analysis and assessment of operating costs, determine the optimum tube dimensions for Robert evaporators to provide a more economical design.

Computational fluid dynamics modelling was intended to be undertaken in the project but this had to be largely curtailed because of the time and cost required for fabrication and installation of the evaporator test rig and for the time required to conduct the experimental program and analyse the results. Despite this the objectives of the project in terms of defining the optimum tube dimensions for Robert evaporators has been achieved.

Comments on the Experimental Program

Heat transfer measurements were undertaken in a single tube evaporator rig for nine stainless steel tubes of three different diameters and three different lengths, for operating conditions corresponding to the conditions at the 1st, 3rd and 5th effects. The measurements were undertaken at three brix values, two headspace pressures, two pressure differences and four juice levels within the heating tube. In addition replicate tests were undertaken for four tubes (two different diameters and two different lengths) for the operating conditions corresponding to the 1st and 5th effects.

The designation for the diameters of the tubes was S (Small), M (Medium) and L (Large) being for 38.1 mm, 44.45 mm and 50.8 mm outside diameters (OD) respectively. The tube lengths were 2, 3 and 4 m. Thus a code M2 was for the tube of 2 m length and 44.45 mm outside diameter. This M2 tube is the tube traditionally used in evaporators in Australian factories.

Each of the heating tubes was fitted with four gutters on the outside of the tube to collect and drain condensate to an external container. Four gutters which were spaced equidistantly along the length of the tube were installed on each tube. Thus HTC values could be calculated from the condensate collected for the four individual sections on the tube and the overall HTC values calculated from the total condensate rates on the tube.

The test program was undertaken at typical industrial conditions but a few characteristics of the rig meant that the heat transfer performance was slightly different from that experienced in industrial evaporators. These factors included:-

- the drainage of condensate on the outside of the tube was from four positions whereas condensate in industrial evaporators drains to the bottom plate;
- the single tube was combined with an adjacent downtake for juice flow to the base of the evaporator. This configuration is expected to reduce the juice flow down the heating tube to a greater extent compared with the flow that may be occurring in an industrial evaporator with downtakes located more distantly on average from heating tubes; and
- the tubes were new and clean for the tests (i.e. without any scale deposits). Industrial evaporator tubes even after a clean would generally have a slight deposit of scale which would reduce the heat transfer.

The replicate tests with the four tubes demonstrated a high level of consistency with the heat transfer results of the original test program with the nine tubes. This consistency provided confidence in the determinations of the heat transfer performance for the nine tubes at the different operating conditions.

Summary of the Research Outputs

Capital cost model

A capital cost model for the Robert evaporator was developed for 2000, 3000, 4000 and 5000 m² vessels with 2 m, 3 m, and 4 m tube lengths and 38.10 mm, 44.45 mm, and 50.80 mm tube outside diameters.

The results showed that the conventional evaporator for which Australian factories almost universally use 2 m tubes of 44.45 mm outside diameter is more expensive than using the other tubes except for evaporators with 2 m tubes of 50.8 mm outside diameter.

Relative to the conventional evaporator, cost savings in the ex-works cost of ~12% are likely in using 3 m long tubes of 44.45 mm OD and ~15% if 3 m long tubes of 38.10 mm OD are used. Further savings are made by the use of 4 m long tubes but the incremental cost reduction is less than increasing the tube length from 2 to 3 m. Longer tube vessels have smaller diameter and considerably less mass on the structure and foundations than the conventional evaporator, and so additional savings through reduced installation costs would be achieved.

Heat transfer performance of tubes of different dimensions

The experimental investigations were undertaken to determine the HTC for the nine tubes at the operating conditions corresponding to the typical conditions in the 1st, 3rd and 5th effects (the *Original432* dataset). Replicate tests were undertaken for M2, S2, M3 and S3 tubes to understand the tube length and tube diameter interaction and to determine the consistency in the results (the *Replicate128* dataset).

The selection of two headspace pressures and two pressure differences for each set of test conditions provided heat transfer data (heat flux and HTC) for four temperature differences between the vapour in the steam chest and the boiling juice.

Analysis of the HTC results showed that tube length and tube diameter interaction is significant, meaning that the choice of tube length and diameter cannot be independent of each other in selecting a high level of heat transfer performance. The data showed that for tube lengths of 3 m and longer, small diameter tubes are preferred; as brix increases HTC decreases and at higher headspace pressure the HTC values are generally higher. The effect of headspace pressure was attributed to the lower viscosity of the juice at the higher boiling temperature when the headspace pressure is higher.

For each tube at each set of processing conditions (juice brix, headspace pressure and pressure difference) HTC measurements were undertaken at four juice levels. In all cases a particular juice level provided a maximum HTC value (HTC_{max}) for those conditions.

For many tests the variation of HTC with juice level was not a consistent gradually changing variation, but often quite discontinuous. This result is unexpected but interestingly replicated closely in the two datasets.

Two interesting observations were made for 2 m tubes of 44.45 and 38.1 diameter at Brix-20:-

- M2 tubes: The general pattern was a faster decline in HTC at juice levels below the optimum compared with juice levels above the optimum;
- S2 tubes: The general pattern was a faster decline in HTC at juice levels above the optimum compared with juice levels below the optimum i.e. opposite behaviour than for the M2 tubes at Brix-20.

HTC_{max} results were determined from the *Original432* dataset. An analysis of variance determined that tube diameter is more important than tube length in affecting HTC_{max} . As brix increases, HTC_{max} decreases. For Brix-20, higher HTC_{max} values were achieved at 38.1 and 44.45 mm tube diameter. For Brix-35 and Brix-70, higher HTC_{max} values were achieved at 44.45 mm tube diameter. For Brix-35 the tube of 38.1 mm diameter and 3 m length (S3) also provided good heat transfer performance.

Analysis of the optimum juice levels corresponding to HTC_{max} values showed that as brix increases, optimum juice level increases. The effects of tube length and headspace pressure on optimum juice level were not consistent across the dataset. It was found that for tubes of 38.1 and 50.8 mm diameters, the optimum juice level increased with increase in pressure difference while for 44.45 mm tube diameter the optimum juice level decreased with increase in pressure difference.

Empirical relationships were developed for HTC_{max} and optimum juice level (expressed as the actual level in the tube in mm). The empirical relationship for HTC_{max} was

$$HTC = B^{-0.4901} T_j^{1.3582} VCC^{0.8877} \quad 0.1$$

where B is the brix of the juice,

T_j is the temperature of the juice, °C

VCC is the vapour condensation coefficient, kg/h/m²

This relationship showed good agreement with the measured results ($R^2 = 0.94$) and with industry values although the experimental data were slightly higher than typical industry values at Brix-20.

The empirical relationship for optimum juice level (mm) was

$$JL_{opt} = T_L^{0.7253} B^{0.4544} \Delta T^{-0.1122} \quad 0.2$$

where T_L is the tube length, mm

ΔT is the temperature difference between the vapour and juice, °C

Understanding the boiling patterns in the single tube

The HTC values for the individual sections of the tube of the *Original432* dataset were analysed to determine variations relative to the overall HTC value. Six HTC patterns were identified of which four patterns accounted for more than 90% of the results. The test conditions for each of these four HTC patterns were qualitatively and quantitatively analysed to determine which tube dimensions and operating conditions were most common for each of these patterns. The relationship between these HTC patterns and the magnitudes of the overall HTC of the tube was also investigated. Those conditions which provided *Uniform* boiling (wherein the HTC of each of the four tube sections was within 15% of the overall HTC) provided the highest overall HTC for all effect positions. The boiling pattern that provided the second highest overall HTC was *Low HTC at bottom* for which the bottom section of the tube had a HTC value more than 15% below the overall HTC value.

The other two HTC patterns of the four patterns that collectively accounted for more than 90% of the results were *Low HTC at top* and *Low HTC at an intermediate* section of the tube. Both these patterns resulted in a lower overall HTC than the other two patterns.

In general terms, *Uniform* boiling conditions are more likely to be established for boiling at Brix-20 with high headspace pressure. *Uniform* boiling appears to form in the tubes of all three diameters. For tubes of 38.1 mm diameter, tubes of 4 m length produced *Uniform* boiling whereas for tubes of 44.45 mm and 50.8 mm diameter *Uniform* boiling was more likely to be achieved with the shorter tubes.

The second favoured boiling pattern with *Low HTC at bottom* was likely to be established for all three brix values, and particularly for Brix-20 and Brix-70. Tubes S3, M3 and M4 were shown to be more likely to produce this boiling pattern at Brix-20. For Brix-70, tubes with diameter 44.45 mm and 50.8 mm appeared more likely to produce this boiling pattern than the 38.1 mm tube. A higher pressure difference also enhanced the formation of this boiling pattern.

A boiling mechanism was proposed for each of the four dominant boiling patterns. It was concluded that annular flow did not exist in the single tube evaporator. The *Uniform* boiling pattern was determined to be bubbly/slug flow boiling for the whole tube length while the *Low HTC at bottom* pattern was of similar boiling behaviour but contained bubbly flow at the bottom section.

A new mechanism termed as “dry out” was identified to occur in the tube for the *Low HTC at top* pattern. This mechanism was observed to occur more frequently for long tubes and low operating juice levels where insufficient juice is able to rise to the top of the tube and boiling is restricted to the bottom section of the tube.

For the boiling pattern with *Low HTC at the intermediate* section no boiling pattern was identified. The literature suggests that a *Boiling Crisis* or *Critical Heat Flux* can exist whereby bubbles can adhere to the inner surface of the tube and act as an insulating blanket to heat transfer. However this behaviour is only expected where very large temperature differences between the vapour and liquid exist and would not be expected in a juice evaporator.

The formation of a specific boiling pattern cannot be independently set in practice. However, setting the operating conditions for the evaporator close to the optimum conditions will likely ensure that *Uniform* or *Low HTC at bottom* boiling patterns are formed and good heat transfer performance is achieved.

Selecting the optimum tube dimensions

The experimental program showed that the traditional 44.45 mm diameter, 2 m tube provides good heat transfer performance across the full set of processing conditions typically found in a quintuple evaporation station. Tubes of 38.1 mm OD and/or longer tubes (3 or 4 m length) provided comparable (or perhaps slightly inferior) heat transfer performance to the traditional tube at the 1st effect position, and superior heat transfer performance at the 3rd effect position.

Evaporator vessels with the traditional tube are more expensive than evaporator vessels comprising tubes of smaller diameter and/or greater length. Thus cost savings of ~20% should be possible by using tubes such as 38.1 mm outside diameter and 3 m length at the 3rd effect position. Even larger savings are achieved with 4 m long tubes. However Australian factories are unlikely to utilise 4 m long tubes in Robert evaporators and so the favoured tubes for the 1st to 3rd effects positions are S3 and M3. For the 4th and 5th effect positions the traditional tube (M2) is favoured.

An important benefit from using smaller diameter and longer tubes is that the juice volume is smaller than in an evaporator with traditional tube dimensions. For a 1st effect evaporator operating in a high steam efficiency configuration (typically at high boiling temperature and with large heating surface area at the 1st effect), the smaller juice volume and shorter residence time would result in reduced sucrose losses through hydrolysis and hence provide increased revenue for the factory. This aspect reinforces the benefit of using S3 or M3 tubes at the 1st effect position.

When an increase in heating surface area in the 1st to 3rd effects is required in order to increase the juice processing capacity of the set and/or to suit an upgrade for a more steam efficient configuration, a financially attractive option may be to replace the existing calandria of 44.45 mm and 2 m tubes with a calandria comprising smaller diameter and longer tubes. Tubes of 38.1 mm or 44.45 mm diameter and 3 m length (S3 or M3) are recommended for the replacement calandrias. Increases in heating surface area of 75% and 50% respectively into existing evaporator bodies are achievable. Replacing the calandria in an existing vessel should be much less expensive than installing a new evaporator. However this option is only feasible if the body of the evaporator is in good condition.

CFD modelling

Computational Fluid Dynamics (CFD) was undertaken to examine the capabilities of the software (ANSYS CFX software) for simulating the boiling behaviour at the specified experimental conditions. Development of a suitable model would lead to the use of CFD modelling in the optimisation of evaporator calandria design. The geometries of the tubes and storage tank in the experimental rig were closely modelled and attempts were made to incorporate the physics of heat transfer and boiling, in order to reproduce the different boiling mechanisms and corresponding heat transfer rates.

Three sets of calandria tube geometries involving different initial flow and heat transfer conditions were modelled. These three conditions were identified from analysis of the experimental results as exhibiting consistent and substantially different flow and heat transfer behaviour.

The preliminary results are encouraging but show more extensive modelling is required to obtain confidence in the approach used for the CFD modelling. Further modelling is required to identify and validate the most appropriate techniques. Work from the nuclear industry which has just recently been published provides good information which can be utilised in future modelling of rising film tube evaporators (and calandria tubes in vacuum pans).

Conclusions

The investigations have determined that tubes S3 and M3 are preferable for use in Robert evaporators at the 1st to 3rd effects and would result in cost savings of ~20% for new installations. These tubes also provide the benefit at the 1st effect position (and also at the 2nd effect) in steam efficient configurations of having smaller juice volumes than the traditional M2 tube and so would result in reduced sucrose loss through hydrolysis. The replacement of a calandria in an existing evaporator comprising M2 tubes with S3 or M3 tubes may also be a very cost effective way to increase the heating surface area substantially (e.g., by up to 75% using S3 tubes). For the 4th and 5th effect positions the traditional tube (M2) is favoured.

Acknowledgements

The investigations in this project were undertaken by Omkar Thaval for his PhD thesis "Investigating the effect of tube dimensions and operating conditions on heat transfer performance in a rising film

vertical tube evaporator". This thesis was undertaken at the Queensland University of Technology, Brisbane. Omkar is thanked for his effort and commitment to undertaking this study and completing the onerous experimental program. The management and staff at Rocky Point Mill are thanked for hosting Omkar and the evaporator rig for the experimental trials.

The funding for the project which was provided by Sugar Research Australia and Sugar Research Limited is gratefully acknowledged.

TABLE OF CONTENTS

ABSTRACT.....	1
EXECUTIVE SUMMARY	3
TECHNICAL SUMMARY.....	5
Aim of the Research Program	5
Comments on the Experimental Program	5
Summary of the Research Outputs.....	6
Capital cost model.....	6
Heat transfer performance of tubes of different dimensions	6
Understanding the boiling patterns in the single tube.....	7
Selecting the optimum tube dimensions.....	8
CFD modelling	9
Conclusions	9
Acknowledgements.....	9
TABLE OF TABLES	15
TABLE OF FIGURES	17
1. BACKGROUND.....	19
1.1. Issues addressed in this study.....	19
1.2. Design and operation of Robert evaporators	19
1.3. Outline of the investigations.....	20
1.4. Evaporator tubes evaluated in the study.....	20
2. PROJECT OBJECTIVES	21
3. OUTPUTS, OUTCOMES AND IMPLICATIONS	21
3.1. Outputs	21
3.2. Outcomes and Implications	22
4. INDUSTRY COMMUNICATION AND ENGAGEMENT	22
4.1. Outputs for adoption by sugar factories.....	22
4.2. Industry engagement during course of project	23
4.3. Industry communication messages	24
4.4. Example of adoption by industry	24
5. METHODOLOGY.....	24
5.1. Overview of methodology	24
5.2. Capital cost of evaporators	24
5.3. Experimental determinations of heat transfer performance of tubes of different dimensions at different operating conditions	25

5.4.	Examination of HTC patterns along the tube length and postulation of boiling behaviour in the tube.....	26
5.5.	Selection of the optimum tube dimensions for the different effect positions.....	26
5.6.	Computational Fluid Dynamics modelling	26
6.	RESULTS AND DISCUSSION.....	27
6.1.	Capital cost of evaporators.....	27
6.1.1	Number of tubes	27
6.1.2	Vessel internal diameter	27
6.1.3	Material costs.....	28
6.1.4	Capital costs (ex works).....	28
6.1.5	Installation costs	29
6.1.6	Overall comments on cost analysis.....	30
6.1.7	Other considerations in designing Robert evaporators with different tube dimensions.	30
6.1.8	Summary of results from the capital cost analysis	33
6.2.	Experimental determinations of heat transfer performance of tubes of different dimensions at different operating conditions	33
6.2.1.	General comments on heat transfer performance.....	33
6.2.2.	Experimental procedure	34
6.2.3.	Experimental rig	34
6.2.4.	Experimental design.....	35
6.2.5.	Experimental program	37
6.2.6.	Experimental procedure	38
6.2.7.	Analysis of potential errors in the operating conditions	38
6.2.8.	Analysis of potential errors in the measurement of condensate flows.....	41
6.2.9.	Effect of tube dimensions and operating conditions on heat flux and HTC	41
6.2.10.	Comparison of the pilot evaporator HTC values with industrial HTC values	44
6.2.11.	Visual observations of the boiling behaviour.....	45
6.2.12.	Comparison of the overall HTC results for the <i>Original432</i> and <i>Replicate128</i> datasets	46
6.2.13.	Interaction of tube diameter and length on HTC values	47
6.2.14.	Analysis of the results of the <i>Original432</i> tests	47
6.2.15.	Analysis of HTC_{max} results	49
6.2.16.	Analysis of optimum juice level	51
6.2.17.	Empirical relationships for HTC_{max} and optimum juice level (in mm)	53
6.3.	Examination of HTC patterns along the tube length and postulation of boiling behaviour in the tube.....	57

6.3.1.	Overview	57
6.3.2.	Comparison of the HTC values for the individual tube sections for the <i>Original432</i> and <i>Replicate128</i> datasets	57
6.3.3.	Identification of HTC patterns.....	58
6.3.4.	Determination of factors influencing the boiling patterns	58
6.3.5.	Analysis of variance of HTC values for the four sections of the heating tubes	59
6.3.6.	Analysis of variance of the HTC values for individual sections corresponding to overall HTC_{max}	60
6.3.7.	Boiling mechanism	61
6.3.8.	Boiling patterns that provide superior heat transfer performance.....	62
6.4.	Selection of the optimum tube dimensions for the different effect positions.....	63
6.4.1.	General comments.....	63
6.4.2.	Favoured tubes based on HTC_{max}	63
6.4.3.	Capital costs for constructing and installing Robert evaporators using tubes of favoured heat transfer performance	66
6.4.4.	Selection of optimum tube dimensions.....	70
	Basis of selection.....	70
	Estimates of capital cost savings.....	71
	Estimates of operating cost savings.....	71
	Selection of the optimum tube dimension	72
6.4.5.	Retrofitting a calandria into an existing evaporator	73
	Introductory remarks.....	73
	Practical considerations of retrofitting a calandria	73
	Retrofit options	74
	Further design considerations	74
6.5.	CFD modelling results	74
6.5.1.	Description of the CFD model and assumptions.....	74
6.5.2.	Results of the CFD modelling	75
6.5.3.	Discussion on results of CFD modelling	80
7.	CONCLUSIONS.....	81
8.	PUBLICATIONS.....	81
9.	ACKNOWLEDGEMENTS	82
10.	REFERENCES	82
11.	APPENDIX	84
11.1.	Appendix 1 METADATA DISCLOSURE.....	84
11.2.	Appendix 2 Installation costs for Robert evaporators with the favoured tube dimensions	85

Design weight and design costs	85
Foundation and structural costs	87
Insulation and cladding costs	88
11.3. Appendix 3 Details of the CFD modelling.....	91
11.4. Appendix 4 Summary of experimental results for three boiling cases used in CFD modelling	95
(To be completed by the SRA-RFU Program Manager)	Error! Bookmark not defined.

TABLE OF TABLES

Table 1	Code for different tube dimensions.....	20
Table 2	Maximum specific vapour rates for acceptable up flow vapour velocities in the headspace of vessels comprising tubes of 38.1 mm OD and 4 m length.....	32
Table 3	Maximum specific vapour rates for LSEA II louvres in vessels comprising tubes of 38.1 mm OD and 4 m length	33
Table 4	Factors and number of values explored in the experiment.....	36
Table 5	Experimental factors investigated for juice at Brix-20.....	37
Table 6	Experimental factors investigated for juice at Brix-35.....	37
Table 7	Experimental factors investigated for juice at Brix-70.....	37
Table 8	Maximum values, minimum values, mean values and standard deviation of the experimental factors.....	39
Table 9	List of tubes showing high and low HTC for the different processing conditions	43
Table 10	Observations of juice above the top tube plate in the heat transfer experiments	46
Table 11	Analysis of variance of HTC from <i>Original432</i> tests with 4 th order interactions.....	48
Table 12	Analysis of variance of HTC _{max} from <i>Original432</i> tests	51
Table 13	Analysis of variance of the optimum juice level (JL _{opt} -% tube height) corresponding to HTC _{max} from <i>Original432</i> tests	53
Table 14	Typical operating conditions in factory vessels and the predicted HTC from two models ..	55
Table 15	Typical operating conditions in factory vessels and the predicted optimum juice levels (absolute and % tube height).....	57
Table 16	Categorisation and description of the boiling patterns	58
Table 17	Results of observations of the influence of experimental factors on the boiling patterns..	59
Table 18	Summary of significant factors and interactions for the individual section HTC values (<i>Original432</i>)	60
Table 19	Boiling pattern allocation for HTC _{max} results from <i>Original432</i> dataset.....	60
Table 20	Summary of significant factors and interactions for the individual section HTC _{max} (<i>Original432</i>)	61
Table 21	Proposed boiling regimes for boiling patterns.....	62
Table 22	Average HTC _{max} for different boiling patterns at three brix	62
Table 23	Favoured tubes based on HTC _{max} for 1 st , 3 rd and 5 th effect positions	66
Table 24	Heating surface areas of the respective vessels for the favoured tubes for 1 st , 3 rd and 5 th effect positions	67
Table 25	Details of the evaporator vessels with the favoured tube dimensions to equate to the heat transfer performance of a 2000 m ² HSA M2 evaporator	69
Table 26	Details of the evaporator vessels with the favoured tube dimensions to equate to the heat transfer performance of a 5000 m ² HSA M2 evaporator	70
Table 27	Estimate of cost savings from using S3 and M3 tubes in Robert evaporators at the 1 st effect and 3 rd effect instead of using a Robert evaporator with M2 tubes	71
Table 28	Sucrose degradation and operating cost savings for a 5000 m ² evaporator.....	72
Table 29	Evaporator heating surface details for retrofit options.....	74
Table 30	Comparison of the measured condensation rate to the predicted vapour flow rate out of the tube outlet	80

Table 31	Metadata disclosure 1.....	84
Table 32	Cost data for foundations and structure to support the evaporator	87
Table 33	Foundations and structural costs for evaporators comprising the favoured tubes for 1 st , 3 rd and 5 th effect positions (HSA of M2 evaporator of 2000 m ²)	88
Table 34	Foundations and structural costs for evaporators comprising the favoured tubes for 1 st , 3 rd and 5 th effect positions (HSA of M2 evaporator of 5000 m ²)	88
Table 35	Cost data for insulation and cladding of the evaporator.....	89
Table 36	Insulation area and costs for the favoured tubes for 1 st , 3 rd and 5 th effect positions (HSA of M2 evaporator of 2000 m ²)	89
Table 37	Insulation area and costs for the favoured tubes for 1 st , 3 rd and 5 th effect positions (HSA of M2 evaporators of 5000 m ²).....	90
Table 38	Juice properties.....	91
Table 39	Juice vapour properties.....	91
Table 40	Low pressure steam properties	91
Table 41	Summary of experimental results for uniform boiling pattern adopted for CFD modelling (from Appendix L, Table L.1, Thaval (2017))	95
Table 42	Summary of experimental results for boiling pattern with low HTC at top of tube adopted for CFD modelling (from (Appendix M, Table M.1), Thaval (2017)).....	95
Table 43	Summary of experimental results for boiling pattern with low HTC at bottom of tube adopted for CFD modelling (from Appendix N, Table N.1), Thaval (2017)).....	95

TABLE OF FIGURES

Figure 1	Number of tubes for 2000, 3000, 4000 and 5000 m ² vessels with different tube dimensions	27
Figure 2	Vessel ID for 2000, 3000, 4000 and 5000 m ² vessels with different tube dimensions.....	28
Figure 3	Costs of materials for 2000, 3000, 4000 and 5000 m ² vessels with different tube dimensions as fraction of cost of materials for vessels with M2 calandrias	28
Figure 4	Total costs (ex-works) for 2000, 3000, 4000 and 5000 m ² vessels with different tube dimensions as fraction of cost (ex-works) for vessels with M2 calandrias.....	29
Figure 5	Total mass on foundations for 2000, 3000, 4000, and 5000 m ² vessels with different tube dimensions as fraction of the total mass for vessels with M2 calandrias.....	30
Figure 6	Juice volume intensity for 2000, 3000, 4000 and 5000 m ² vessels with different tube dimensions	31
Figure 7	Schematic representation of the single tube evaporator rig.....	34
Figure 8	Pilot evaporator rig	36
Figure 9	Actual average temperature differences for the three brix	40
Figure 10	Target temperature differences for the three brix.....	40
Figure 11	Effect of tube dimensions and operating conditions on heat flux and heat transfer coefficient for test at Brix-20 and ΔT of 6.5 °C	42
Figure 12	Relationship between heat transfer coefficient and heat flux at the optimum juice level at Brix-20 and ΔT of 6.5 °C	43
Figure 13	Comparison of industrial and pilot evaporator HTC values for M2 tube dimension.....	45
Figure 14	Mean values of HTC for each level of each factor for the <i>Original432</i> tests with all results included	47
Figure 15	Mean values of HTC_{max} for each level of each factor from the <i>Original432</i> tests (108 data points)	50
Figure 16	Mean values of $JL_{opt(\%)}$ for each level of each factor from the <i>Original432</i> tests (108 data points)	52
Figure 17	Measured and predicted HTC_{max}	54
Figure 18	Measured and predicted optimum juice level.....	56
Figure 19	Influence of tube length and tube diameter on HTC_{max} for Brix-20.....	64
Figure 20	Influence of tube length and tube diameter on HTC_{max} for Brix-35.....	64
Figure 21	Influence of tube length and tube diameter on HTC_{max} for Brix-70.....	65
Figure 22	Materials and labour costs for evaporators with favoured tubes dimensions for 1 st , 3 rd and 5 th effect positions	68
Figure 23	Predicted vapour volume fraction for uniform boiling case	76
Figure 24	Predicted vapour volume fraction for uniform boiling case (detail for upper half of tube).	76
Figure 25	Predicted vapour volume fraction for uniform boiling case (detail for lower half of tube)	77
Figure 26	Predicted vapour volume fraction for low HTC at top case.....	77
Figure 27	Predicted vapour volume fraction for low HTC at top case (detail for upper half of tube)	78
Figure 28	Predicted vapour volume fraction for low HTC at top case (detail for lower half of tube) ..	78
Figure 29	Predicted vapour volume fraction for low HTC at bottom case	79

Figure 30	Predicted vapour volume fraction for low HTC at bottom case (detail for upper half of tube)	79
Figure 31	Predicted vapour volume fraction for low HTC at bottom case (detail for lower half of tube)	80
Figure 32	Design vessel weight and design costs for evaporators with the favoured tubes for 1 st , 3 rd and 5 th effect positions	86
Figure 33	Mesh achieved for tube volume	92
Figure 34	Mesh achieved for tank volume	92
Figure 35	Momentum convergence.....	93
Figure 36	Energy convergence	93
Figure 37	Turbulence convergence.....	94

1. BACKGROUND

1.1. Issues addressed in this study

The concentration of clarified sugar juice from 15 brix to 70 brix is undertaken in multiple effect evaporators having due regard for energy efficiency, sucrose losses due to hydrolysis, and the capital cost of the installed heat transfer area. The evaporator station is the single largest consumer of process steam (typically at 200-250 kPa abs) in the sugar factory.

Australian sugar factories almost universally use the Robert design throughout the evaporator set. The tubes in the Robert evaporators are typically 2 m long, 44.45 mm outside diameter and 304 stainless steel. The main advantages of the Robert design are acceptably high heat transfer efficiency, low maintenance costs, long service lives, ease of cleaning including chemical and mechanical/hydraulic cleaning, and the robust control of these units due to the buffer volume of juice held in the base of the vessel. However capital costs per unit heating surface area (HSA) are likely to be greater for Robert evaporators than for designs with longer tubes e.g. Kestner evaporators. As well the juice hold-up volume is likely to be greater in the Robert evaporator which increases the potential for sucrose losses, particularly in the early stages of evaporation where boiling temperatures are high. Another disadvantage of Robert evaporators is the large footprint compared with designs comprising the longer tubes.

This project investigates the suitability of tubes of different dimensions to determine those tubes which are preferable, reducing the impact of the negative aspects while maintaining the strong advantages of Robert evaporators. The preferred tubes may differ for the different stages of the evaporator set owing to variations in the operating conditions along the set.

The investigations described in this report are described in detail in the PhD thesis of Omkar Thaval titled “Investigating the effect of tube dimensions and operating conditions on heat transfer performance in a rising film vertical tube evaporator”. This thesis was undertaken at the Queensland University of Technology, Brisbane.

1.2. Design and operation of Robert evaporators

Robert evaporators operate in rising film mode, meaning that the boiling juice and vapour both rise up the tubes due to the formation of the vapour bubbles within the tube.

Processing conditions and/or evaporator designs that achieve a higher overall heat transfer coefficient (HTC) allow reductions in the HSA required to achieve the same rate of evaporation, or achieve higher juice processing rates for the installed areas, or extend the period of operation between cleans. An important benefit of increased HTCs is the ability to achieve the required rate of evaporation with a smaller temperature difference. This benefit is of particular interest to factories seeking to reduce their process steam consumption and fuel usage (Moller *et al.*, 2003; Rose *et al.*, 2009).

The HTC of Robert evaporators depends on factors related to liquid properties and processing conditions (Broadfoot and Dunn, 2007; Wright, 2008). According to literature and industry experience, juice concentration and liquid level (% tube height) have the largest impact on HTC. In rising film evaporators such as Robert evaporators, previous studies have confirmed that an optimum liquid level within the calandria tubes exists for given processing conditions which corresponds to the maximum HTC, (HTC_{max}) (Guo, *et al.*, 1983; Shah and Peacock, 2013; Watson, 1986). Operating the evaporator above or below the optimum level results in reduced heat transfer

performance. The position of the optimum level depends on processing conditions during evaporation.

The effect of tube dimensions on HTC has been investigated previously (Hugot and Jenkins, 1986; Peacock, 2001). However no definitive recommendations have been provided. Some researchers have postulated that tube dimensions should be selected based on the effect position in a multiple effect set.

The new Robert evaporators installed in the industry in the past decade have incorporated a central downtake which preferentially removes the juice from above the top tube plate and passes it to the outlet of the vessel for flow to the next effect. Tubes of 44.45 mm outside diameter, 2.0 m in length have traditionally been used in the Australian industry for all stages of evaporation. There are only a relatively few vessels with different tube lengths or diameters.

1.3. Outline of the investigations

This study presents the results from the experimental investigations using a pilot Robert evaporator to determine the tube dimensions that provide the higher values of HTC_{max} for 1st, 3rd and 5th effect positions in a quintuple set. The capital cost model presented by Thaval and Broadfoot (2014) has been further updated to provide estimates of the cost of installing of evaporator vessels containing tubes of different dimensions. The results of the study are presented to determine the optimum tube dimensions based on considerations of heat transfer performance, capital costs and operational costs such as associated with sucrose hydrolysis.

1.4. Evaporator tubes evaluated in the study

The code for the dimensions of the nine tubes which were evaluated in this project is shown in Table 1.

Table 1 Code for different tube dimensions

Tube length (m)	Tube (mm)	OD	Code
2	38.10	S2	
	44.45	M2	
	50.80	L2	
3	38.10	S3	
	44.45	M3	
	50.80	L3	
4	38.10	S4	
	44.45	M4	
	50.80	L4	

2. PROJECT OBJECTIVES

The aims of the project at the outset were to increase the heat transfer efficiency and reduce the installed investment cost of Robert evaporators by:

- undertaking experimental investigations of the heat transfer of a single rising film tube evaporator in which tubes of different dimensions (diameter and length) were assessed
- incorporating the experimental results into a computational fluid dynamics (CFD) model of a Robert evaporator, and
- applying the results of the CFD modelling to the engineering design of Robert evaporators to determine the optimum tube dimensions.

The study aimed to determine a more economical design for new Robert evaporator installations using tubes with optimum dimensions.

During the course of the project a variation was required to remove the work involving CFD modelling of the evaporator and base the determination on the experimental results, the capital cost analysis and the assessment of operating costs. This change was necessary because the task to design, construct, commission and undertake the comprehensive experimental program was much more time consuming and costly than envisaged at the outset.

Some CFD work was undertaken to check on the vapour flow pattern within the steam chest of the evaporator rig and to develop a model of two phase flow in a single tube. However the CFD modelling work did not investigate the flow patterns of juice in a segment of a Robert evaporator.

3. OUTPUTS, OUTCOMES AND IMPLICATIONS

3.1. Outputs

The main outputs from the project were stated at the outset to be:-

- increased knowledge of the mechanism of rising film evaporation
- knowledge of the effect of tube dimensions on the heat transfer performance for the full range of processing conditions
- expansion of computational fluid dynamic modelling skills within the SRI group at QUT
- knowledge of the optimum tube dimensions for each stage of evaporation
- Robert evaporator designs for the preferred tube dimensions for each stage of evaporation.

In addition the student would develop extensive experimental and computational modelling skills. It was also considered likely that an increased understanding of the mechanism of rising film evaporation would be obtained and this would benefit technologists in operating Robert evaporators.

The above list of project outputs has been satisfied although the expansion of the CFD modelling skills with the SRI Group at QUT has been limited to work on modelling the single tube.

None of the outputs requires further development prior to adoption by sugar factories. The adoption pathway is likely to follow one of two routes when either a new evaporator is to be installed or a replacement calandria fitted into an existing evaporator viz.,

- for sugar factories to approach evaporator equipment manufacturers and specify the required tube dimensions to be incorporated; or

- for sugar factories to request SRI to design the new evaporator or to design the retrofit calandria so the factory could supply that specification to evaporator equipment manufacturers.

The project has shown that evaporator vessels comprising the optimum tube dimensions have substantially reduced juice hold up volume which results in reduced residence time for the juice, and hence offers the prospect for reduced sucrose degradation. This benefit is important for evaporators located at the front of the evaporator set when boiling at high temperatures (such as in a cogeneration factory).

3.2. Outcomes and Implications

The main outcomes of the project will be sugar mills utilising the optimum tube dimensions when installing new Robert evaporators or installing replacement calandrias in existing evaporators.

The benefits to the Australian sugar industry resulting from the outcomes of this project are:

- Economic. Reduced capital costs of installing new juice evaporators. Savings between \$0.1 m and \$0.5 m per vessel are expected compared with using the traditional tubes. Where evaporator vessels are being replaced with a vessel comprising the optimum tube dimensions even greater savings are likely due to reduced craneage as the vessel with optimum tube dimensions is lighter and of smaller diameter. Other financial benefits are obtained through using the optimum tube dimensions through reduced sucrose degradation in the early vessels of a cogeneration factory.
- Environmental. Reduced capital costs for evaporators will make cogeneration and other 'green' projects which require increased energy efficiency in factories more financially viable.
- Social. Development of experimental and modelling skills in the graduate engineer by undertaking this thesis study. As well projects such as this that assist Australian sugar factories to reduce the cost of capital make the milling sector more financially viable.

4. INDUSTRY COMMUNICATION AND ENGAGEMENT

4.1. Outputs for adoption by sugar factories

The project has delivered the following key messages for industry:-

- For a given tube and boiling at certain operating conditions an optimum juice level in the tube exists which provides a maximum HTC (HTC_{max}).
- Favoured tube dimensions were selected based on the values of HTC_{max} at the different operating conditions experienced throughout the set. For the typical operating conditions at the 1st effect the traditional tube M2 and tubes S2, M3, S3 and S4 provided high values of HTC_{max} . At the typical 3rd effect boiling conditions the traditional tube M2 and tubes M3, S3 and M4 provided high values of HTC_{max} . For the typical 5th effect boiling conditions the traditional tube M2 and tube L2 provided high values of HTC_{max} .
- A cost analysis was undertaken which showed that the fabrication and installation costs for evaporators with smaller diameter and/or longer tubes were substantially lower than for evaporators with the traditional M2 tube.
- For evaporators at the 1st effect in a steam efficient configuration (typically high juice boiling temperature and large heating surface areas) tubes of smaller diameter and/or longer tubes than the traditional M2 tube have smaller juice hold up volumes. Consequently the extent

of sucrose hydrolysis would be less in these evaporators than for the M2 tube evaporator owing to the shorter juice residence time for the juice.

- Based on considerations of the HTC performance, capital costs for an installation, operating costs (particularly related to the potential sucrose degradation at the 1st effect) and also practical considerations, the favoured tubes in a quintuple evaporator set are:-
 - For the 1st to 3rd effects, tubes S3 and M3
 - For the 4th and 5th effects, the traditional M2 tube.
- Retrofitting of a calandria comprising S3 or M3 tubes into an existing evaporator with M2 tubes may be a financially attractive alternative to installing a new evaporator in circumstances where additional heating surface area is required. Increases in heating surface areas up to 75 and 50% for the S3 and M3 tubes respectively are possible. The retrofitting of the S3 or M3 tubes is only recommended for evaporators at the 1st to 3rd effect positions, owing to their good heat transfer performance at these positions.
- Boiling patterns with uniform HTC values along the tube length and with low HTC at the bottom of the tube (rather than low HTC in intermediate or the top section of the tubes) were identified when good heat transfer performance is achieved. It was postulated that bubbly and slug flow regimes are dominant under these favoured boiling patterns.

4.2. Industry engagement during course of project

The progress on the project has been communicated to the factory staff at the Regional Research Seminars that are conducted each year in March/April. The table below shows the year of the seminar and the main aspect of the work that was covered.

Year of seminar	Main topics
2014	Description of the experimental program; design of the experimental rig; results of the cost model analysis
2015	Details of the experimental program conducted in the 2014 season at Rocky Point Mill
2016	Selection of the tubes that provided the best heat transfer performance; analysis of HTC patterns along the length of the tube; selection of the recommended based on the HTC and cost considerations
2017	Summary of project outcomes; recommended tube dimensions for the different effects; postulation of the boiling mechanisms in the tubes for the different effect positions and tube dimensions; presentation of case studies for retrofitting a new calandria with tubes of smaller diameter and greater length into an existing evaporator.

Other than the presence of the SRA Communications staff at the Regional Research Seminars there has been no communication with the SRA Adoption staff regarding the project.

A SRA webinar was held on the 22nd April 2015. Representatives from eight milling companies attended the webinar and positive feedback was achieved.

The following conference papers have been presented:-

Thaval OP, Broadfoot, R (2014). Capital cost model for Robert evaporators. *Proceedings of the 36th Annual Conference of the Australian Society of Sugar Cane Technologists*, Gold Coast, Australia.

Thaval OP, Broadfoot, R, Kent GA & Rackemann, DW (2016). Determining optimum tube dimensions for Robert evaporators. *Proceedings of the XXIX International Society of Sugar Cane Technologists Congress, Chiang Mai, Thailand.*

Thaval OP, Broadfoot, R & Kent GA (2017). Boiling mechanism in rising film vertical tube evaporator. Proceedings of the Annual Convention of Sugar Technologists Association of India, Kochi, India.

Two papers for the International Journal of Heat and Mass Transfer are being prepared.

4.3. Industry communication messages

The main message from the project is that factories can make substantial cost savings by using S3 or M3 tubes at the 1st, 2nd and 3rd effects instead of using the conventional M2 tubes. This will apply for new installations and replacement calandrias. The heat transfer coefficients will be comparable to those achieved by the M2 tubes. The traditional M2 tube is favoured at the 4th and 5th effects.

An evaporator comprising a calandria with the S3 or M3 tube also has substantially smaller juice hold up volume than an evaporator of the same heating surface area with the traditional M2 tube. Hence, for situations where the exhaust steam supply to the first effect is at a high saturation temperature e.g. 125 °C, sucrose degradation will be less for the evaporator with the S3 or M3 tubed calandria.

4.4. Example of adoption by industry

SRI recently prepared a design specification for an Australian sugar factory to replace the worn calandria of an existing evaporator containing the traditional tubes of 44.45 mm outside diameter and 2.0 m length, with tubes of smaller diameter and greater length. The heating surface area of the refurbished evaporator increased by 72% and was calculated to provide a substantial increase in the juice processing capacity of the set.

5. METHODOLOGY

5.1. Overview of methodology

The methodology for undertaking the project was:-

- Develop a capital cost model to determine the costs of designing, fabricating and installing Robert vessels of the same heating surface area but with tubes of different dimensions.
- Determine the HTC of tubes with different lengths and diameters operating at different processing conditions.
- Determine the optimum tube dimensions and operating conditions favouring maximum heat transfer coefficient.
- Determine the HTC at different sections of the tube in order to understand the boiling patterns of juice within the tube.
- Postulate a theory on boiling mechanism based on the boiling patterns
- Select the optimum tube dimensions for a particular evaporation duty by considering collectively the heat transfer performance, the capital costs and the operating costs.

5.2. Capital cost of evaporators

The main design parameters for vessels of 2000, 3000, 4000, 5000 m² were calculated for calandrias comprising three tube lengths (2, 3 and 4 m) and three outside diameters (38.1, 44.45 and 50.8 mm).

All tubes were assumed to be stainless steel with a wall thickness of 1.2 mm. The procedure for calculating the capital cost of constructing and installing a particular evaporator was:-

- Given the nominated heating surface area (HSA), tube dimensions, pitch of tubes, number of mini-downtakes, incondensable gas removal arrangements and stay bar details use a tube layout program developed by the Sugar Research Institute (SRI) to calculate the vessel internal diameter (ID) and the number of tubes. The evaporator design was based on the SRI design of Robert evaporator which incorporates radial flow of steam from an external annulus to central offtakes for condensate and noxious gases, a central downtime of the semi-sealed design, inlet juice distributed under the calandria near the outer wall (Moller, et al., 2003; Wright, et al., 2003). For the analysis the specification of the HSA of the evaporator was based on the internal diameter of the tube and the length between the outer faces of the tube plates.
- Develop a database for the costs of tubes of the different dimensions, mild steel plate, time for undertaking fabrication tasks including time for cutting, rolling and welding mild steel plate and installing tubes by expansion, labour costs, project management costs, freight, insulation and cladding, foundation construction costs (materials and labour) (Thaval and Broadfoot, 2014; Thaval, 2017).
- Develop a spreadsheet to:-
 - Design the evaporator for the specified tube dimensions and HSA using the tube plate layout determined above.
 - Calculate the mass of materials needed
 - Calculate the costs of fabrication and installation
- Calculate the juice hold-up volume in the evaporator to allow calculation of the sucrose degradation through hydrolysis for specified juice processing conditions.
- Calculate the potential for juice entrainment for the specific evaporators. Smaller diameter and longer tubes allow higher HSA to be installed into a given diameter of evaporator. Limitations to the evaporation rate or requirements for longer strakes, additional de-entrainment equipment were determined and allowed for in the design.

5.3. Experimental determinations of heat transfer performance of tubes of different dimensions at different operating conditions

The procedure undertaken to determine the heat transfer coefficients of the tubes of different dimensions at different operating conditions was:-

- Design the experimental program based on heat transfer measurements on a single tube. In total nine tubes were tested, being the same nine tubes investigated in the capital cost analysis.
- Design, construct and install the test evaporator rig at a sugar factory.
- Undertake the extensive test program of measuring heat transfer performance for each of the nine tubes at the 48 different processing conditions determined for the test program (designated *Original432* test program). The experiments for four tubes were repeated for the different processing conditions for two of the three brix values (total of 32 tests for each tube) (designated *Replicate128* test program).
- Analyse the experimental data for potential errors and consistency of HTC values in repeat measurements.
- Analyse the heat transfer data using various techniques including:
 - Qualitative assessments using plots of data

- Magnitude of mean HTC values attributed to single operating parameters
- Analysis of variance for statistical significance. These assessments include determinations of interactions between the tube dimensions and process conditions
- Determination of the juice level in the tube that maximises the HTC value (HTC_{max}), for a given set of processing conditions.
- Conduct analysis of variance of the HTC_{max} values to determine the parameters that are of statistical significance.
- Determine correlations for HTC_{max} and optimum juice level in terms of tube dimensions and the processing conditions.

5.4. Examination of HTC patterns along the tube length and postulation of boiling behaviour in the tube

The procedure undertaken to define the likely boiling behaviour in the tubes at the different operating conditions was:-

- Examine the consistency of the HTC patterns along the length of the tube by analysing the results for the corresponding tests in the Original432 and Replicate128 datasets.
- Identify the various HTC patterns which existed among the full range of test conditions and determine which patterns were more common and under which test conditions.
- Undertake a qualitative investigation of the factors influencing the HTC patterns.
- Conduct an analysis of variance of the effects of the processing conditions on the HTC values for the individual tube sections for the test conditions that produced HTC_{max} values.
- Determine the predominant boiling patterns when HTC_{max} values were achieved and determine the influence that the various processing parameters have at those conditions.
- Postulate the boiling mechanism in the tube corresponding to the different HTC patterns.
- Determine the boiling patterns in the tube that provide superior heat transfer performance.

5.5. Selection of the optimum tube dimensions for the different effect positions

The procedure which was undertaken to determine the optimum tube dimensions for a rising film tube (Robert) evaporator at the different effect positions involved consideration of three aspects:-

- The heat transfer performance of the tubes and in particular the HTC_{max} data;
- The capital costs to construct and install an evaporator with the different tubes; and
- The operating costs of using an evaporator with a particular tube. Operating costs are associated with sucrose loss through hydrolysis and potential for juice entrainment into the discharged vapour.

5.6. Computational Fluid Dynamics modelling

The overall aim of the Computational Fluid Dynamics (CFD) study was to examine the capabilities of the software for simulating the boiling behaviour at the specified experimental conditions. This would lead to the use of CFD modelling in the optimisation of evaporator calandria design. The geometries of the tubes and storage tank in the experimental rig were closely modelled and attempts were made to incorporate the physics of heat transfer and boiling, in order to reproduce the different boiling mechanisms and corresponding heat transfer rates.

Three sets of calandria tube geometries involving different initial flow and heat transfer conditions were modelled. These three conditions were identified from analysis of the experimental results as

exhibiting consistent and substantially different flow and heat transfer behaviour. The three conditions were:

- Uniform boiling at all four sections of the tube
- Low heat transfer coefficient at the top of the tube.
- Low heat transfer coefficient at the bottom of the tube.

6. RESULTS AND DISCUSSION

6.1. Capital cost of evaporators

6.1.1 Number of tubes

The number of tubes for each tube dimension is shown in Figure 1. The L4 tube dimension requires the fewest tubes. Calandrias with tube dimensions S4 require 42 % fewer tubes than the conventional M2 calandria for the same HSA. As a consequence a calandria with S4 tubes will provide cost savings in drilling and honing of the holes in the tube plates, inserting and expanding the tubes.

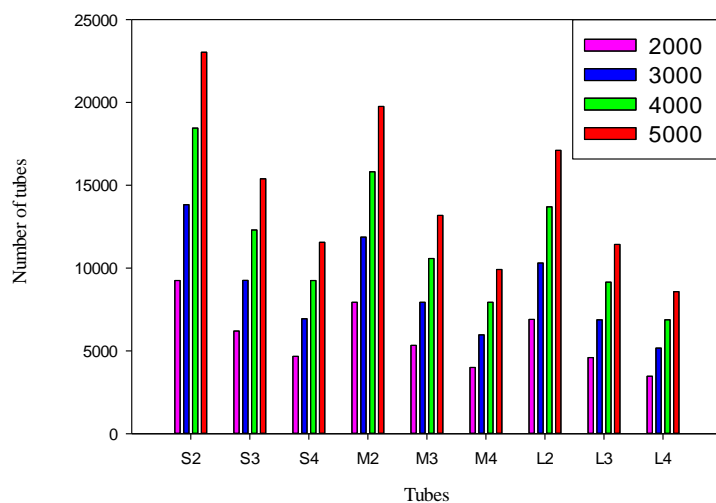


Figure 1 Number of tubes for 2000, 3000, 4000 and 5000 m² vessels with different tube dimensions

6.1.2 Vessel internal diameter

Figure 2 shows the vessel internal diameter (ID) for calandrias with the different tube dimensions. The vessel ID is the factor which determines the footprint for the vessel, the mass of steel in the vessel, the volume of juice held in the vessel at the normal operating level, the total mass of the vessel and contents for the design of the supporting structure and foundations, and the cross-sectional area in the vapour space for the up flow of vapour and housing for de-entrainment louvres. Smaller vessels are attractive on all counts apart from a potential impact on juice level control owing to a reduced buffer volume of juice and higher up flow vapour velocities. The diameter of the vessel is reduced by 33% when the S4 tube dimensions are used rather than the conventional tube dimensions, M2.

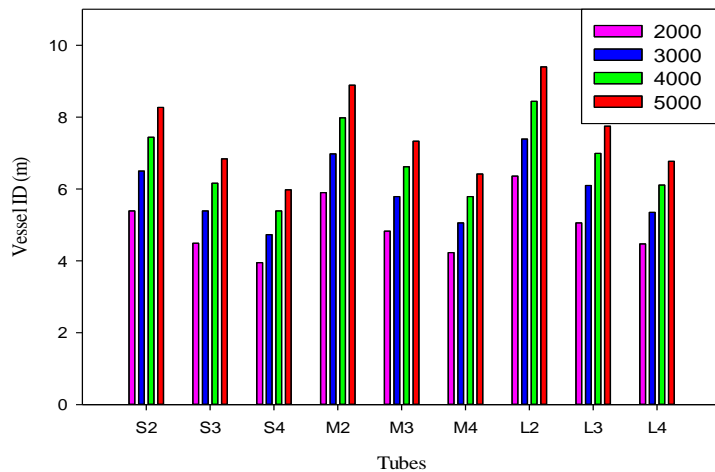


Figure 2 Vessel ID for 2000, 3000, 4000 and 5000 m² vessels with different tube dimensions

6.1.3 Material costs

Figure 3 shows the costs of materials (without fabrication costs) for vessels with calandrias of different tube dimensions. The data for each HSA are presented relative to the materials costs for a vessel of the same HSA comprising the conventional tube dimensions, M2.

As expected, for evaporators with the same tube diameter, the material costs are lower where calandrias of longer tubes are used as the vessel diameter is reduced. For a fixed tube length, the calandrias comprising 44.45 mm OD tubes have the lowest cost of materials for the vessel and heating tubes. This is partly because of the lower cost of the 44.45 mm OD tubes per m² of HSA than the 38.10 mm and 50.80 mm OD tubes.

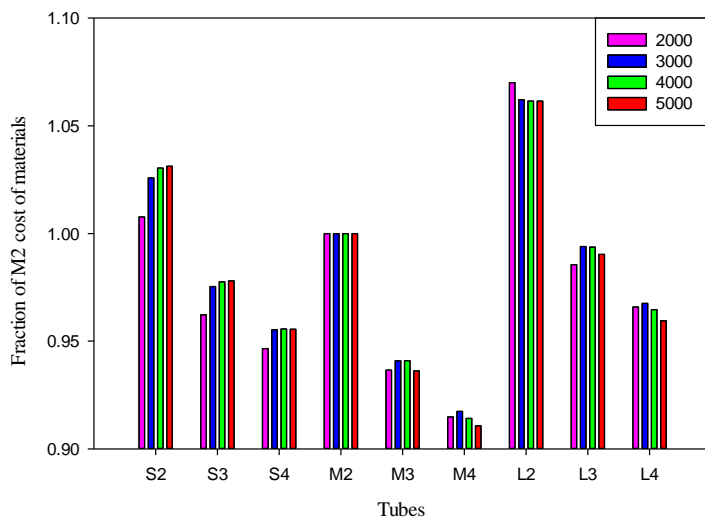


Figure 3 Costs of materials for 2000, 3000, 4000 and 5000 m² vessels with different tube dimensions as fraction of cost of materials for vessels with M2 calandrias

6.1.4 Capital costs (ex works)

Figure 4 shows the capital costs (ex-works) for the evaporator with calandrias of different dimensions. As for Figure 3 the data for each HSA are expressed relative to the costs of vessels of

the same HSA with calandrias of M2 tubes. As expected the material and labour costs are lower for vessels with long tubes and small diameter and greater for vessels with short tubes and large diameter. Comparison of the data in Figure 4 and Figure 3 shows the impact of labour costs in manufacturing the vessels and inserting and expanding the heating tubes into the calandrias.

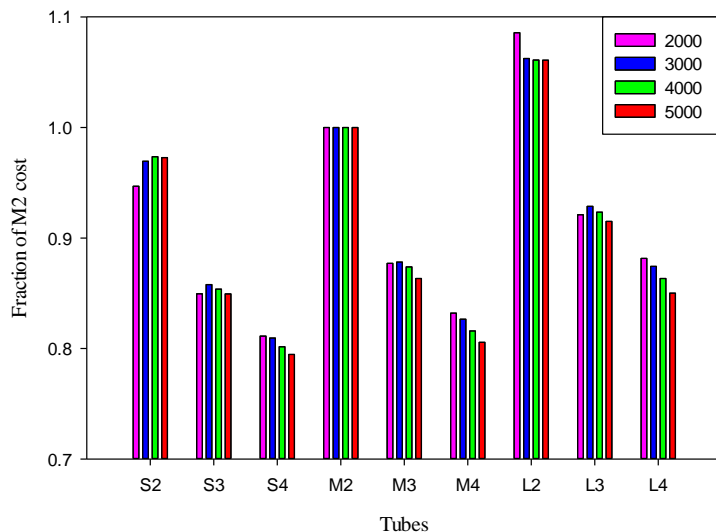


Figure 4 Total costs (ex-works) for 2000, 3000, 4000 and 5000 m² vessels with different tube dimensions as fraction of cost (ex-works) for vessels with M2 calandrias

The data in Figure 4 show the length of tube has a strong impact on capital costs. For example increasing the tube length from 2 m to 3 m provides a 13 to 15% cost saving. Incrementally there is a larger cost saving in increasing the tube length from 2 m to 3 m than from 3 m to 4 m. This finding is to be expected.

Smaller diameter tubes provide a capital cost saving but this is of lesser influence than the length of the tube. For the same length of tube the cost saving in using tubes of 38.10 mm OD is only 3 to 5% compared with tubes of 44.45 mm OD. This result is strongly dependent on the cost of tube per m² of HSA (Thaval and Broadfoot, 2014).

One clear observation from Figure 4 is that the evaporators with the conventionally used tube dimensions M2 are more expensive than all the other tube arrangements except for evaporators with L2 tubes.

6.1.5 Installation costs

The installation costs include the costs of the foundations and structure to support the evaporator, and insulation and cladding costs. The installation costs are likely to be proportional (probably not linearly) to the weight of the vessel used for the design of the foundations and structure design (i.e., the vessel weight and the weight of both the calandria and juice side full of condensate and juice respectively).

Figure 5 shows the total mass on the foundations for the vessels with different tube dimensions. The mass of juice is calculated for juice of 40 brix. The data for each HSA are presented relative to the values for M2. Comparing the S4 tube design with the conventional M2 tube design, a 40% reduction in the mass on the foundations and structure is calculated.

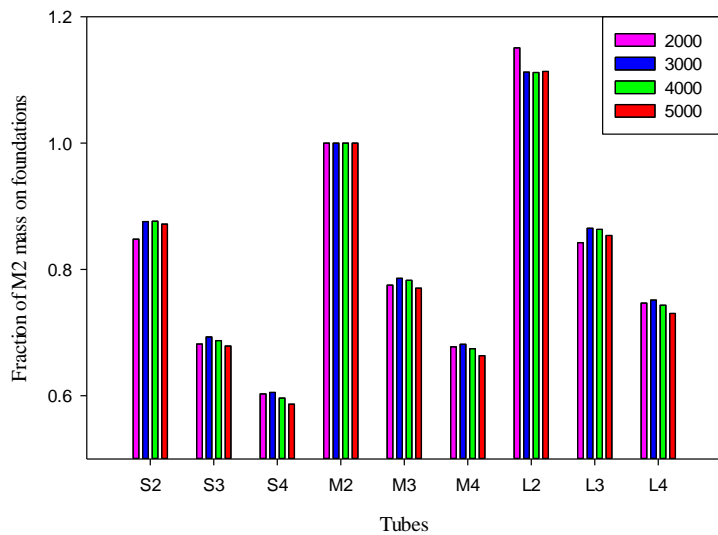


Figure 5 Total mass on foundations for 2000, 3000, 4000, and 5000 m² vessels with different tube dimensions as fraction of the total mass for vessels with M2 calandrias

Another benefit with the S4 tube design, and in general for small diameter vessels, is the smaller footprint which gives an additional saving on installation costs. The costs of locating a vessel within an existing factory are generally proportional to the footprint, although these costs are very site specific. Thus, in some situations, considerable savings may also be obtained for the smaller footprint of vessels with smaller body diameter.

Craneage costs for installing the vessel are affected by the mass of the vessel and also access to the location for the vessel, which depends on the site for the new evaporator. The data in Figure 3 provide a reasonable indication of the relative masses (empty vessels) to be lifted into position.

6.1.6 Overall comments on cost analysis

The cost analysis shows that the values for M2 calandria for the cost of materials, total costs (ex-works) and the mass on foundations are significantly higher than the values for calandrias with longer tubes and, to a lesser extent, with smaller diameter. Vessels comprising S4 tubes have the smallest vessel diameter, lowest cost ex works and smallest mass on the foundations.

6.1.7 Other considerations in designing Robert evaporators with different tube dimensions

The potential for sucrose degradation and entrainment of juice droplets in the up flow vapour have to be considered when designing an evaporator.

Juice hold up volume and potential sucrose degradation

The extent of sucrose degradation that occurs in the juice evaporation process is a function of the juice conditions (pH, temperature and brix) and the residence time. The evaporation conditions that are likely to experience high levels of sucrose degradation are where high levels of steam economy are sought e.g., where extensive vapour bleeding is undertaken and where the process steam supplied to the calandria of effect 1 is at higher pressure. For these stations large evaporation areas are provided in the front end of the set and the boiling temperatures are high (e.g., 118 °C). These arrangements provide longer residence times for the juice at high temperatures, thus providing conditions conducive to higher rates of sucrose degradation.

There is potential with the use of smaller diameter vessels associated with calandrias comprising smaller diameter, longer tubes that the juice volume per unit heating surface area can be reduced. Figure 6 shows the calculated juice volume intensity (litres of juice in the evaporator at normal operating levels per m^2 of HSA) for evaporators using tubes of different dimensions. These values are determined for the base of the evaporator having a fixed gap between the bottom tube plate and the base of the evaporator at the outer wall (300 mm) and angles in a W shaped bottom of 15 degrees (outer plate) and 30 degrees (inner plate). The juice operating level is set at 35% of the tube height. The data show that calandrias comprising longer tubes of smaller diameter should allow operation with a shorter residence time for the juice and hence provide reduced potential for sucrose degradation. In this regard the benefits of using longer tubes of smaller diameter would be greater at the front end of the set where the rates of sucrose degradation are faster and reductions in the residence time for juice would be very beneficial.

Of note in Figure 6 vessels with calandrias using the conventional tubes M2 provide the second largest juice volume intensity, second only to vessels with L2 tubes. Vessels with S4 tubes have juice volume intensities of $\sim 6 L/m^2$ compared with vessels with M2 tubes of $\sim 11 L/m^2$.

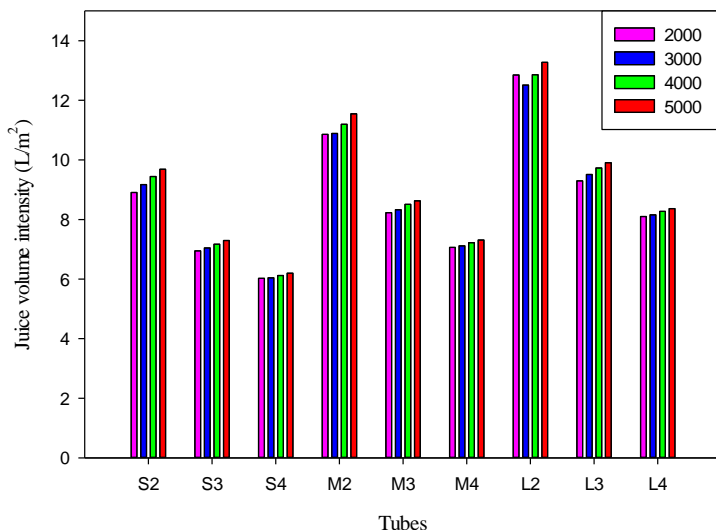


Figure 6 Juice volume intensity for 2000, 3000, 4000 and 5000 m^2 vessels with different tube dimensions

De-entrainment considerations

In practice the de-entrainment of droplets of juice from the vapour stream passing to the next vessel is achieved through:

- the provision of a large distance from the boiling level of the juice to the de-entrainment system, thus providing the opportunity for droplets to disengage from the up flow of vapour and fall back, and
- the de-entrainment equipment itself.

Vessels of smaller diameter produce a stronger up flow velocity for the same vapour rate and so the intensity of droplets impinging on the de-entrainment system is likely to be increased. For the investigations in this paper a constant stroke height above the top tube plate of 5 m is assumed. This height is common in the current installations of Robert evaporator.

Table 2 shows the maximum specific vapour rates that produce acceptable vapour up flow velocities. The data are shown for calandrias comprising tubes of 38.10 mm OD and 4 m long, in evaporators of 2000 and 5000 m², for vapour pressures of 13, 80 and 160 kPa abs. The calculation is based on a maximum allowable up flow velocity of 1 m/s for 160 kPa abs, 5 m/s for 80 kPa abs and 9 m/s at 13 kPa abs. These values have been chosen as being typical of the maximum velocities that are adequately handled in industrial evaporators.

Table 2 Maximum specific vapour rates for acceptable up flow vapour velocities in the headspace of vessels comprising tubes of 38.1 mm OD and 4 m length

Vapour pressure, kPa abs	Maximum specific vapour rate*, kg/h/m ²	
	Vessel of 2000 m ²	Vessel of 5000 m ²
13	18	16
80	18	17
160	20	19

* Specific vapour rate is vapour rate per unit HSA.

As a guide for calandrias of 38.10 mm OD but with shorter tubes than 4 m the maximum specific vapour rates that can be accommodated are 30% greater for 3 m tubes and 75% greater for 2 m tubes than shown in Table 2.

It is apparent from the data in Table 2 that the vapour velocities and potential impact on entrainment must be considered when designing an installation of a calandria with high heating surface area per unit cross-sectional area of vessel. Up flow vapour velocities are likely to be of greatest concern at the front end of the set (vapour pressures of 160 kPa abs) where specific vapour rates of 22 to 30 kg/h/m² are usual. At the tail end of the set specific vapour rates are often less than 18 kg/h/m², particularly for energy efficient installations. As well it is unlikely that calandrias with tubes of 38.10 mm OD and 4 m length would be suitable for the final vessel from the point of view of effectively producing rising film boiling.

Consideration has been given to the specific vapour rates that could be accommodated by a de-entrainment system of LSEA II louvres (a common design used in Australian factories) installed in the headspace of the evaporator comprising calandrias of different dimensions. For the study the louvre face was assumed to be a square with the corners located 200 mm from the circular shell. A safety margin for the installed louvre area of 30% above the minimum area required for breakthrough of the droplets in the vapour stream exiting the louvres was allowed. The results show, as expected, the vessels of smallest diameter (viz., calandrias comprising 38.10 mm OD tubes and 4 m long) have the lowest specific vapour rate that can be accommodated. The vessels with the capacity to process the highest vapour rate comprise calandrias of 50.80 mm OD tubes, 2 m long.

The data in Table 3 indicate that for almost all practical operating conditions, sufficient LSEA II louvre area can be installed in the headspace of the vessels, without the need for increasing the diameter of the headspace or installing an external separator. It is only at the final effect conditions that the vapour rate may exceed the breakthrough velocity and, for these conditions, it is unlikely that calandrias of these dimensions would be suitable for the final vessel.

Table 3 Maximum specific vapour rates for LSEA II louvres in vessels comprising tubes of 38.1 mm OD and 4 m length

Vapour pressure kPa abs	Maximum specific vapour rate kg/h/m ²
13	16
80	35
160	47

6.1.8 Summary of results from the capital cost analysis

A capital cost model for Robert evaporator was developed for 2000, 3000, 4000 and 5000 m² vessels with 2 m, 3 m, and 4 m tube lengths and 38.10 mm, 44.45 mm, and 50.80 mm tube outside diameter.

The results show that the conventional evaporator with 2 m tubes of 44.45 mm outside diameter is more expensive than all the other tube arrangements except for evaporators with 2 m tubes of 50.8 mm outside diameter.

Relative to the conventional evaporator, cost savings in the ex-works cost of ~12% are likely in using 3 m long tubes of 44.45 mm OD and ~15% if 3 m long tubes of 38.10 mm outside diameter tubes are used. Further savings are made by the use of 4 m long tubes but the incremental cost reduction is less than increasing the tube length from 2 to 3 m. Longer tube vessels have smaller diameter and considerably less mass on the structure and foundations than the conventional evaporator, and so additional savings through reduced installation costs would be achieved.

Vessels comprising longer tubes and smaller diameter have a lower juice volume per unit of heating surface area. This feature is likely to be important for vessels early in the evaporator set to reduce the residence times at high temperatures when high process steam pressures are used.

The vapour up flow velocities and the impact on the de-entrainment system will need to be considered for vessels comprising smaller diameter, longer tubes.

The results from this analysis were used in conjunction with the results of heat transfer efficiency measurements for calandrias of different tube dimensions to allow the optimum Robert evaporator vessel design to be determined for the different evaporation duties.

6.2. Experimental determinations of heat transfer performance of tubes of different dimensions at different operating conditions

6.2.1. General comments on heat transfer performance

Higher HTCs allow reductions in the HSA required to achieve the same rate of evaporation, achieve higher juice processing rates for the installed areas, or extend the period of operation between cleans. In addition, an important benefit of increased HTCs is the ability to achieve the required rate of evaporation with a smaller temperature difference. This benefit is of particular interest to factories seeking to reduce their process steam consumption and fuel usage (Moller *et al.*, 2003; Rose *et al.*, 2009).

6.2.2. Experimental procedure

The methodology for a test on an installed tube involved obtaining juice of the required brix, filling the evaporation rig to the required level in the heating tube, setting the headspace pressure and setting the steam chest pressure to the required values. For these conditions a specific temperature difference (ΔT) exists between the steam side of the heating tube and the average boiling temperature of the juice. For the imposed processing conditions each test results in a certain heat flux from which the HTC is calculated.

6.2.3. Experimental rig

The schematic arrangement of the single tube evaporator developed for this experiment can be seen in Figure 7. The pilot plant evaporator rig, the accessories, the control system, the data logging system and the commissioning are described by Thaval (2017).

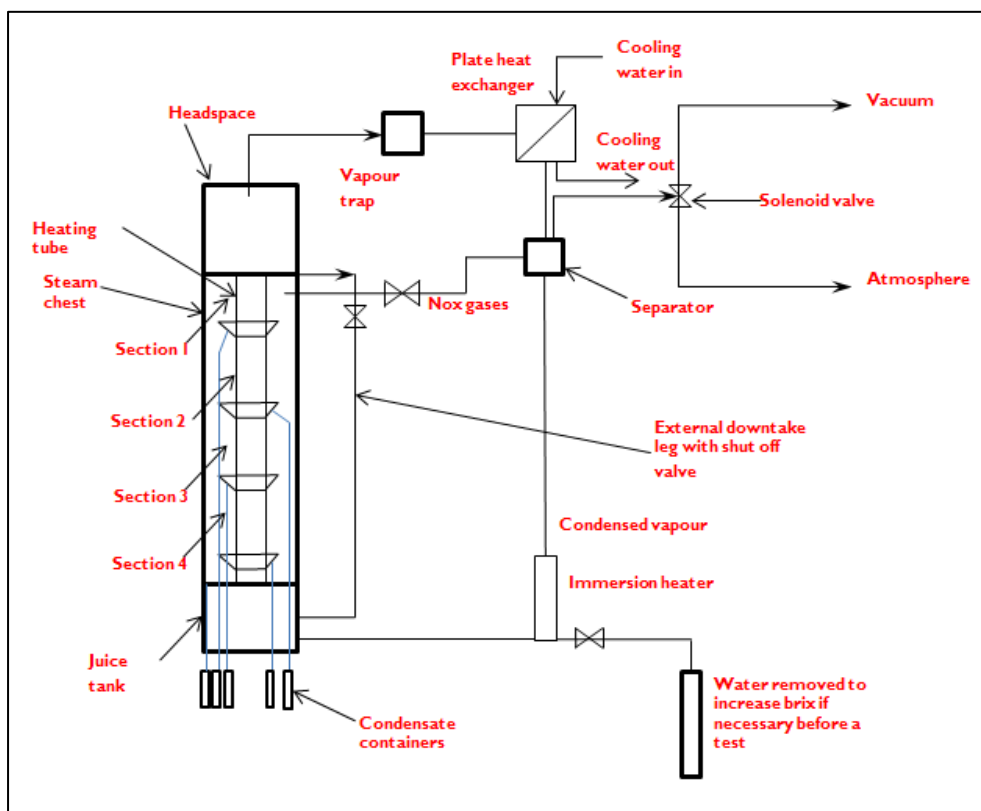


Figure 7 Schematic representation of the single tube evaporator rig

The four main components are the juice tank located below the heating tube, the heating tube, the steam chest around the heating tube and the headspace above the heating tube. The juice held in the vessel fills the juice tank and partly fills the heating tube. The juice inside the tube boils and produces vapour which passes through the headspace of the vessel and is condensed in a plate heat exchanger which is supplied with cooling water. The condensed vapour flows to a separator under vacuum or atmospheric pressure, depending on the test conditions. The condensate from the separator is heated with an immersion heater to the boiling temperature of the juice before returning to the juice tank.

The single stainless steel heating tube is encased in a steam chest allowing the steam which enters the steam chest to condense on the outside of the heating tube. The steam was distributed inside

the steam chest via two pipes which extended the full height of the steam chest and were located on opposite sides of the steam chest. These pipes contained equally spaced holes to distribute the steam and direct the steam away from the heating tube. This arrangement was essential to ensure that the condensate on the outside of the tube was not disturbed by the incoming steam. A CFD model was developed to verify that the velocity of steam near the heating tube was very low.

The condensate on the outside of the heating tube was collected in four gutters which were located equidistantly along the length of the tube. The condensate from each gutter was drained under gravity to its individual container located below the evaporator. A fifth container collected the condensate from the bottom tube plate. Each container was fitted with a pressure transducer at its base to provide a continuous measurement of the head (height) of condensate in the container.

Noxious (incondensable) gases were removed from the steam chest through two pipes within the steam chest which were connected to the condensed vapour separator. The arrangement of the noxious gas removal pipes within the steam chest was similar to that for the steam entry pipes, thus ensuring the noxious gases did not accumulate within the steam chest and were withdrawn uniformly along the full height of the steam chest.

Juice samples were taken at the beginning and end of each test to check that the brix of the juice had not changed substantially through the test. Experience showed that the brix remained reasonably consistent through the course of a test.

The boiling juice that collected above the heating tube could fall back into the heating tube or pass to the juice tank via an external juice return line (downtake).

Figure 8 shows a photograph of the pilot evaporator rig, control unit and the computer to log the data.

6.2.4. Experimental design

The experimental factors selected were tube length, tube diameter, juice brix, juice level, headspace pressure and pressure difference between the steam chest and the headspace. Steam rate was not a controlled variable in the experimental procedure. Instead, the steam chest pressure and the headspace pressure were controlled to nominated set points and the difference in pressure between the steam chest and headspace determined the resulting steam rate.

Table 4 shows the experimental factors and number of levels for each of the factors. The nine tubes which were selected were the same as those considered in the capital cost analysis (see Table 1). The test program was structured to encompass the practical operating conditions that are typical of industrial evaporators for the 1st effect (typically Brix-20), 3rd effect (typically Brix-35) and 5th effect (typically Brix-70) of a quintuple evaporator set.



Figure 8 Pilot evaporator rig

Table 4 Factors and number of values explored in the experiment

Factor	Number of values
Tube length (T_L , m)	3
Tube diameter (T_D , mm)	3
Brix, (B°)	3
Juice level, (JL,% tube height)	4
Headspace pressure (HS, kPa abs)	2
Pressure difference (ΔP , kPa)	2

The juice level, headspace pressure and pressure difference factors were selected to be consistent with the brix of juice according to where that brix is achieved in an evaporator set and to encompass the usual parameter range achieved in Robert evaporators in Australian sugar factories.

The experimental factors which were investigated for Brix-20, Brix-35 and Brix-70 juices are shown in Table 5, Table 6 and Table 7. It should be noted that in subsequent tables the following terminologies are used.

- HS1 and HS2: These are the two headspace pressure and HS1 is the higher of the two.
- DP1 and DP2: These are the two pressure differences and DP1 is the lower of the two.
- JL1, JL2, JL3 and JL4: These are the four juice levels and the order from the lowest to the highest is JL1 to JL4.

Table 5 Experimental factors investigated for juice at Brix-20

Factor	Level 1	Level 2	Level 3	Level 4
Tube length (T_L , m)	2	3	4	-
Tube diameter (T_D , mm)	38.1	44.45	50.8	-
Juice level, (JL,% tube height)	20	30	40	50
Headspace pressure (HS, kPa abs)	149	126	-	-
Pressure difference (ΔP , kPa)	33	45	-	-

Table 6 Experimental factors investigated for juice at Brix-35

Factor	Level 1	Level 2	Level 3	Level 4
Tube length (T_L , m)	2	3	4	-
Tube diameter (T_D , mm)	38.1	44.45	50.8	-
Juice level, (JL,% tube height)	20	35	45	60
Headspace pressure (HS, kPa abs)	94	72	-	-
Pressure difference (ΔP , kPa)	35	50	-	-

Table 7 Experimental factors investigated for juice at Brix-70

Factor	Level 1	Level 2	Level 3	Level 4
Tube length (T_L , m)	2	3	4	-
Tube diameter (T_D , mm)	38.1	44.45	50.8	-
Juice level, (JL,% tube height)	30	45	55	70
Headspace pressure (HS, kPa abs)	29	22	-	-
Pressure difference (ΔP , kPa)	42	60	-	-

6.2.5. Experimental program

Thaval (2017) describes the basis for the order of the test program. The nine tubes were selected for testing in a random order. For each tube, the brix and juice level combinations were selected for testing in a random order. For each of the brix and juice level combinations, the headspace pressure and pressure difference combinations were selected for testing in a random order.

With six experimental factors at the chosen number of levels, the design of the experiment included 432 tests with different parameters. As stated these 432 tests are referred to as *Original432*. Using an analysis of variance (ANOVA) of the whole plot consisting of a 3 x 3 factorial experiment, the tests

provided information on the significance of tube length and tube diameter factors individually, but no information was available on the interaction between tube length and tube diameter.

A replicated experiment was conducted to examine the tube length and tube diameter interaction. The four tubes investigated in the replicate experiment were M2, S2, M3 and S3. To reduce the number of tests in the replicates, brix levels of 20 and 70 only were selected. Juice levels, headspace pressure and pressure difference factors were kept the same values as for the *Original432* experiment. A total of 128 tests were conducted in this second experiment which is referred to as *Replicate128*. The replicated experiments were conducted after the whole *Original432* test program was completed and so, on average, were conducted several weeks after the corresponding test in the *Original432* test program. During this time the cane would have matured further and the composition of impurities varied to at least some (unknown) extent.

6.2.6. Experimental procedure

Details of the procedure used to conduct the experiments are provided by Thaval (2017). Once the appropriate conditions (juice brix, juice level, headspace pressure and pressure difference) were established in the tube, steady boiling conditions were established before logging of the data commenced. For each test, data were logged for all the operating conditions and for the height of condensate collected in each reservoir. The sections of the tube were designated section 1 to 4 with section 1 being the top section and section 4 being the bottom section. The condensate collected from the bottom tube plate was designated section 5. Each test was conducted for approximately 20 to 25 minutes, ensuring a period of steady condensate collection was obtained before moving on to the next test.

The height of condensate (mm) collected in each reservoir was logged and plotted against time (minutes). A linear regression was fitted and for most cases $R^2 \sim 1$ was determined indicating steady boiling conditions had been reached.

Using the total condensate rate on the outside of the tube (being the sum of the condensate rates for the four sections), the latent heat of vapour in the steam chest, the area of the tube (based on the outside diameter and distance between the outer faces of the tube plates) the HTC value was calculated. The effective temperature difference used to calculate the HTC value was the difference between the saturation temperature of the vapour in the steam chest and the boiling temperature of the juice (calculated as saturation temperature at the headspace pressure plus the boiling point elevation for the juice). The vapour condensation coefficient (VCC) for the test is calculated from the total condensate rate for the four sections of the tube divided by the heating surface area of the tubes.

6.2.7. Analysis of potential errors in the operating conditions

The operating conditions of the experimental program were selected such that the differences between the levels of each factor were sufficiently large to cause a change in heat transfer response.

- Juice level was set to a precision of 5 mm and the juice level measured after the run was in close agreement to the initial value, to within 5 to 10 mm of the initial level.
- Headspace pressure was tightly controlled to set point and the variation in process value from the set value was negligible for each run.
- Juice brix was selected by collecting juice from the appropriate factory evaporators and, when necessary, reducing the brix by dilution with water to within 1 – 2 units of the required brix. The brix of the sample was measured before and after the test and for most tests there

was little change. For some tests targeting Brix-20 the factory juice sample was slightly below Brix-20. For tests at Brix-70 the variation in juice brix was greatest as a small amount of evaporation of water from the juice effects a quite large change in brix of the juice.

- Calandria pressure was able to be controlled closely to the set point for most tests. However, for some of the Brix-20 tests the calandria pressure of 194 kPa abs (149 kPa abs headspace pressure and 45 kPa pressure difference) was not able to be achieved since the vapour supply from the factory was at a lower pressure.

Table 8 shows the maximum, minimum, mean and standard deviation values for the experimental factors, including the values of the calculated temperature differences.

Table 8 Maximum values, minimum values, mean values and standard deviation of the experimental factors

Effect	Factor	Set point	Maximum value	Minimum value	Mean	Standard deviation
1	B	20	21.7	14.2	18.2	1.7
	ΔP_1	33	33	33	33.0	0.0
	ΔP_2	45	45	35	40.0	3.2
	ΔT_1	5.6	5.9	5.6	5.7	0.1
	ΔT_2	6.5	6.7	6.4	6.5	0.1
	ΔT_3	7.7	7.8	6.1	7.0	0.5
	ΔT_4	8.9	8.9	8.6	8.8	0.1
3	B	35	38.5	34	36.1	1.3
	ΔP_1	35	35	35	35.0	0.0
	ΔP_2	50	50	50	50.0	0.0
	ΔT_1	7.9	8.0	7.7	7.8	0.1
	ΔT_2	9.8	10.8	9.6	10.2	0.2
	ΔT_3	11.2	11.2	10.9	11.1	0.1
	ΔT_4	13.5	13.6	13.3	13.5	0.1
5	B	70	74	65	69.5	2.3
	ΔP_1	42	42	42	42.0	0.0
	ΔP_2	60	60	60	60.0	0.0
	ΔT_1	17.2	21.7	16	18.8	1.3
	ΔT_2	20.9	24.0	19.7	21.8	1.0
	ΔT_3	23.3	24.4	22.1	23.2	0.6
	ΔT_4	27.4	28.5	26.2	27.4	0.6

Figure 9 shows the actual average temperature differences and Figure 10 shows the target temperature differences for the three brix. It is evident that, for most of the test conditions, the actual average temperature difference was in close agreement with the target temperature difference.

For Brix-20, the actual temperature difference corresponding to the headspace pressure of 149 kPa abs and pressure difference of 45 kPa was not achieved. However the actual average

temperature difference was shown to be statistically different from the other three temperature differences for Brix-20.

Overall the assessment of the differences in process values for the different test conditions concluded that the experiment was well controlled and the achieved values for the operating conditions were statistically different from each other.

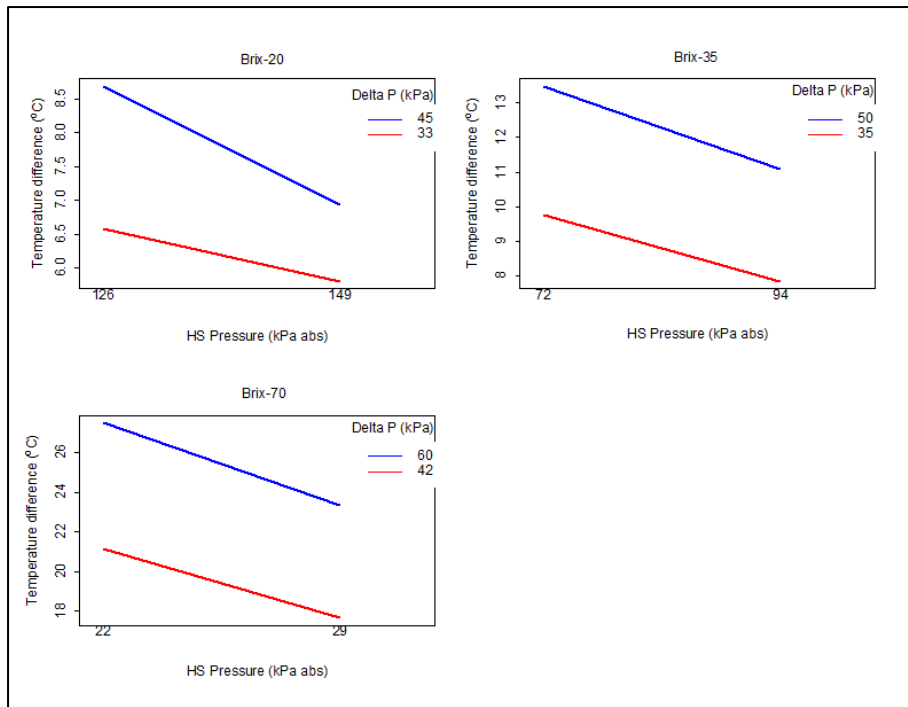


Figure 9 Actual average temperature differences for the three brix

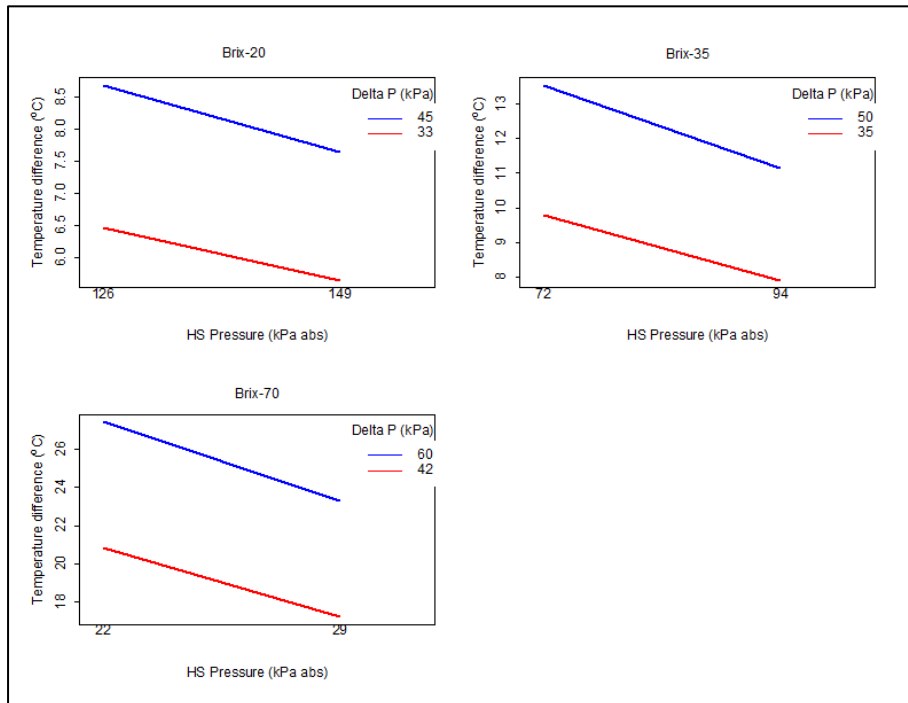


Figure 10 Target temperature differences for the three brix

6.2.8. Analysis of potential errors in the measurement of condensate flows

Thaval (2017) describes a comprehensive investigation that was undertaken to determine if the measured condensate rate for any of the four sections of the heating tube may be in error due to either condensate separating from the tube and not being drained from a gutter to the reservoir or a gutter overflowing. The investigations based on several assessments concluded that there was no evidence of overflowing of gutters or condensate separating from the tube.

One of the assessments was to compare the condensate collection rates for the individual sections of the tubes for the same test conditions in the *Original432* test program with the results in the *Replicate128* test program. The replicate tests showed very good consistency in the results for the individual sections of the heating tubes with the data for the *Original432* test.

Consequently, the measured data on the individual sections of the heating tube were considered to be reliable and suitable for determination of the overall HTC and investigations of the mechanism of heat transfer occurring at the individual sections of the heating tube.

6.2.9. Effect of tube dimensions and operating conditions on heat flux and HTC

The experimental program was designed to induce a heat flux through the imposed temperature difference between the heating steam and the boiling juice for a given brix and operating juice level. The HTC was then calculated based on the heat flux, the heating surface area of the tube and the effective temperature difference. Four temperature differences were imposed for each level of juice brix. This section describes the initial observations of the effects of tube dimensions and operating conditions on the heat flux and the heat transfer coefficient.

Thaval (2017) provides the experimental results from the *Original432* tests and the *Replicate128* tests.

Thaval (2017) presents plots of HTC versus heat flux for each imposed temperature difference with the plots arranged in groups of four for each juice brix value. In total 12 plots were provided. As an example Figure 11 shows a plot of HTC versus heat flux for an imposed temperature difference for the test at Brix-20 and a temperature difference of 6.5 °C. The plot shows the results for the nine tubes and four juice levels. As expected these data lie on a straight line with slope equal to $1/\Delta T$ and the maximum HTC occurs when the heat flux is greatest, and likewise the minimum HTC occurs when the heat flux is lowest.

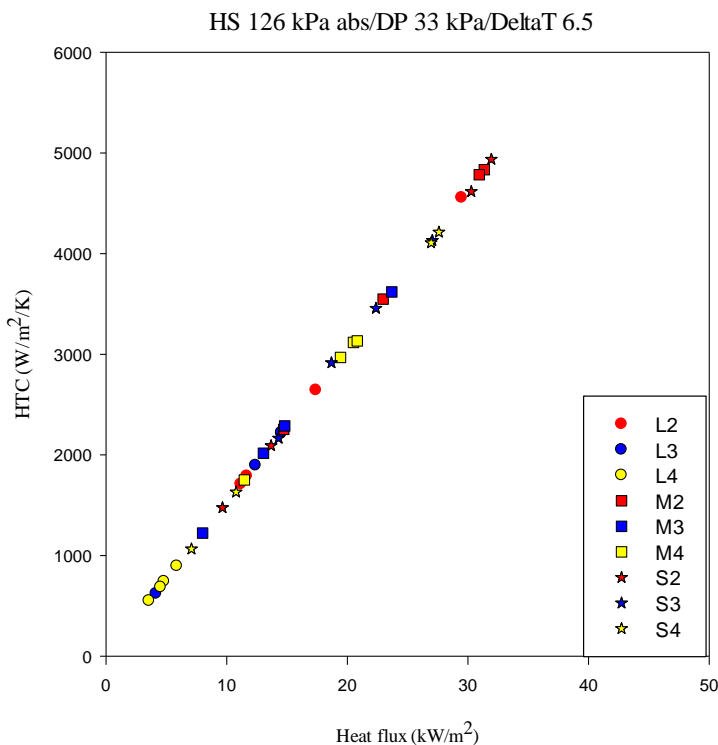


Figure 11 Effect of tube dimensions and operating conditions on heat flux and heat transfer coefficient for test at Brix-20 and ΔT of 6.5 °C

The data from the 12 plots showed:-

- For each juice brix, headspace pressure and pressure difference, for each individual tube, there is an optimum juice level which achieved the maximum heat flux and maximum HTC for that tube and processing conditions;
- For each set of operating conditions and for each tube operating at its optimum juice level, each tube was able to achieve a certain peak value of heat flux and HTC. For a given set of processing conditions certain tubes provide a higher level of heat transfer efficiency than other tubes. Thus for each set of conditions a specific tube operating at its optimum juice level achieved the maximum heat flux and maximum HTC for the imposed operating conditions; and
- The maximum HTC values were much greater for the tests at Brix-20 compared with Brix-35 and likewise for Brix-35 compared with Brix-70.

Thaval (2017) provided plots of HTC versus heat flux for each of the test conditions at Brix-20, Brix-35 and Brix-70 for the juice level that provided the maximum HTC (and heat flux) for each of the nine tubes. These plots showed the maximum HTC and heat flux that was obtained for each tube at the nominated processing conditions, and consequently showed which tube provided the highest heat flux and highest HTC for the imposed processing conditions.

Figure 12 shows the maximum HTC and heat flux values for the nine tubes corresponding to the conditions shown in Figure 11 (Brix-20 and ΔT of 6.5 °C). The data in Figure 12 show that the five tubes showing HTC values above 4000 W/m²/K are S2, M2, L2, S4, and S3.

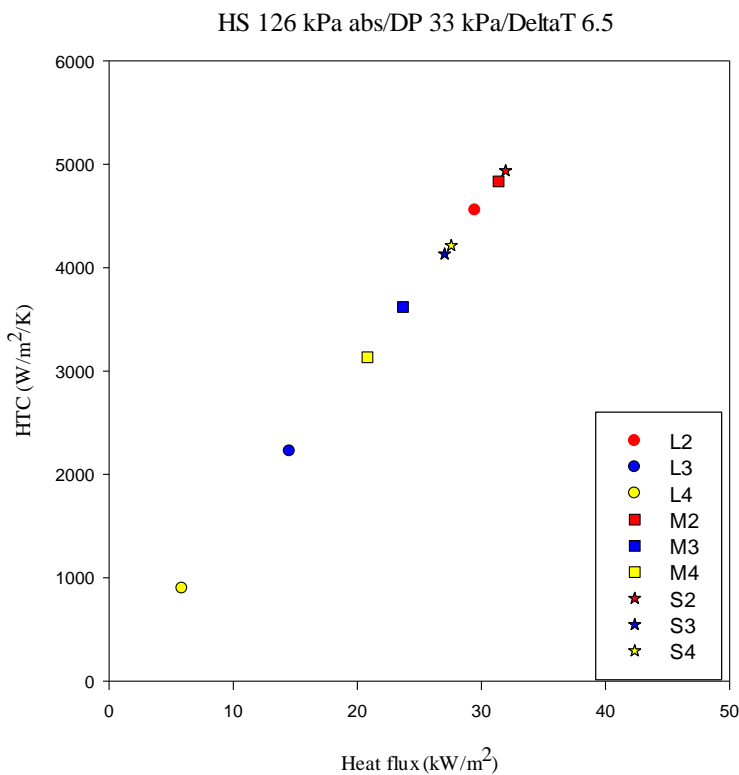


Figure 12 Relationship between heat transfer coefficient and heat flux at the optimum juice level at Brix-20 and ΔT of 6.5 °C

Table 9 lists the tubes in the order of highest HTC first to lowest HTC last for the tests at the three brix values. The HTC values for the three brix values are further divided into two categories being: for Brix-20 by HTC values above or below 4000 W/m²/K; for Brix-35 by HTC values above or below 2500 W/m²/K; for Brix-70 by HTC values above or below 500 W/m²/K.

Table 9 List of tubes showing high and low HTC for the different processing conditions

Brix	Test conditions	Tubes demonstrating good HTC	Tubes demonstrating poor HTC
		(>4000 W/m ² /K)	(<4000 W/m ² /K)
20	HS:149/ΔP:33/DeltaT:5.6	L3, M2, S2, S4, L2, M3, S3	L4, M4
	HS:149/ΔP:45/DeltaT:7.6	S2, M2, M3, S4	S3, M4, L2, L3, L4
	HS:126/ΔP:33/DeltaT:6.5	S2, M2, L2, S4, S3	M3, M4, L3, L4
	HS:126/ΔP:45/DeltaT:8.7	S2, M3, S3, M4, S4	M2, L2, L3, L4
35		(>2500 W/m ² /K)	(<2500 W/m ² /K)
	HS:94/ΔP:35/DeltaT:7.9	S3, M3, M4, M2	S2, S4, L2, L3, L4
	HS:94/ΔP:50/DeltaT:11.2	M3, S3 M4, L2, M2	S2, S4, L3, L4
	HS:72/ΔP:35/DeltaT:9.79	L2, M4, M3	S2, S3, S4, M2, L3, L4
70	HS:72/ΔP:50/DeltaT:13.5	M4	L2, L3, L4, M2, M3, S2, S3, S4
		(>500 W/m ² /K)	(<500 W/m ² /K)
	HS:29/ΔP:42/DeltaT:17.2	L2, M2, S3	S2, S4, M3, M4, L3, L4
	HS:29/ΔP:60/DeltaT:23.3	M2, L2, L3	S2, S3, S4, M3, M4, L4
	HS:22/ΔP:42/DeltaT:20.9	M2, L2, S2	S3, S4, M3, M4, L3, L4
	HS:22/ΔP:60/DeltaT:27.4	S2, L3	S3, S4, M2, M3, M4, L2, L4

Other observations from the plots of HTC versus heat flux for the tests on the nine tubes were:

- For tests at Brix-20 the maximum heat flux was obtained for the test at the highest ΔT. This corresponded to the test at the lower headspace pressure and larger pressure difference. However for the tests at Brix-35 and Brix-70 the maximum heat flux was at the higher headspace pressure and larger pressure difference. This corresponded to the second highest ΔT. The difference in these results is attributed to the stronger dependence of HTC on juice viscosity at higher juice brix values.
- For tests at Brix-20, Brix-35 and Brix-70 the maximum HTC values were obtained for the tests at the higher headspace pressure (i.e. higher boiling temperature).

6.2.10. Comparison of the pilot evaporator HTC values with industrial HTC values

Figure 13 shows HTC values for Australian industrial evaporators (which predominantly use the M2 tube) and the pilot evaporator HTC values for M2 tube dimension. The industrial HTC values are for different evaporator sets operating under different conditions e.g. vapour bleeding schemes.

The data in Figure 13 show that the pilot evaporator HTC values are slightly higher than for the industrial vessels, especially for the 1st effect conditions. For the 3rd and 5th effect conditions, HTC values for both the pilot evaporator and industrial vessels are in close proximity. Most importantly, the HTC values for the industrial and pilot evaporators show the same trend with brix, temperature difference and juice temperature.

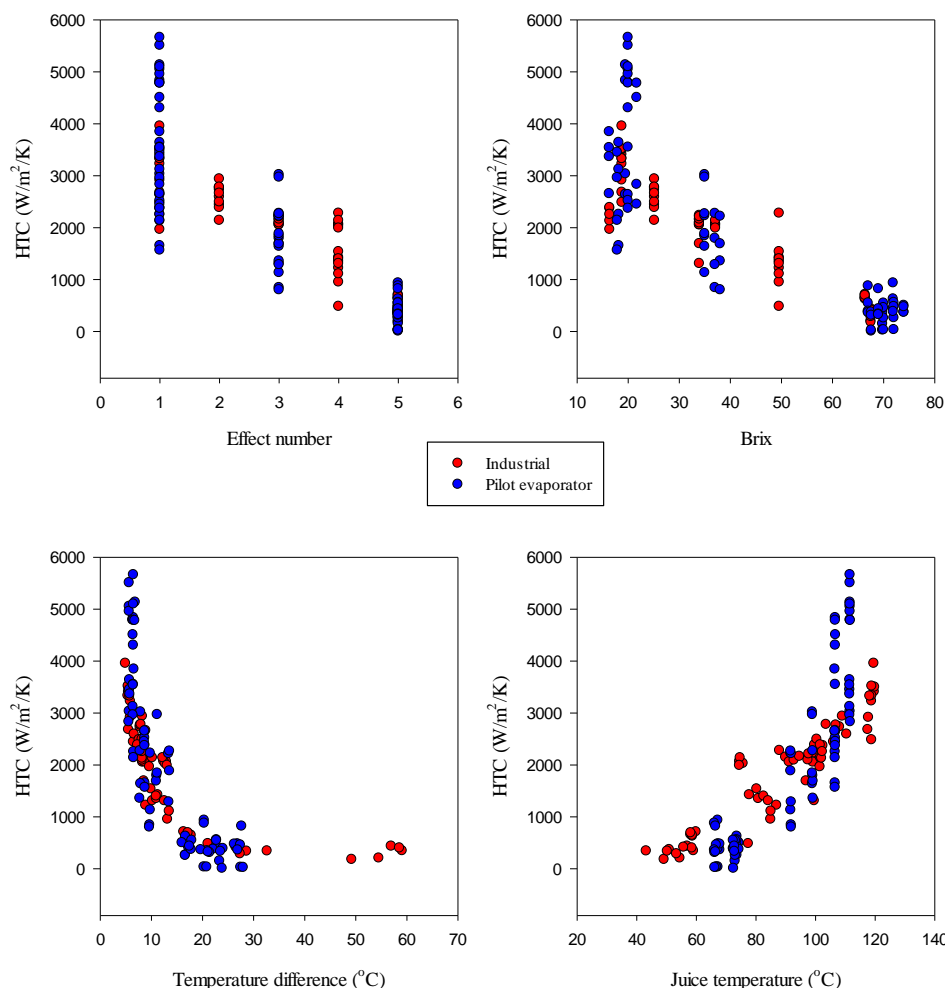


Figure 13 Comparison of industrial and pilot evaporator HTC values for M2 tube dimension

Reasons why the pilot evaporator may produce higher HTC values than industrial evaporators include:-

- The heating tubes in the pilot evaporator were brand new and clean. After each day's tests they were boiled with water to maintain this cleanliness;
- Juice was only boiled in the pilot evaporator tubes for considerably shorter periods than in industrial evaporators.
- The gutters removed the condensate from the outside of the tubes, thus reducing the resistance to heat transfer provided by the condensate film; and
- A downtime was installed for the single heating tube. As a consequence it is likely that, compared with an industrial evaporator, a greater proportion of the pool of juice above the top tube plate in the experimental rig returned to the juice tank through the downtime line as opposed to running down inside the heating tube.

6.2.11. Visual observations of the boiling behaviour

The headspace of the single tube evaporator was fitted with a sight glass which allowed the movement of juice and froth above the top tube plate to be observed. In industrial evaporators the preferred boiling conditions generally show a vigorous boiling juice and froth layer above the top

plate for a height of 200 to 300 mm. The boiling behaviours in the experimental rig were noted while conducting the experiments. The boiling behaviours were allocated to one of three patterns as shown in Table 10.

Table 10 Observations of juice above the top tube plate in the heat transfer experiments

Behaviour	Description and comments
No visible juice above top plate	For these tests low HTC values were usual.
Visible juice above top plate	Small layer of juice/froth evident. Most common behaviour. Good HTC values were usual.
Substantial juice head above top plate	Consistent boiling head of 50 to 250 mm above the top plate. Generally highest HTC values and correspond to the optimum juice level.

6.2.12. Comparison of the overall HTC results for the *Original432* and *Replicate128* datasets

Thaval (2017) provides plots of overall HTC versus juice level for each processing condition for the four tubes (M2, S2, M3, S3) and Brix-20 and Brix-70 to compare the repeatability of the results for the *Original432* and *Replicate128* datasets. Very similar patterns between the two datasets were obtained.

The juice level corresponding to the maximum HTC values (HTC_{max}) are the same for the two datasets for the S2, M3 and S3 tubes and for all except one set of conditions for the M2 tube. There is good agreement for the values of HTC_{max} between the two datasets for S2, M3 and S3 tubes. For some unknown reason the HTC_{max} values for the M2 tube are more variable than for the S2, M3 and S3 tubes.

The plots of overall HTC versus juice level show very strong replication of the profiles in the two datasets. For many tests the variation of HTC with juice level was not a consistent gradually changing variation, but often quite discontinuous. This result is unexpected but interestingly replicated closely in the two datasets.

Two interesting observations were made from the profiles for juice at Brix-20 and with 2 m long tubes:-

- M2 tubes: The general pattern is a faster decline in HTC at juice levels below the optimum level with juice levels above the optimum. This pattern agrees with the observations of Broadfoot and Dunn (2007) for their work with M2 tubes;
- S2 tubes: The general pattern is a faster decline in HTC at juice levels above the optimum level compared with juice levels below the optimum i.e. opposite behaviour than for the M2 tubes at Brix-20.

The good repeatability of the HTC patterns shown in the replicate datasets increases the confidence in the results obtained in the *Original432* dataset. The consistency of the results between the two datasets suggests that juice properties such as surface tension variation were not influencing the heat transfer performance and the boiling juice pattern to a large extent. This conclusion is made because the replicate tests were undertaken on average several weeks after the initial tests.

The HTC versus juice level patterns demonstrated that headspace pressure and pressure difference (and corresponding ΔT) also affect the optimum juice level and the maximum HTC.

6.2.13. Interaction of tube diameter and length on HTC values

Analysis of the HTC results from the *Original432* dataset showed that tube length and tube diameter interaction is significant. Thus, the selection of tube length and tube diameter is not independent of each other in relation to achieving good heat transfer performance. Analysis of the replicate data confirmed the result.

6.2.14. Analysis of the results of the *Original432* tests

Figure 14 shows the mean values of HTC for each of the experimental factors at each level for the *Original432* dataset. It was found that tube length and tube diameter alone do not affect the HTC significantly. The most important factor affecting HTC was the brix of the juice. As expected from industrial experience, higher HTC was achieved at lower brix and HTC was lower at higher brix.

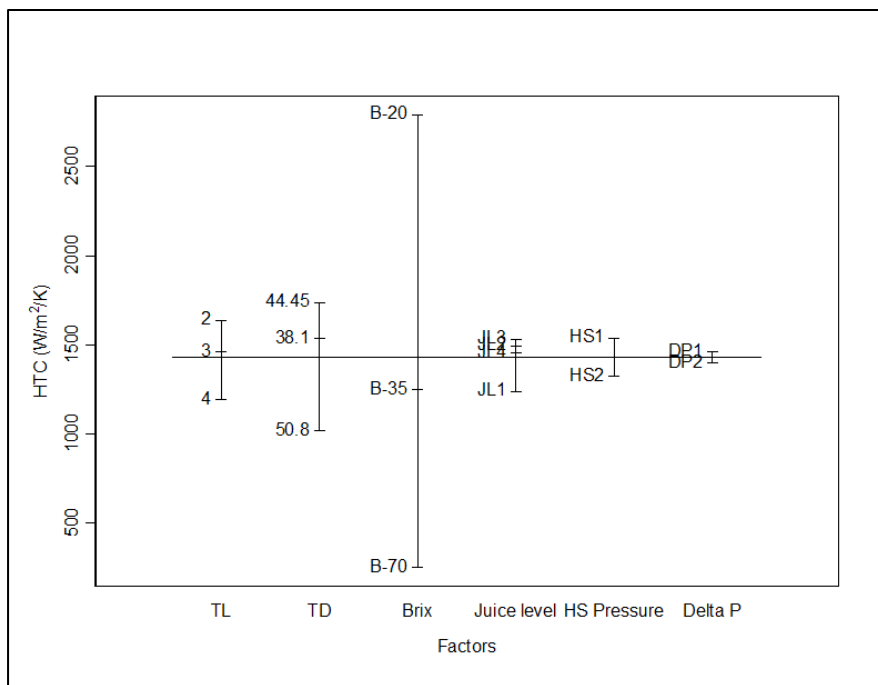


Figure 14 Mean values of HTC for each level of each factor for the *Original432* tests with all results included

Thaval (2017) presents the results of an analysis of variance (ANOVA) for the *Original432* HTC values. The ANOVA was undertaken for a split-split-plot design with whole plot for tube dimensions, subplot for juice brix and juice level and sub-sub-plot for headspace pressure and pressure difference. The same procedure was applied to all ANOVA undertaken for all datasets.

Table 11 presents the results of the analysis of variance of the HTC values of the *Original432* dataset. Significant interactions (to the 0.05 level) were achieved up to the 4th order. Two main factors (B, HS), three 2nd order interactions (B:HS, T_D:B, T_D:JL), two 3rd order interaction (T_L:T_D:B, T_L:T_D:HS) and one 4th order interaction (T_L:T_D:B:HS) were identified with a level of significance less than 0.05. Those parameters or combinations of parameters showing a low value for the significance level in the tables of ANOVA results (as in Table 11) indicate a strong influence on the HTC value.

Table 11 Analysis of variance of HTC from Original 432 tests with 4th order interactions

Source	Degrees of freedom	Mean square	Variance ratio	Significance level
T _L	2	6562399	0.69	—
T _D	2	21762038	2.28	—
Residuals	4	9548502		
B	2	230647154	245.15	0.000
JL	3	2569618	2.73	—
T _L :B	4	1868540	1.99	—
T _L :JL	6	890671	0.95	—
T _D :B	4	9562815	10.16	0.000
T _D :JL	6	3354494	3.57	0.011
B:JL	6	2106656	2.24	—
T _L :T _D :B	8	3278353	3.48	0.008
T _L :T _D :JL	12	1005306	1.07	—
T _L :B:JL	12	789134	0.84	—
T _D :B:JL	12	1666036	1.77	—
Residuals	24	940844		
HS	1	5271514	15.17	0.000
ΔP	1	264281	0.76	—
T _L :HS	2	947255	2.73	—
T _L :ΔP	2	65834	0.19	—
T _D :HS	2	96601	0.28	—
T _D :ΔP	2	96802	0.28	—
B:HS	2	3138628	9.03	0.000
B:ΔP	2	858313	2.47	—
JL:HS	3	273703	0.79	—
JL:ΔP	3	46677	0.13	—
HS:ΔP	1	46190	0.13	—
T _L :T _D :HS	4	1389868	4.00	0.004
T _L :T _D :ΔP	4	179391	0.52	—
T _L :B:HS	4	564882	1.63	—
T _L :B:ΔP	4	1091752	3.14	—
T _L :JL:HS	6	748109	2.15	—
T _L :JL:ΔP	6	166142	0.48	—
T _L :HS:ΔP	2	832428	2.40	—
T _D :B:HS	4	1148956	3.31	—
T _D :B:ΔP	4	383181	1.10	—
T _D :JL:HS	6	467756	1.35	—

Source	Degrees of freedom	Mean square	Variance ratio	Significance level
T _D :JL:ΔP	6	187437	0.54	—
T _D :HS:ΔP	2	281050	0.81	—
B:JL:HS	6	404672	1.16	—
B:JL:ΔP	6	74783	0.22	—
B:HS:ΔP	2	76723	0.22	—
JL:HS:ΔP	3	565762	1.63	—
T _L :T _D :B:HS	8	1172778	3.38	0.002
T _L :T _D :B:ΔP	8	298091	0.86	—
T _L :T _D :JL:HS	12	360754	1.04	—
T _L :T _D :JL:ΔP	12	164010	0.47	—
T _L :T _D :HS:ΔP	4	286797	0.83	—
T _L :B:JL:HS	12	244066	0.70	—
T _L :B:JL:ΔP	12	242668	0.70	—
T _L :B:HS:ΔP	4	384196	1.11	—
T _L :JL:HS:ΔP	6	96163	0.28	—
T _D :B:JL:HS	12	320568	0.92	—
T _D :B:JL:ΔP	12	258218	0.74	—
T _D :B:HS:ΔP	4	455442	1.31	—
T _D :JL:HS:ΔP	6	497655	1.43	—
B:JL:HS:ΔP	6	613441	1.77	—
Residuals	116	347431		

Thaval (2017) presents interaction plots for the significant interactions.

The main conclusions from the ANOVA on the *Original432* dataset were:-

- Brix is the dominating factor affecting HTC;
- Tube length and tube diameter interaction was found to be significant. It was concluded that for 2, 3 and 4 m tube length, tubes of 44.45, 38.1 and 44.45 mm diameter respectively showed higher HTC than the tubes of other diameters;
- The effects of juice level and headspace pressure on HTC were not consistent within the dataset.

6.2.15. Analysis of HTC_{max} results

For each brix and associated processing conditions, HTC was calculated at four juice levels of which one juice level was found to be the optimum juice level. This optimum juice level corresponds to HTC_{max}. The HTC_{max} values were determined from the plots of HTC versus juice level. For the *Original432* dataset 108 values of HTC_{max} were obtained.

Figure 15 shows the mean values of HTC_{max} for all the experimental factors at each level. It is evident from Figure 15 that brix is the dominant factor affecting HTC_{max}.

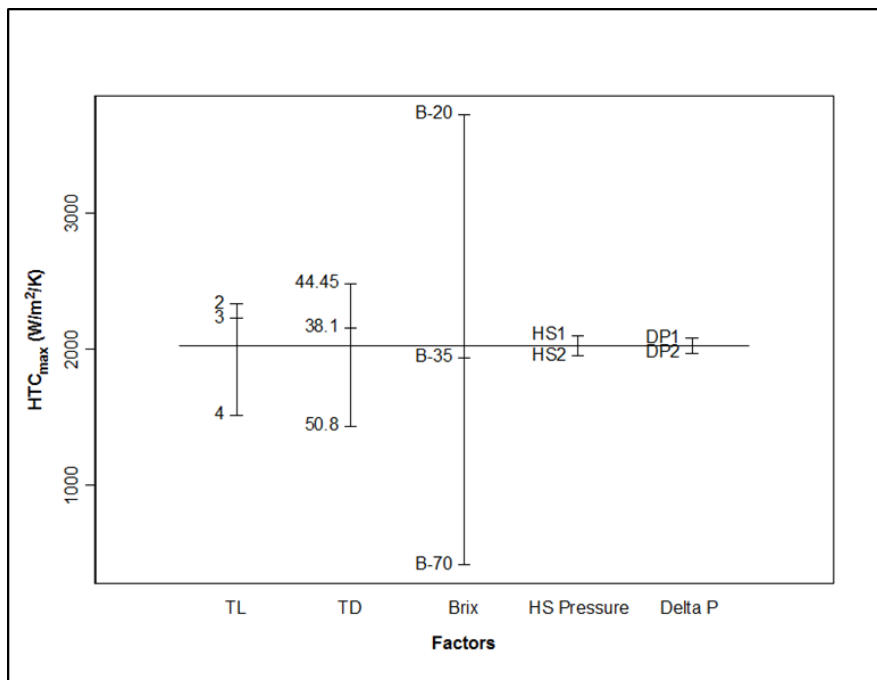


Figure 15 Mean values of HTC_{\max} for each level of each factor from the *Original432* tests (108 data points)

Table 12 shows the analysis of variance of HTC_{\max} for the *Original432* dataset. Two main effects (B, HS) and one 3rd order interaction ($T_D:B:HS$) were identified with significance level less than 0.05.

Thaval (2017) concluded the following from the analysis of variance for HTC_{\max} :-

- Higher brix results in lower HTC_{\max} and vice versa.
- Tube diameter is more important than tube length in influencing HTC_{\max} .
- For tubes of 38.1 mm diameter, headspace pressure has little influence on HTC_{\max} . For tubes of 44.45 mm and 50.8 mm outside diameter, higher headspace pressure generally provides substantially higher values of HTC_{\max} ; and
- For Brix-20 higher HTC_{\max} values are achieved for tubes of 38.1 mm and 44.45 mm outside diameter. For Brix-35 and Brix-70, higher HTC_{\max} values are achieved for tubes of 44.45 mm outside diameter.

Table 12 Analysis of variance of HTC_{max} from Original432 tests

Source	Degrees of freedom	Mean square	Variance ratio	Significance level
T _L	2	7605799	4.31	—
T _D	2	9027073	5.12	—
Residuals	4	1763889		
B	2	96679890	62.58	0.000
T _L :B	4	1356587	0.88	—
T _D :B	4	3724704	2.41	—
Residuals	8	1544845	—	—
HS	1	1284893	4.38	0.043
ΔP	1	794988	2.71	—
T _L :HS	2	471666	1.61	—
T _L :ΔP	2	132652	0.45	—
T _D :HS	2	735357	2.51	—
T _D :ΔP	2	29695	0.10	—
B:HS	2	774050	2.64	—
B:ΔP	2	442284	1.51	—
HS:ΔP	1	16133	0.05	—
T _L :T _D :HS	4	509971	1.74	—
T _L :T _D :ΔP	4	169562	0.58	—
T _L :B:HS	4	222860	0.76	—
T _L :B:ΔP	4	356036	1.21	—
T _L :HS:ΔP	2	947662	3.23	—
T _D :B:HS	4	1087098	3.70	0.013
T _D :B:ΔP	4	263404	0.90	—
T _D :HS:ΔP	2	31442	0.11	—
B:HS:ΔP	2	24413	0.08	—
Residuals	36	293421		

6.2.16. Analysis of optimum juice level

Figure 16 shows the mean values of optimum juice level (% tube height) for the Original432 tests. It is observed that optimum juice level is lower for lower brix and increases with increase in brix. This observation agrees closely with practical experience with industrial Robert evaporators.

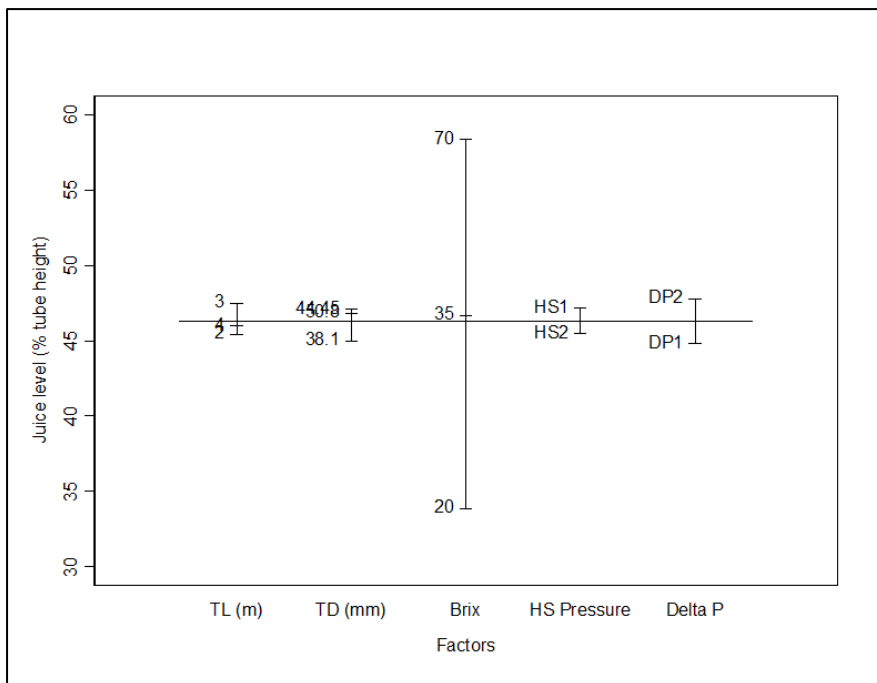


Figure 16 Mean values of $JL_{opt}(\%)$ for each level of each factor from the *Original432* tests (108 data points)

Table 13 shows the analysis of variance of optimum juice levels corresponding to HTC_{max} from the *Original432* dataset. One main source (B), one 2nd order interaction ($T_D:\Delta P$) and one 3rd order interaction ($T_L:B:HS$) were identified with significance level less than 0.05.

Thaval (2017) concluded the following from the analysis of variance for optimum juice level:-

- For juice at higher brix the optimum juice levels (as % of tube height) is higher.
- The effect of tube length and headspace pressure on optimum juice level was not consistent across the full dataset. It was found that, in general, for tubes of 38.1 and 50.8 mm diameter the optimum juice level increases with increase in pressure difference while, for tubes of 44.45 mm diameter, optimum juice level decreases with increase in pressure difference. Among these results there was some variability in the effect for the different brix values.
- When the effect of juice level was examined in terms of the absolute level (in mm) a more consistent pattern of lower optimum juice level for higher pressure difference was found. This behaviour is generally observed in industrial Robert evaporators.

Table 13 Analysis of variance of the optimum juice level (JL_{opt} -% tube height) corresponding to HTC_{max} from Original432 tests

Source	Degrees of freedom	Mean square	Variance ratio	Significance level
T_L	2	41.89	0.26	—
T_D	2	46.06	0.28	—
Residuals	4	163.77		
B	2	5381.48	18.27	0.001
$T_L:B$	4	110.65	0.38	—
$T_D:B$	4	587.73	2.00	—
Residuals	8	294.5	—	—
HS	1	75	0.84	—
ΔP	1	237.03	2.66	—
$T_L:HS$	2	4.86	0.05	—
$T_L:\Delta P$	2	100.23	1.13	—
$T_D:HS$	2	0.69	0.01	—
$T_D:\Delta P$	2	321.06	3.60	0.037
B:HS	2	202.77	2.28	—
B: ΔP	2	195.37	2.19	—
HS: ΔP	1	0.92	0.01	—
$T_L:T_D:HS$	4	173.26	1.95	—
$T_L:T_D:\Delta P$	4	24.88	0.28	—
$T_L:B:HS$	4	284.72	3.20	0.024
$T_L:B:\Delta P$	4	46.06	0.52	—
$T_L:HS:\Delta P$	2	264.12	2.97	—
$T_D:B:HS$	4	190.97	2.14	—
$T_D:B:\Delta P$	4	52.31	0.59	—
$T_D:HS:\Delta P$	2	143.28	1.61	—
B:HS: ΔP	2	250.92	2.82	—
Residuals	36	89.07		

6.2.17. Empirical relationships for HTC_{max} and optimum juice level (in mm)

Thaval (2017) developed empirical relationships for HTC_{max} and optimum juice level from the Original432 dataset.

The best empirical relationship for HTC_{max} was found to be:

$$HTC_{max} = B^{-0.4901} T_j^{1.3582} VCC^{0.8877} \quad 6.1$$

where B is the brix of the juice,

T_j is the temperature of the juice, °C

VCC is the vapour condensation coefficient, kg/h/m²

Brix is the dominating factor affecting HTC_{max} followed by the temperature of the juice which is a function of the headspace pressure in the vessel. As vapour bleeding changes, VCC values of the effects change and the developed equation takes this into account when predicting the HTC_{max} of the effect.

Figure 17 shows the measured and predicted HTC_{max} . The predictions from the empirical model provide a good match with measured HTC_{max} ($R^2 = 0.94$) and are in general agreement with industry values.

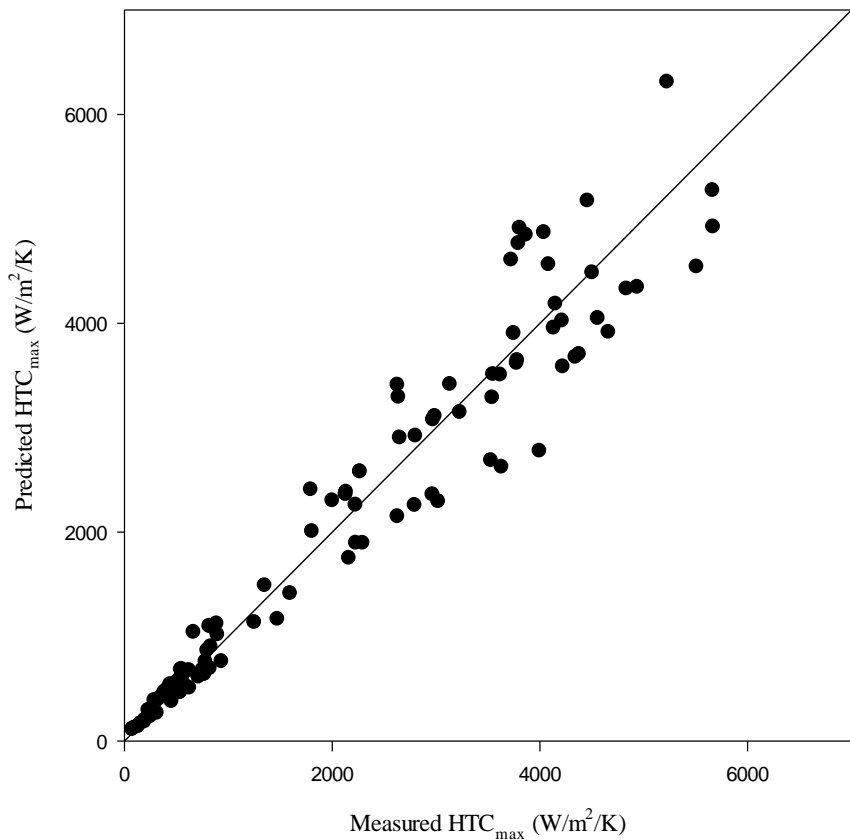


Figure 17 Measured and predicted HTC_{max}

The correlation for HTC_{max} shows that, as brix increases HTC_{max} decreases and, as temperature of the juice and VCC increase, HTC_{max} increases. In industrial evaporators factory the juice level in the individual evaporator vessels is controlled to approximate the optimum juice level and so the HTC is close to the HTC_{max} value.

Table 14 shows examples of the typical operating conditions in factory vessels and the predicted empirical HTC from two models viz., Equation 6.1 and AusTyp (Australian Typical as defined by Wright, 2008). The AusTyp formula is extensively used for predicting HTC_{max} values when undertaking evaporator simulations. The 'AusTyp' does not contain the VCC parameter and often shows higher HTC_{max} than the 'Equation 6.1' correlation.

The incorporation of VCC into equation 6.1 is an important inclusion in the correlation to allow improved simulations of evaporator stations which incorporate extensive bleeding of vapour (i.e. for stations that often experience very low VCC values).

Table 14 Typical operating conditions in factory vessels and the predicted HTC from two models

Brix	Temperature of juice (°C)	VCC (kg/h/m ²)	HTC (W/m ² /K)	
			Equation 5.1	AusTyp
17	115	25	2734	3086
20	115	25	2524	2918
25	115	25	2263	2690
17	110	20	2111	2949
17	110	25	2574	2949
17	110	35	3469	2949
17	110	40	3906	2949
35	105	25	1696	2134
35	100	25	1587	2031
35	95	25	1480	1928
35	100	15	1008	2031
35	100	20	1302	2031
35	100	25	1587	2031
70	60	10	250	733
70	60	15	359	733
70	60	20	463	733
65	60	15	372	805
70	65	15	400	795
70	75	15	486	920

Developing an empirical relationship for juice level (% tube height) did not give a robust correlation. However, the empirical relationship developed with absolute juice level (mm) resulted in a better correlation.

Step-wise regression was undertaken to determine the parameters in the empirical model. The best empirical relationship for optimum juice level ($JL_{opt\,(mm)}$) was given by:

$$JL_{opt\,(mm)} = T_L^{0.7253} B^{0.4544} \Delta T^{-0.1122} \quad 6.2$$

where T_L is the tube length, mm
 B is the brix of the juice,
 ΔT is the temperature difference between the steam and juice, °C

Figure 18 shows the predicted and measured values of $JL_{opt\,(mm)}$. The data are differentiated for lengths of 2, 3 and 4 m. The correlation coefficient R^2 for the match of the predicted values is 0.61.

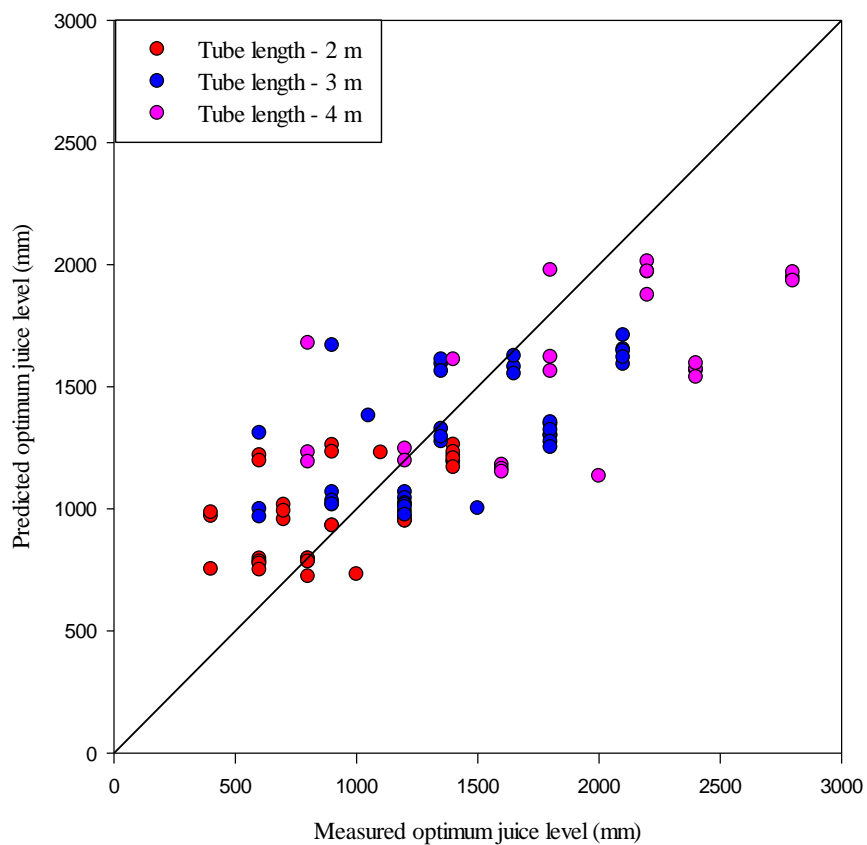


Figure 18 Measured and predicted optimum juice level

Table 15 shows the typical operating conditions in factory vessels and the predicted optimum juice levels (absolute and %tube height). The predictions for optimum juice level for tube length of 2 m are above the accepted values in the Australian industry. The predicted effects of processing conditions on optimum juice level are in agreement with observations in industrial evaporators. For example, operation at a higher juice brix requires a higher juice level to be set to maximise HTC and operation at a higher temperature difference requires a slightly lower juice level to be set to maximise the HTC.

The correlation incorporates a tube length term such that for longer tubes the optimum juice level (mm) is higher, which is logical.

Table 15 Typical operating conditions in factory vessels and the predicted optimum juice levels (absolute and % tube height)

Tube length (m)	Brix	ΔT (°C)	Optimum juice level (mm)	Optimum juice level (% tube height)
2000	20	5	807	40
2000	35	6	1020	51
2000	20	7	777	39
2000	35	7	1002	50
2000	70	20	1221	61
2000	70	12	1293	65
3000	70	20	1638	55
3000	70	12	1735	58
3000	15	5	950	32
3000	20	6	1061	35
3000	20	7	1043	35
3000	35	8	1325	44
4000	15	5	1171	29
4000	35	8	1633	41

6.3. Examination of HTC patterns along the tube length and postulation of boiling behaviour in the tube

6.3.1. Overview

The different patterns of HTC values for the individual sections of the heating tubes were investigated for the different operating conditions and, based on these patterns, different boiling mechanisms were proposed.

Thaval (2017) provides details of the investigations into the heat transfer patterns leading to the proposed mechanism of boiling in the heating tubes for the different operating conditions.

6.3.2. Comparison of the HTC values for the individual tube sections for the *Original432* and *Replicate128* datasets

The HTC of the individual sections of the four tubes in the replicate dataset were compared to the HTC of the individual sections from the corresponding original dataset.

Tests with Brix-20 juice demonstrated a high level of consistency in the results for the two series of tests. The results showed 97% of the individual section HTC values in the two datasets were within 15% of each other.

Tests with Brix-70 juice showed a much lower level of consistency with 56% of the tests providing HTC values within 15% of each other. The larger discrepancy for Brix-70 is probably attributable to the larger variation in brix among the Brix-70 tests than the Brix-20 tests and the effect of the variation in brix on HTC was proportionally much greater for the Brix-70 tests than for the Brix-20 tests.

6.3.3. Identification of HTC patterns

The patterns of HTC for the individual sections of the tubes were found to be different for the different operating conditions. The different HTC for the different tube sections indicates that different boiling patterns were present for the different test conditions.

Six boiling patterns were identified in the *Original432* and *Replicate128* datasets and these patterns are presented in Table 16.

Table 16 Categorisation and description of the boiling patterns

Category of boiling pattern	Description of category
Uniform boiling along the tube	HTC of all the four sections of the tube are within 15% of the overall HTC
Non uniform boiling; low HTC at the top section	HTC at top section >15% below the overall HTC; HTC for other tube sections within 15% or >15% above overall HTC
Non uniform boiling; low HTC at the bottom section	HTC at bottom section >15% below the overall HTC; HTC for other tube sections within 15% or >15% above overall HTC
Non uniform boiling; low HTC at an intermediate section (i.e. section 2 and/or 3)	HTC at intermediate section (section 2 and/or 3) >15% below the overall HTC; HTC for other tube sections within 15% or >15% above overall HTC
Non uniform boiling; low HTC at the top and bottom section	HTC at top and bottom section >15% below the overall HTC; HTC for other tube sections within 15% or >15% above overall HTC
Non uniform boiling; low HTC at top and intermediate section (i.e. section 1 and 2 or 3)	HTC at top and intermediate section (section 1 and 2 or 3) >15% below the overall HTC; HTC for other tube sections within 15% or >15% above overall HTC

The non-uniform boiling – low HTC at the top of the heating tube was found to be the most common boiling pattern for both the *Original432* and *Replicate128* datasets. Non-uniform boiling with low HTC at the bottom section was found to be the next most common pattern. The first four patterns listed in Table 16 account for ~90% of the data and only these four patterns are considered in more detail.

6.3.4. Determination of factors influencing the boiling patterns

A qualitative analysis of the *Original432* dataset was undertaken to understand the influence that tube dimensions and operating conditions have on the formation of the different boiling patterns. The results of these observations are summarised in Table 17.

Table 17 Results of observations of the influence of experimental factors on the boiling patterns

HTC patterns	Factors which have a strong influence on the HTC pattern
Uniform	2 m tube length Brix-20 Higher juice levels Higher headspace pressure
Non uniform; low HTC at top	Brix-35 and Brix-70 Lower juice levels
Non uniform; low HTC at bottom	4 m tube length 44.45 mm tube diameter Brix-20 and Brix-70 Higher juice levels
Non uniform; low HTC at intermediate section	2 m tube length 38.1 mm tube diameter Lower headspace pressure

6.3.5. Analysis of variance of HTC values for the four sections of the heating tubes

Analysis of variance was undertaken for the individual section HTC values to determine the experimental factors affecting the HTC values of the individual sections. Table 18 shows the single parameters and interactions that were found to have a significant effect on the HTCs for the four sections at the 0.05 level of significance. The 4th order interaction ($T_L:T_D:B:HS$) was found to be significant for all four sections. Section 1 of the tube is the top section and section 4 is the bottom section.

Thaval (2017) provides information on the interactions of the different tube dimensions and operating parameters on the HTC patterns.

Table 18 Summary of significant factors and interactions for the individual section HTC values (*Original432*)

Tube section	Factor identified with significance level less than 0.05			
	Single parameter	2 nd order interaction	3 rd order interaction	4 th order interaction
Section 1	B, HS	T _D :B, T _D :JL, T _D :HS	T _L :T _D :B T _L :T _D :HS T _L :B: ΔP	T _L :T _D :B:HS
Section 2	B, JL, HS, ΔP	T _D :B, T _D :JL, B:JL, B:HS, B:ΔP	T _L :T _D :B T _L :T _D :HS T _L :B:ΔP T _L :HS:ΔP	T _L :T _D :B:HS
Section 3	B, HS	T _D :B, T _D :JL	T _L :T _D :B T _L :T _D :HS T _L :JL:HS T _D :B:HS	T _L :T _D :B:HS
Section 4	B, HS	T _L :B, T _D :B, T _L :HS, B:HS, B: ΔP	T _L :T _D :B T _L :T _D :HS T _L :JL:HS T _D :B:HS T _L :B:HS JL:HS:ΔP	T _L :T _D :B:HS

6.3.6. Analysis of variance of the HTC values for individual sections corresponding to overall HTC_{max}

Of greater interest is to understand the patterns of HTC for operation at the optimal juice levels, that is for the HTC_{max} results, for the nine tubes and test conditions of juice brix, headspace pressure and pressure difference.

Table 19 shows the allocation of the boiling patterns for the HTC_{max} results from the *Original432* dataset.

Table 19 Boiling pattern allocation for HTC_{max} results from *Original432* dataset

Boiling pattern	Percentage of data in this category
Uniform	18.5
Non uniform; low HTC at top	30.6
Non uniform; low HTC at bottom	28.7
Non uniform; low HTC at intermediate section	11.1
Non uniform; low HTC at top and bottom	1.9
Non uniform; low HTC at top and intermediate	5.6
No particular pattern	3.7

Table 20 presents a summary of the factors and interactions for the individual section HTC values corresponding to the overall HTC_{max} that were found to be significant at the 0.05 level. Brix was identified as a significant factor for all the sections. T_D:B:HS is identified as significant for sections 1, 2 and 3.

Table 20 Summary of significant factors and interactions for the individual section HTC_{max}
(Original432)

Tube section	Factor identified with significance level less than 0.05		
	Single parameter	2nd order interaction	3rd order interaction
Section 1	B, HS	$T_D:B, T_D:HS$	$T_D:B:HS, T_L:HS: \Delta P$
Section 2	B, HS, ΔP	$T_D:B$	$T_L:HS:\Delta P, T_D:B:HS$
Section 3	B	-	$T_D:B:HS$
Section 4	T_L, B	-	-

Thaval (2017) provides information on the interactions of the different tube dimensions and operating parameters on the HTC patterns. Both tube diameter and tube length were found to affect the individual HTC values for conditions corresponding to the overall HTC_{max} . For specific conditions, headspace pressure and pressure difference are also important factors affecting the HTC values of the individual sections for the tests corresponding to the HTC_{max} values.

6.3.7. Boiling mechanism

The various patterns of HTC values for the individual sections of the heating tube are attributed to variations in the boiling patterns for the juice within the tube. Thaval (2017) determined that for the test conditions which are typical of industrial Robert evaporators, annular flow did not exist in the single tube. The reason for this is because, as discussed in the next section, the highest overall HTC_{max} was obtained for the uniform HTC pattern and it would not be possible to produce annular boiling pattern in the bottom section of the tube. Annular boiling pattern occurs when the juice boiling pattern has progressed from vapour bubbles dispersed through the liquid phase (bubble/slug flow) to a phase where a core of vapour exists in the middle of the tube and a liquid layer and small bubbles are adjacent to the tube wall. Hence, it was postulated that bubble and slug flow were dominant in the single tube evaporator. Slug flow occurs when the vapour bubble dispersed through the liquid (bubble flow) coalesce to occupy a large proportion of the cross-section of the tube, but remain as separate bubbles. The HTC for bubble flow is lower than the HTC in the slug flow regime as the larger (slug) bubbles cause greater turbulence in the juice at the wall of the tube and hence increase the heat transfer rate. The presence of a sub-cooled liquid region in the base of the tube was dismissed since the juice entering the base of the heating tube was heated and should be close to the temperature for boiling at the headspace pressure. The only suppressing effect on boiling would be the hydrostatic head of the juice.

Table 21 presents the proposed boiling mechanisms for the various HTC patterns which have been identified. The term “dry out” is proposed here to describe the situation where the tube surface is not fully wetted by liquid.

Table 21 Proposed boiling regimes for boiling patterns

Boiling pattern	Section 1	Section 2	Section 3	Section 4
Uniform boiling	Bubble/slug	Bubble/slug	Bubble/slug	Bubble/slug
Low HTC at top	Dry out	Bubble/slug	Bubble/slug	Bubble/slug
Low HTC at bottom	Bubble/slug	Bubble/slug	Bubble/slug	Bubble
Low HTC at intermediate	Bubble/Slug	Not known	Not known	Bubble/slug

The two dominant flow regimes in the single evaporator tube, and most likely in industrial rising film tube evaporators, are bubble and slug flow. Low HTC at the bottom is likely associated with high hydrostatic head (e.g. long tubes) while low HTC at the top of the tube most likely indicates drying out (probably intermittent drying out) of the tube surface i.e. insufficient wetting. No mechanism was proposed to describe the circumstance with low HTC at an intermediate section. The literature indicates that this pattern may exist for certain heat exchangers where temperature differences are very high e.g. >100 °C and vapour blanketing can occur (Hong Chae Kim et al., 2000). However, these conditions do not exist in sugar juice evaporators and the mechanism is not evident.

While the proposed boiling mechanisms relate to the single heating tube used in the experimental rig the proposed boiling mechanisms are likely to provide a reasonable description of the boiling mechanisms in industrial vertical tube rising film evaporators. One cause of any differences, if they exist, between the boiling patterns for the single tube and the tubes in an industrial evaporator is the influence of a potentially larger juice quantity in industrial evaporators pooling above the tube plate, thus affecting the juice flow rising in an individual tube. For the single tube evaporator rig the downtime was closer on average than the average distance between heating tubes and downtakes in industrial evaporators, thus reducing the potential pooling of juice above the tube plate.

It is to be noted that the effect of gutters on the outside of the tube may slightly influence the boiling patterns. The boiling patterns of industrial tubes when a thicker condensate layer would exist at the base of the tube may show a slightly different boiling pattern, resulting from a slightly lower HTC at the bottom of the tube.

6.3.8. Boiling patterns that provide superior heat transfer performance

Table 22 presents the average overall HTC_{max} values for the four dominant boiling patterns for Brix-20 (1st effect), Brix-35 (3rd effect) and Brix-70 (5th effect). The uniform boiling pattern shows the highest HTC_{max} for all the three brix values. The pattern with low HTC at the bottom provides the next highest average overall HTC_{max} values followed by the pattern with low HTC at an intermediate position. These two patterns provide reasonably similar average overall HTC_{max} values. The boiling pattern with low HTC at the top shows the lowest HTC_{max} values for all the three brix. Thus boiling conditions that result in a low HTC at the top section are the least favoured.

Table 22 Average HTC_{max} for different boiling patterns at three brix

Boiling pattern	% of results	Brix-20	Brix-35	Brix-70
Uniform boiling	18	4593	2899	512
Low HTC at top	31	2431	1701	370
Low HTC at bottom	29	3939	2616	468
Low HTC at intermediate	10	3733	2443	475

In general terms, uniform boiling conditions are more likely to be established for boiling at Brix-20 with high headspace pressure. Uniform boiling appears to form in the tubes of all three diameters. For tubes of 38.1 mm diameter, tubes of 4 m length produced uniform boiling whereas for tubes of 44.45 mm and 50.8 mm diameter uniform boiling was more likely to be achieved with the shorter tubes.

The second favoured boiling pattern having low HTC at the bottom was likely to be established for all three brix values, and particularly for Brix-20 and Brix-70. Tubes S3, M3 and M4 were shown to be more likely to produce this boiling pattern at Brix-20. For Brix-70, tubes with diameter 44.45 mm and 50.8 mm appeared more likely to produce this boiling pattern than the 38.1 mm tube. A higher pressure difference also enhanced the formation of this boiling pattern.

6.4. Selection of the optimum tube dimensions for the different effect positions

6.4.1. General comments

The selection of the optimum tube dimensions for a rising film tube evaporator at a particular effect position takes into account the heat transfer performance (HTC_{max}), the capital and installation costs and the operating costs (such as losses resulting from sucrose degradation and entrainment losses). The work undertaken in this project allows the optimum (preferred) tube dimensions for the 1st, 3rd and 5th effects in a quintuple set to be determined and, by inference, the preferred tube dimensions for the 2nd and 4th effects.

6.4.2. Favoured tubes based on HTC_{max}

Figure 19, Figure 20 and Figure 21 show the HTC_{max} results for the nine tube dimensions for the typical operating conditions corresponding to Brix-20, Brix-35 and Brix-70 respectively. Each data value shown in Figure 19 to Figure 21 is the average of the HTC_{max} values for two headspace pressures and two pressure differences, *i.e.*, the average of the four ΔT values for the tests at the nominated juice brix. These figures show which tubes provide good and poor heat transfer performance for the typical conditions for the 1st, 3rd and 5th effect positions in a quintuple set.

It is evident from Figure 19 for Brix-20 (1st effect) that tubes of small and medium diameter (38.1 and 44.45 mm) show high HTC_{max} values and tubes M2, S2, M3, S3 and S4 provide HTC_{max} values close to or above 4000 W/m²/K. It is seen that tubes with large diameter (50.8 mm) provide consistently lower HTC_{max} values than tubes with 38.1 and 44.45 mm tube diameter, for all the tube lengths. The lowest HTC_{max} value is for the L4 tube.

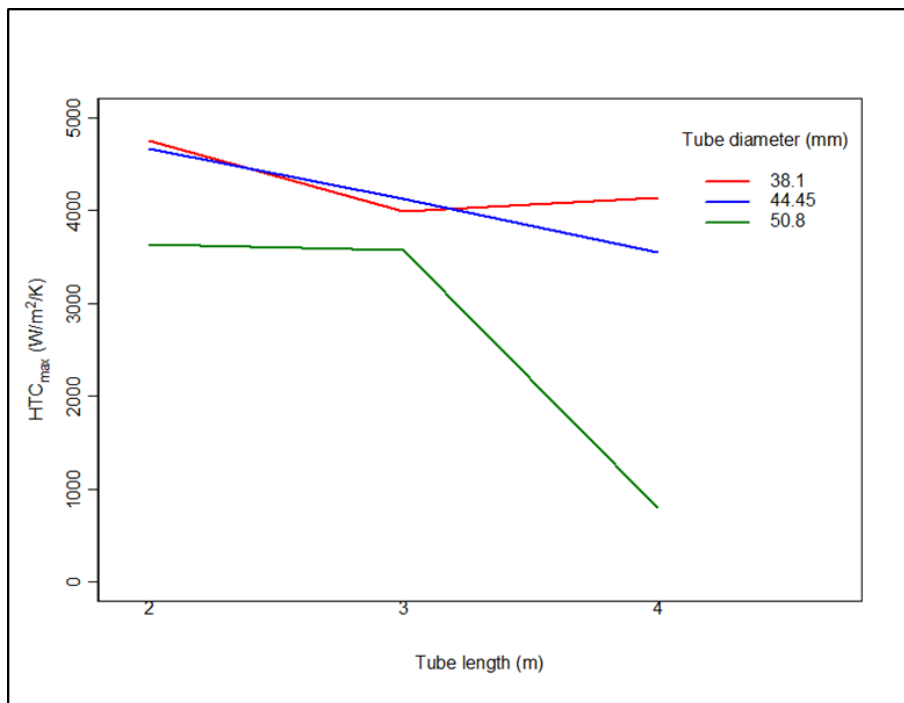


Figure 19 Influence of tube length and tube diameter on HTC_{max} for Brix-20

Figure 20 shows the HTC_{max} results for Brix-35 (3rd effect). This result is somewhat confounding. The reason for the variable data for the tubes of 38.1 mm diameter with different length is not known. Compared to the M2 tube dimensions (traditional tube), M3, S3, and M4 tube dimensions show higher HTC_{max}. Tubes S4 and L4 show very poor heat transfer performance.

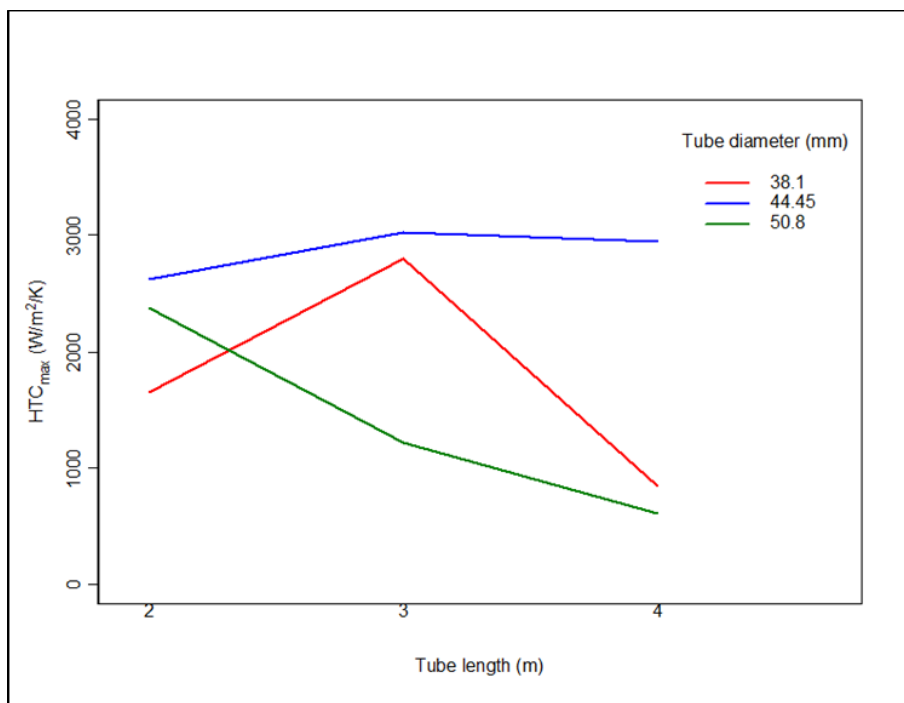


Figure 20 Influence of tube length and tube diameter on HTC_{max} for Brix-35

Figure 21 shows that for Brix-70 (5th effect), tube dimensions giving the highest HTC_{max} are M2 and L2. Tube lengths of 3 and 4 m result in very low HTC_{max} . Tube L4 provides very poor heat transfer performance for juice at Brix-70.

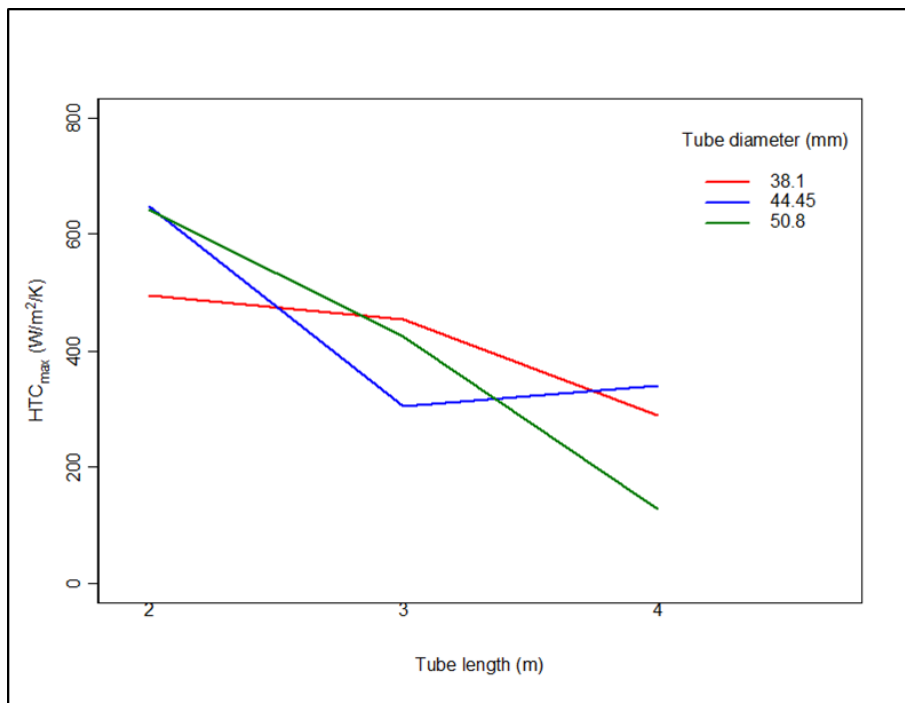


Figure 21 Influence of tube length and tube diameter on HTC_{max} for Brix-70

Table 23 shows those tube dimensions which provided good heat transfer performance for each effect position and the average HTC_{max} value for those tubes. Also shown in Table 23 is the ratio of HTC_{max} to the HTC_{max} value for M2.

Examination of the data in Table 23 shows that for the 1st effect M2 and S2 have the highest HTC_{max} , for the 3rd effect M3 and M4 have the highest HTC_{max} and for the 5th effect M2 and L2 have similar HTC_{max} values. Each of the tubes shown in Table 23 is considered appropriate to achieve good heat transfer performance at the nominated processing conditions. The traditional M2 tube has shown good heat transfer performance for each effect position.

Table 23 Favoured tubes based on HTC_{max} for 1st, 3rd and 5th effect positions

Effect number	Tube with good heat transfer performance	Average HTC_{max} value (W/m ² /K)	Ratio of HTC_{max} to HTC_{max} for M2
1	M2	4660	1.00
	S2	4740	1.02
	M3	4240	0.91
	S3	3990	0.86
	S4	4140	0.81
3	M2	2620	1.00
	M3	3030	1.16
	S3	2800	1.07
	M4	2950	1.13
5	M2	650	1.00
	L2	640	0.98

6.4.3. Capital costs for constructing and installing Robert evaporators using tubes of favoured heat transfer performance

The capital costs of evaporators comprising the favoured tube dimensions as shown in Table 23 are calculated using the cost model described in section 6.1. In order to account for the differences in heat transfer performance as defined by HTC_{max} , the areas of the vessels were selected so that $HTC_{max} \times$ heating surface area (HSA) is constant for a nominated HSA for an M2 evaporator. Thus the evaporators with the different tube dimensions would have the same evaporation capacity, for a given ΔT .

The cost analysis from section 6.1 was undertaken in more detail for the favoured tubes for evaporators of 2000 m² and 5000 m² (based on evaporators with M2 tubes). The areas of the respective vessels for the favoured tubes, having the same $HTC_{max} \times$ HSA as for the M2 evaporator, are shown in Table 24 for M2 evaporators of 2000 and 5000 m².

Table 24 Heating surface areas of the respective vessels for the favoured tubes for 1st, 3rd and 5th effect positions

Effect number	Tube with good heat transfer performance	HSA for 2000 (m ²)	HSA for 5000 (m ²)
1	M2	2000	5000
	S2	1960	4900
	M3	2200	5490
	S3	2330	5810
	S4	2250	5620
3	M2	2000	5000
	M3	1720	4310
	S3	1870	4670
	M4	1770	4420
5	M2	2000	5000
	L2	2040	5100

The basis of costs for labour, materials, designs etc. were discussed in section 6.1. Figure 22 shows the materials and labour costs for evaporators with the favoured tubes for the 1st, 3rd and 5th effect positions relative to the M2 evaporator. The costs of materials for the 1st effect position are higher for small diameter and long tubes. This result is due to the increased heating surface areas of the vessels with small diameter and long tubes, compared with the M2 tube dimensions. However, the labour costs are reduced up to 20% for vessels comprising small diameter and long tubes due to the smaller vessel diameter and fewer tubes to be installed.

For the 3rd effect position, the materials and labour costs both show a reduction of ~20% for vessels with medium diameter and long tubes. For the 5th effect position, the M2 tube dimensions show lower materials and labour costs than for an evaporator with the L2 tube dimensions.

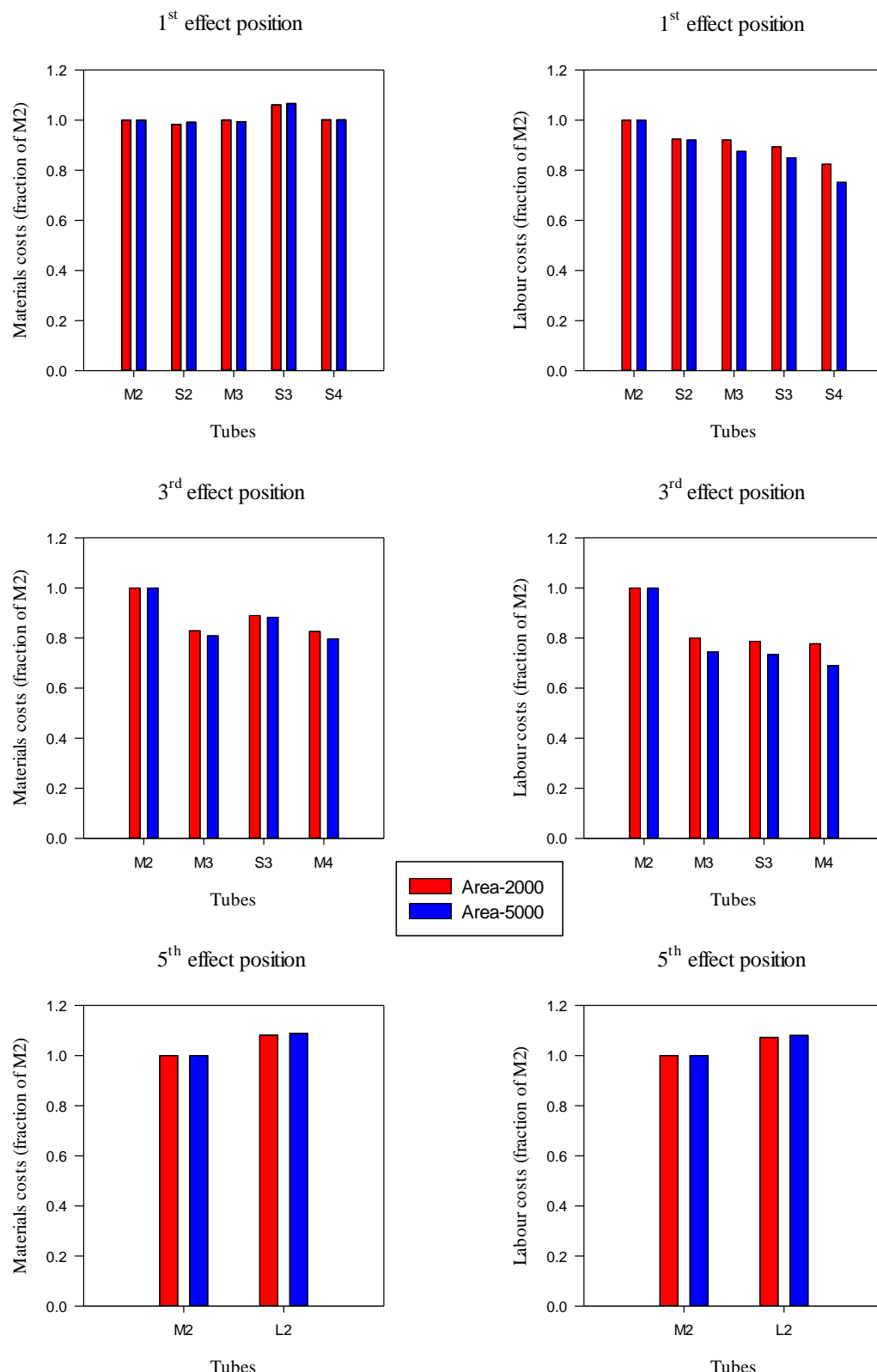


Figure 22 Materials and labour costs for evaporators with favoured tubes dimensions for 1st, 3rd and 5th effect positions

Section 6.1 did not consider the installation costs such as foundations and supporting structure and insulation costs. Details of these costs for evaporators comprising the favoured tube dimensions for the 1st, 3rd, and 5th effect positions are provided in Appendix 11.2.

Table 25 and Table 26 provide design details and total costs of the evaporators with the favoured tube dimensions having equivalent heat transfer performance to 2000 m² and 5000 m² evaporators with M2 tubes respectively. The juice level in the tubes is the optimum level determined from the experimental investigations (see section 6.2.16). The optimum juice level affects the juice level intensity (juice volume per m² of HSA).

The data in Table 25 and Table 26 show that, at the 1st and 3rd effect positions, the diameter of the vessel is reduced by ~18% and the mass on foundations reduced by ~20% when S3 tube dimensions are used compared to the conventional M2 tube dimensions. The juice level intensity is reduced by ~40% with S3 tube dimensions compared with using the M2 tube. These reductions are even greater when S4 tube dimensions are used.

Table 25 Details of the evaporator vessels with the favoured tube dimensions to equate to the heat transfer performance of a 2000 m² HSA M2 evaporator

Effect	Code	Area (m ²)	No. of tubes	Vessel ID (m)	Optimum juice level in tubes	Design vessel weight (t)	Juice intensity, (L/m ²)	Total cost (M AUD)
1	M2	2000	7590	5.78	35%	322	9.27	1.28
	S2	1960	8770	5.34	33%	278	7.56	1.21
	M3	2200	5574	5.02	35%	279	7.34	1.21
	S3	2330	6986	4.80	30%	259	5.76	1.23
	S4	2250	5024	4.15	28%	221	4.71	1.14
3	M2	2000	7590	5.78	56%	322	11.65	1.28
	M3	1720	4354	4.49	60%	225	10.07	1.03
	S3	1870	5578	4.35	50%	214	7.58	1.05
	M4	1770	3374	4.01	47%	205	7.72	1.01
5	M2	2000	7590	5.78	40%	322	9.83	1.28
	L2	2040	6718	6.20	70%	366	15.24	1.37

Table 26 Details of the evaporator vessels with the favoured tube dimensions to equate to the heat transfer performance of a 5000 m² HSA M2 evaporator

Effect	Code	Area (m ²)	No. of tubes	Vessel ID (m)	Optimum juice level in tubes	Design vessel weight (t)	Juice intensity, (L/m ²)	Total cost (M AUD)
1	M2	5000	18986	8.89	35%	762	10.35	2.58
	S2	4900	21900	8.20	33%	652	8.40	2.46
	M3	5490	13890	7.67	35%	642	7.91	2.39
	S3	5810	17304	7.32	30%	593	6.20	2.44
	S4	5620	12576	6.31	28%	496	4.99	2.22
3	M2	5000	18986	8.89	56%	762	12.73	2.58
	M3	4310	10920	6.85	60%	512	10.53	1.99
	S3	4670	13924	6.62	50%	485	7.98	2.06
	M4	4420	8432	6.06	47%	453	7.96	1.89
5	M2	5000	18986	8.89	40%	762	10.91	2.58
	L2	5100	16814	9.55	70%	874	16.59	2.80

For the 1st effect position cost savings of between 4 and 10% are indicated by using evaporators with favoured smaller diameter and/or longer tubes compared with evaporators with the M2 tube.

Larger cost savings (18 to 20%) are indicated for evaporators with the favoured smaller diameter and/or longer tubes at the 3rd effect position because of the superior HTC_{max} of these tubes relative to the M2 tubes at the 3rd effect. For the 5th effect position the evaporator with the M2 tube is the lower cost option.

6.4.4. Selection of optimum tube dimensions

Basis of selection

Many factors are considered by factory management in selecting the appropriate tube dimensions including heat transfer performance, installed cost, access to site for installing the evaporator (crane hire etc.), availability of replacement tubes, potential sucrose degradation, potential entrainment of juice in the vapour flow and perceived risk in departing from previously used tube dimensions. If the assessment is based largely on installed cost, given appropriate heat transfer is achieved and the other factors are acceptable, then the data in Table 25 and Table 26 indicate that evaporators with S4, M4 and M2 tubes are preferred for the 1st effect, 3rd effect and 5th effect respectively. This result applies to both the 2000 m² and 5000 m² vessels.

Discussions with Australian factory staff indicated that there is stronger interest in using 3 m long tubes rather than 4 m long tubes in future installations of Robert evaporators. There are two main reasons for this viz., (1) use of 4 m long tubes would be a major departure from the traditional 2 m long tubes, and (2) the up flow vapour velocity for the same VCC would be more than double compared with that for the M2 tube which is likely to cause overloading of the juice de-entrainment louvres within the vessel, as discussed in section 6.1.7. The industry already has a few Robert evaporators with 38 mm diameter tubes at the 1st effect position (Watson, 1986) and at Millaquin and Rocky Point Mills and so the use of smaller diameter tubes at the 1st effect and 3rd effect positions is likely to be perceived as low risk.

It is for these reasons that the interest from the industry for future installations into Robert evaporators will be in comparing S3 and M3 tubes with the traditional M2 tubes.

Estimates of capital cost savings

Table 27 shows the cost savings in using S3 and M3 tubes in the 1st and 3rd effect positions relative to using evaporators with M2 tubes. For the 5th effect, the M2 tube dimensions are preferred based on both the HTC and capital costs.

Table 27 Estimate of cost savings from using S3 and M3 tubes in Robert evaporators at the 1st effect and 3rd effect instead of using a Robert evaporator with M2 tubes

Tube dimensions	Saving in installed cost relative to cost of M2 evaporator (AUD)	
	1 st effect	3 rd effect
2000 m² HSA		
S3	48,000	222,000
M3	61,000	245,000
5000 m² HSA		
S3	139,000	519,000
M3	188,000	591,000

The cost savings for the S3 and M3 tubes relative to the M2 tubes are substantially greater for the 3rd effect than for the 1st effect because the heat transfer performance of S3 and M3 tubes in the 3rd effect is superior to that for the M2 tubes. For the 1st effect the S3 and M3 tubes provide slightly inferior heat transfer performance than the M2 tubes but overall the savings on installation costs of the S3 and M3 tubes outweigh the influence of slightly inferior heat transfer performance. The cost savings from using S3 tubes instead of M2 tubes are ~5% for the 1st effect and ~20% for the 3rd effect. The cost savings are greater for the M3 tubes than for the S3 tubes at both the 1st and 3rd effect positions. As expected the cost savings are greater for the evaporator of larger HSA.

Estimates of operating cost savings

For the use of S3 and M3 tubes at the 1st and 3rd effects de-entrainment of juice from the up flow vapour should be able to be effectively achieved using conventional louvre systems located within the head space of the evaporator. The cross-sectional area available in the top of the evaporator should be sufficient to install the required area of de-entrainment louvres. Hence, for most practical applications, the de-entrainment of juice should be managed adequately for similar costs compared to the M2 evaporator.

Under certain circumstances sucrose degradation during juice evaporation can be a major operational cost, resulting in a loss of revenue for the factory.

The extent of sucrose degradation that occurs in the juice evaporation process is a function of the juice conditions (pH, temperature and brix) and the residence time (Vukov, 1965). The evaporation conditions that are likely to experience large sucrose losses are where high levels of steam economy are sought, e.g., where extensive vapour bleeding is undertaken and where the process steam pressure is high. Several studies have shown that under these conditions the majority of sucrose degradation that occurs during evaporation is in the first evaporation stage (Purchase, et al., 1987; Schaffler, et al., 1985; Rackemann and Broadfoot, 2017). Sucrose losses should be low (<0.1% of

sucrose in clarified juice) when minimal vapour bleeding is undertaken and the process steam pressure is 200 kPa abs or lower.

As noted in Table 25 and Table 26, Robert evaporators with different tube dimensions have markedly different juice hold up volumes per m² of HSA. Evaporator vessels with lower juice volume intensities will provide shorter residence times for the juice and hence experience reduced sucrose loss through hydrolysis.

Using the correlation developed by Vukov (1965), the sucrose losses in a 1st effect evaporator have been calculated for evaporators with the favoured tube dimensions, based on the evaporation capacity being equivalent to that of a 5000 m² M2 evaporator. The results and the assumed processing conditions are shown in Table 28. For the assumed conditions the vapour loading would be 24 kg/h per m² of HSA. The average juice residence time in each evaporator is calculated for operation at the optimum juice level (see Table 26). In all cases, due to the smaller juice holdup volume than for an M2 evaporator, the calculated sucrose loss is less than for the M2 evaporator.

Table 28 also shows the estimated increase in annual revenue that would be expected for an Australian factory utilising a 5000 m² evaporator at the 1st effect in an energy efficient plant. It was assumed that the cane/sugar mass ratio is 7 (typical of Australian factories), the annual crop is 1.3 million t of cane, sugar price is AUD 400 per t, molasses price is AUD 120 per t, and final molasses is of 45 purity and 78 dry substance. The values of the discounted increases in revenues for a 10 year period (using a discount rate of 15%) from reduced sucrose losses relative to using a M2 evaporator are also shown in Table 28.

These results demonstrate that for a factory intending to use Robert evaporators at the 1st effect in a situation where a large HSA is required to suit vapour bleeding arrangements and a high boiling temperature will be used, serious consideration should be given to using smaller diameter and longer tubes than M2, e.g., S3 or S4.

Table 28 Sucrose degradation and operating cost savings for a 5000 m² evaporator

Process conditions for 1st effect:

Juice inflow: 425 m³/h, 90 purity, 16 brix

Conditions in vessel: 22 brix, 119 °C and pH 6.8 at 20 °C

Parameter	M2	S2	M3	S3	S4
Residence time, min	10.1	8.0	8.4	7.0	5.4
Predicted sucrose degradation (%)	0.40	0.32	0.34	0.28	0.22
Annual saving in reduced sucrose loss relative to the loss for a M2 evaporator (AUD)		75,000	56,000	112,000	168,000
Discounted value* over 10 years of increased revenue due to reduced sucrose loss relative to the loss for an M2 evaporator (M AUD)		0.45	0.34	0.67	1.01

* Discount rate of 15% per annum

Selection of the optimum tube dimension

New Robert evaporator vessels comprising S3 and M3 tubes provide installation costs savings of 5 to 7% at the 1st effect and 20 to 22% at the 3rd effect compared with an M2 Robert evaporator, for the

same evaporation capacity. While S4 tubes at the 1st effect and M4 tubes at the 3rd effect are well suited to these applications, providing good heat transfer performance and would provide greater cost savings, Australian mills are unlikely to utilise a 4 m long tube in a Robert evaporator. Thus S3 and M3 tubes are the favoured tubes for the 1st and 3rd effects from a cost and heat transfer point of view.

The S3 and M3 tubes are also recommended for the 2nd effect on the basis that the operating conditions for the 2nd effect are intermediate between the conditions for the 1st and 3rd effects.

For the installation of a Robert evaporator at the 1st effect in a factory seeking to reduce the process steam consumption to a low level, major operational cost savings are achieved for evaporators with S3 and M3 tubes compared to an evaporator with M2 tubes, owing to the lower juice volume intensity of the evaporators with the S3 and M3 tubes. Reduced sucrose degradation would occur in the 1st effect vessel as a result of the shorter residence time for the juice at the high boiling temperature. Use of an evaporator with S3 tubes provides a larger increase in revenue compared with the use of the M3 tubes because of the lower juice volume intensity.

For the 5th effect a Robert evaporator with the traditional M2 tube is favoured. The M2 tube is also recommended for the 4th effect as for many evaporator stations, particularly for the steam efficient configurations, the brix of juice in the 4th effect is quite high (e.g. 60 brix) and so the processing conditions are not markedly different from those for the 5th effect.

6.4.5. Retrofitting a calandria into an existing evaporator

Introductory remarks

When an evaporator station requires the installation of additional area the usual procedure is to install another evaporator at the appropriate position or to replace an existing evaporator with a new vessel of larger HSA to debottleneck the capacity. However, consideration should be given to whether it may be feasible to replace the calandria comprising M2 tubes of an existing evaporator with a calandria having favoured tubes being longer or of smaller diameter. The experimental investigations have shown that this change could be feasible at the 1st to 3rd effect positions. Obviously retrofitting a new calandria is only feasible if the remainder of the vessel body has adequate service life.

Practical considerations of retrofitting a calandria

When factories are upgrading the evaporator station to increase the capacity and/or changing the configuration to suit increased steam efficiency, larger heating surface areas are required. When increased steam efficiency is being sought the additional area will likely be placed in the effects upstream of the effect from which maximum vapour bleeding is undertaken. In most scenarios the additional area is required in one, or perhaps two, of the first three effects in a quintuple set. In these circumstances retrofitting of a new calandria into an existing vessel may be feasible.

If a calandria is to be replaced with one of larger heating surface area, smaller diameter and/or longer tubes would be used. Some additional practical matters have to be considered.

When an existing calandria is replaced with a new calandria comprising longer tubes, the height of the vessel will most likely be increased in order to retain de-entrainment efficiency. It is preferable to retain the base of the vessel at its current position, and consequently the top cone and vapour offtake pipe will be raised. These costs must be taken into account in the financial assessment to determine the viability of the retrofit. If the top of the headspace cannot be lifted due to height limitations, lowering the bottom remains the only option. In most cases this option will be feasible if

the evaporators are located at a sufficient elevation above the ground floor level. Consideration will need to be given to the transfer of the juice from one vessel to the next due to the different elevation of the juice operating level and base of the retrofitted evaporator.

Retrofit options

Design calculations have been undertaken for typical 2000 m² and 5000 m² Robert evaporators comprising M2 tubes (internal diameters of vessels being 5.78 and 8.89 m respectively) being replaced with calandrias using S3 and M3 tube dimensions, with the pitch of tubes set at the minimum according to Australian Standards for a pressure vessel. For this retrofit the top of the vessel would be 1 m higher. The HSAs for the retrofitted evaporators are shown in Table 29.

Table 29 Evaporator heating surface details for retrofit options

Original HSA of M2 evaporator	Details of evaporator with S3 tubes		Details of evaporator with M3 tubes	
	Number of tubes	HSA (m²)	Number of tubes	HSA (m²)
2000	10430	3500	7590	3000
5000	26034	8740	18986	7500

The data in Table 29 show that using S3 tubes the HSA is increased by 75% and using M3 tubes the HSA is increased by 50%. These are large increases in area and would be sufficient to suit most applications for a retrofit. If a smaller increase in area is required then it would be feasible to increase the pitch of the tubes (resulting in fewer tubes being installed) or reducing the height of the tubes (*e.g.* use 2.8 m tubes).

Further design considerations

The large increases in area that can be achieved by retrofitting S3 or M3 tubes will increase the vapour rate from the vessel substantially. Most likely, increased area for the de-entrainment louvres will be needed. Retrofitting a calandria at the 3rd effect position with S3 tube dimensions (previous one being M2 tube) would result in higher HTC with an enhanced area. In such cases, increasing the strake height further than the suggested 1 m and providing more louvre area may be necessary to avoid entrainment of juice. If these options are not sufficient, more efficient louvres designs must be installed.

6.5. CFD modelling results

6.5.1. Description of the CFD model and assumptions

The detail of the models is shown in Appendix 11.3. The experimental data from Thaval (2017) for the three cases which were used for the modelling are detailed in Appendix 11.4.

The modelling was carried out with the ANSYS CFX software. Steady state modelling was performed, that is, the simulation was not progressed in time via a transient simulation. A pseudo time step was used to allow convergence of the solution. Therefore, the modelling was aimed at simulating the steady state behaviour observed in the experimental tests. The volume fractions of juice and vapour were defined at the beginning of the simulation in order to define the static juice height, with corresponding pressures defined along the tube height. A Eulerian multi-fluid approach was used with three fluids defined as:

- a. A liquid (water) which could evaporate, modelled as a continuous fluid.
- b. A 'brix' liquid dispersed as globules in the water, i.e. a dispersed fluid, with a given globule diameter. The 'brix' liquid could not evaporate.
- c. A gaseous vapour modelled as a dispersed fluid with a given bubble diameter. The vapour could condense and become water.

Heat transfer was allowed to occur between the three fluids, as well as mass transfer between the water and the vapour for evaporation.

Consistent with the experimental testing, any vapour that exited the top of the tube was returned to an inlet at the bottom tank, as water at the same mass flow rate, and at the temperature of the bulk water in the tank. Any water and 'brix' liquid that exited the top of the tube was also returned at the same mass flow rate, and at the temperature of the bulk water in the tank. This was not fully consistent with the temperature of the juice that may have flowed out of the tube and back into the tank in the physical experiments. However, the temperature difference would be small and not expected to significantly affect the bulk temperature of the tank fluid volume.

Another difference from the experimental arrangement is that the top of the tube is modelled as an outlet (which would show the net transfer of fluid), whereas in reality some juice that is ejected from the top of the tube from the ebullition process may also fall back into the tube (or accumulate around the top of the tube and drain into the tube).

The heat transfer was calculated by the CFD simulation using the tube wall temperature which was calculated from the saturated steam pressure and was an input to the CFD model.

The RPI (Rensselaer Polytechnic Institute) (Kurul and Podowski, 1991) model was used as the base wall boiling model. This is the same base model used by Stephens (2001) for modelling natural circulation and ebullition in sugar vacuum pans, as well as currently used for modelling boiling flow in tubes of nuclear plants (Hohne et al., 2017).

Gravity and buoyancy were modelled.

6.5.2. Results of the CFD modelling

Appendix 11.3 shows that the CFD simulations reach steady state quickly (within half an hour). Ideally lower residual¹ values (see the convergence response data) are desired; however lower values may not be possible for the boiling simulations where the dynamic multiphase conditions are averaged to provide a steady state solution. The residual is also directly linked to the size of the mesh elements (error is linked to the iterative variation in properties as the system of equations is solved across the distance between mesh elements) which inversely affects the simulation time.

The predicted vapour volume fractions for the three boiling cases are shown in Figure 23 to Figure 31.

Perusing the results, as a general conclusion, the predictions look promising but the detail of the mechanisms may not be sufficiently modelled with the Eulerian multi-fluid approach. In particular, there is almost always a high value of vapour volume fraction predicted adjacent to the tube wall, with an increasing volume fraction moving towards the middle of the tube as juice rises in the tube. That is, the formation of 'separate bubbles' and their movement away from the wall is not being explicitly or realistically modelled. As the results are 'time averaged' in a steady state simulation,

¹ The residual measures an iterative solution's convergence, as it quantifies the error in the solution of the system of equations.

transient simulations may be required to capture this bubble behaviour more accurately after an initial steady state has been achieved.

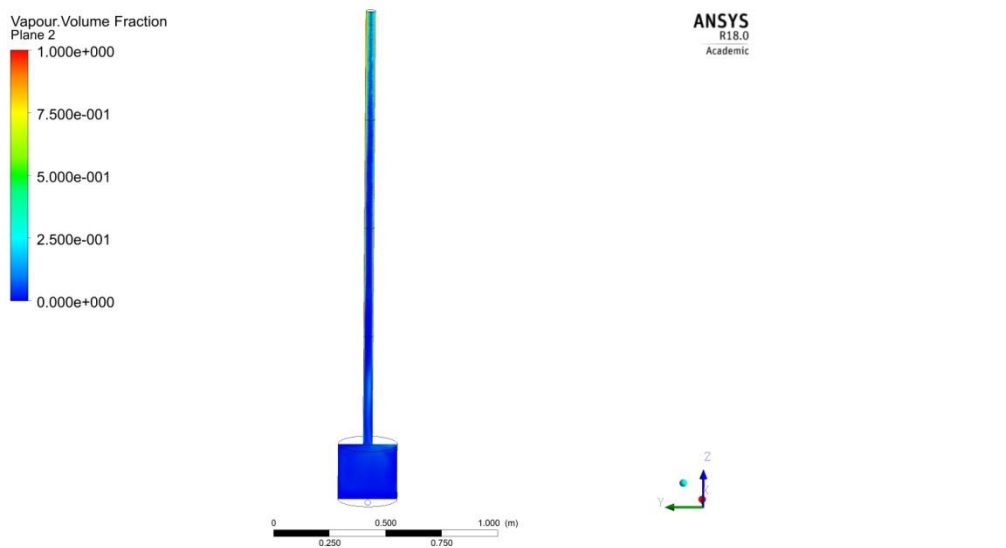


Figure 23 Predicted vapour volume fraction for uniform boiling case

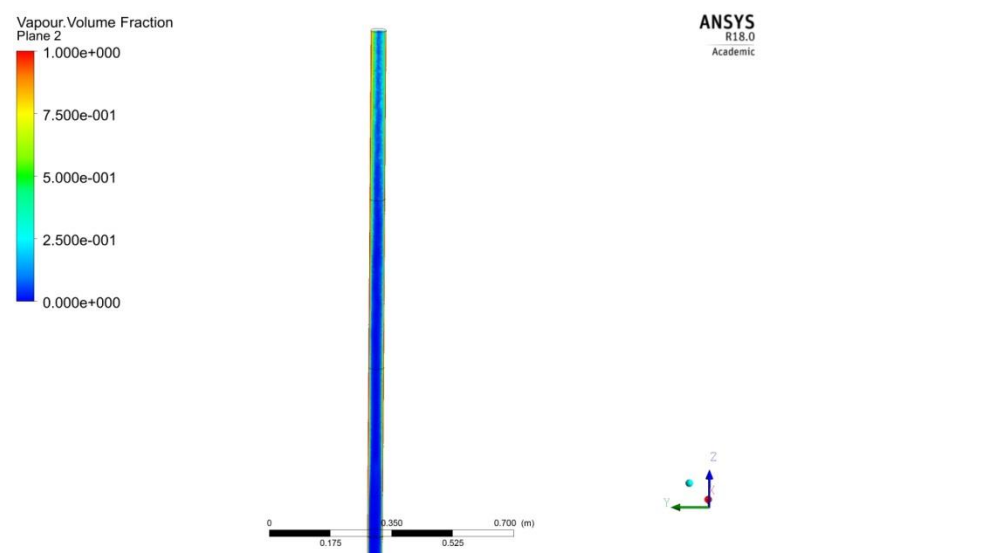


Figure 24 Predicted vapour volume fraction for uniform boiling case (detail for upper half of tube)

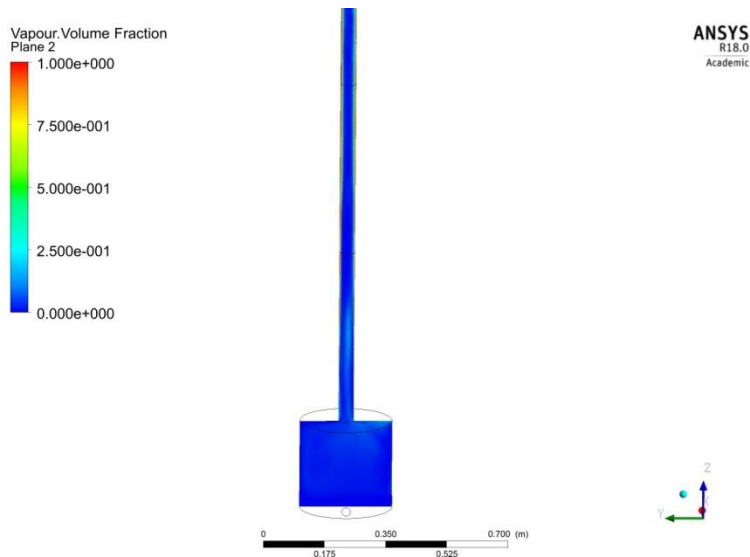


Figure 25 Predicted vapour volume fraction for uniform boiling case (detail for lower half of tube)

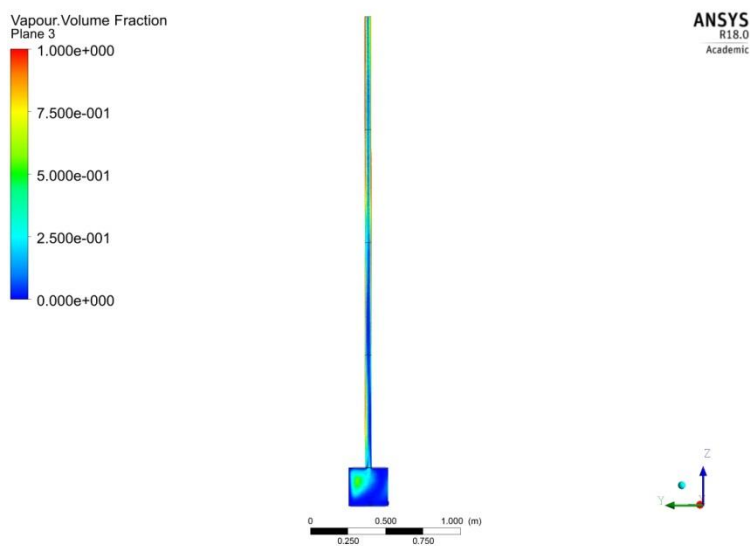


Figure 26 Predicted vapour volume fraction for low HTC at top case

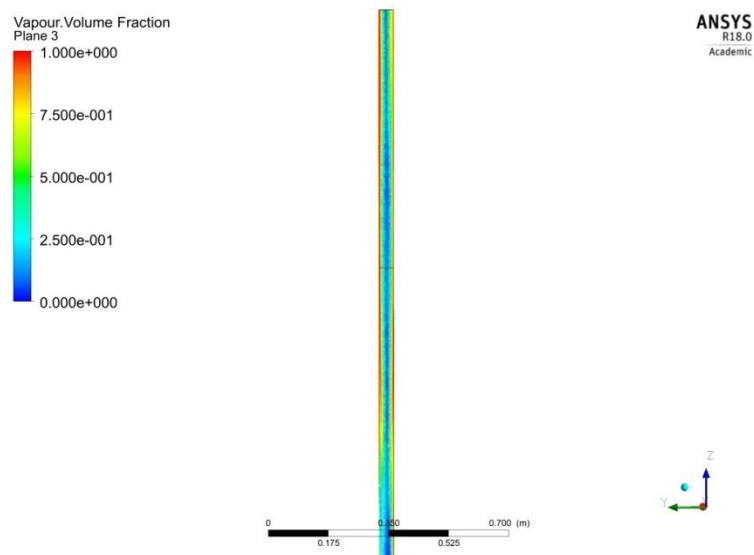


Figure 27 Predicted vapour volume fraction for low HTC at top case (detail for upper half of tube)

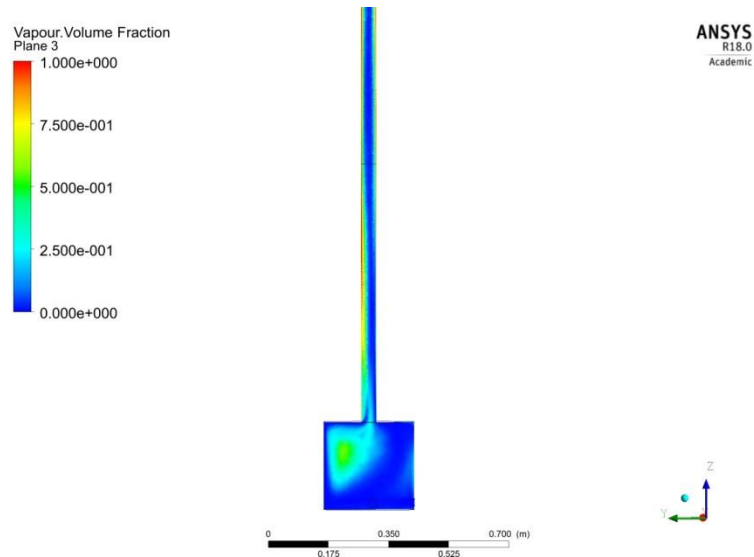


Figure 28 Predicted vapour volume fraction for low HTC at top case (detail for lower half of tube)

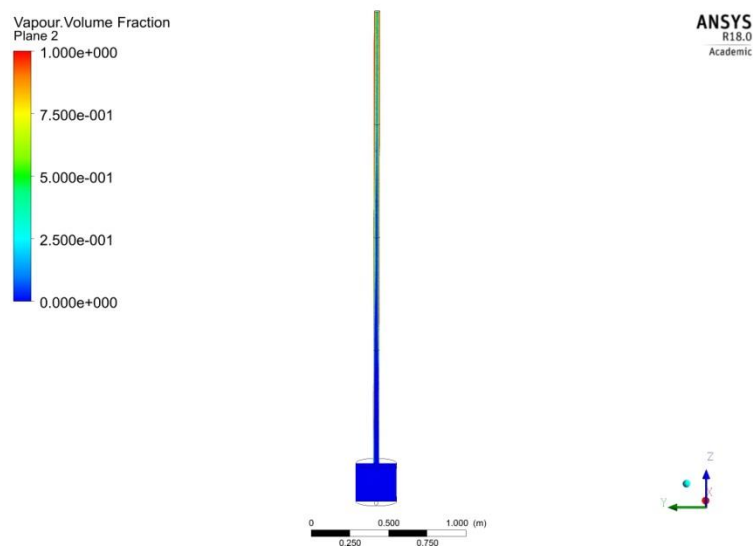


Figure 29 Predicted vapour volume fraction for low HTC at bottom case

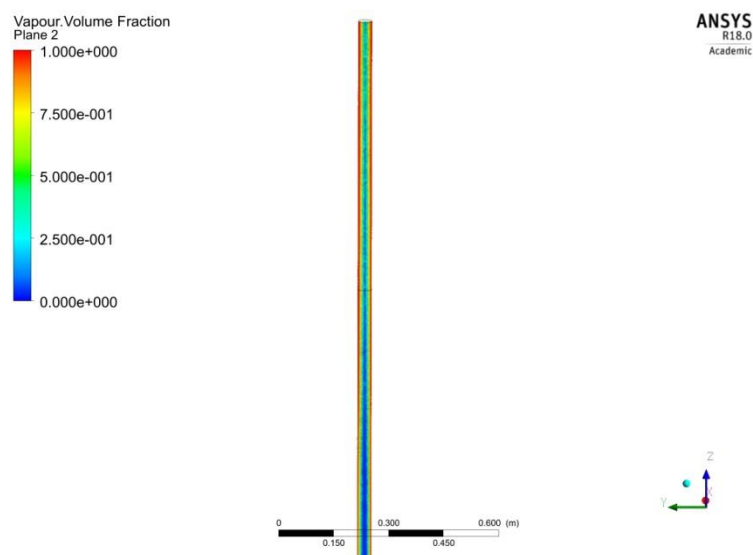


Figure 30 Predicted vapour volume fraction for low HTC at bottom case (detail for upper half of tube)

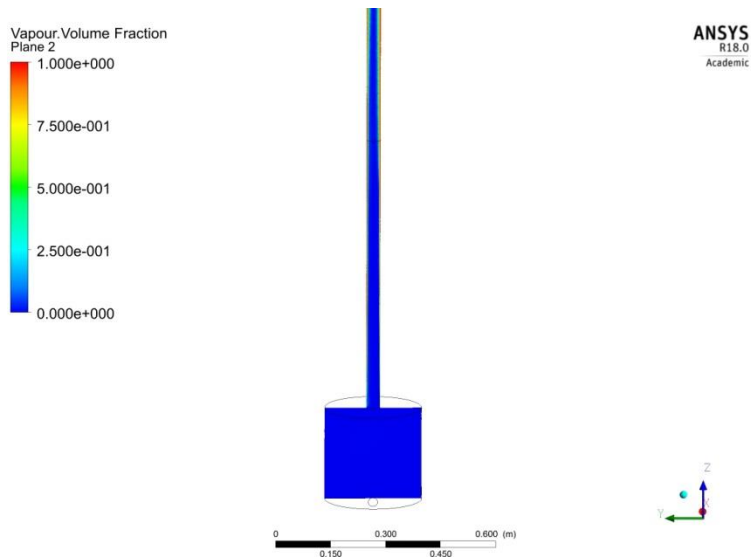


Figure 31 Predicted vapour volume fraction for low HTC at bottom case (detail for lower half of tube)

A comparison of the measured condensation rate to the predicted vapour flow rate out of the tube outlet is shown in Table 30. Table 30 also shows the predicted flow rates out of the tube outlet for liquid and 'brix' liquid. Although no comparison can be made to experimental values as they were not measured in the experiments, the predicted flow rates can provide an estimate of the tendency for juice to be dragged up the tube, i.e. the drag forces applied by the vapour flow to the juice, and may be useful in the future to validate the CFD models.

Table 30 Comparison of the measured condensation rate to the predicted vapour flow rate out of the tube outlet

Case	Measured heat transfer rate Steam condensation rate (kg/s)	Predicted tube outlet flows		
		Vapour	Liquid	'Brix' liquid
		(kg/s)	(kg/s)	(kg/s)
Uniform boiling pattern	0.003934	0.00304	0.412	0.175
Low HTC at top	0.000973	0.00391	5.814	3.334
Low HTC at bottom	0.002461	0.00403	0.417	0.0799

Although the predicted vapour flow (0.00304 kg/s) out of the tube for the uniform case agrees fairly well with the measured value (0.003934 kg/s), there is poor agreement between the measured and predicted rates with the other cases. The 'Low HTC at top' case (which is for the high brix of 70 which is expected to be harder to model) has a strange pattern predicted, where a vapour fraction is predicted inside the tank, therefore this prediction is likely to be incorrect.

6.5.3. Discussion on results of CFD modelling

The preliminary results are encouraging but show more extensive modelling is required to obtain confidence in the approach used for the CFD modelling. Further modelling is required to identify and validate the most appropriate techniques such as:

- Bubble size, bubble growth, coalescence and break up models, particularly with properties changing with height within the tube and hydrodynamic pressure. These models have a large and direct impact on the flow profile and hence heat transfer.
- Treatment of multiple fluids. Is the current dispersed phase approach for vapour and brix adequate?

A literature review on recent advances in modelling a boiling tube in other industries shows that there have been significant advances. In particular, a recent paper from the nuclear industry (Hohne et al., 2017) provides the modelling detail required to advance the modelling of the Thaval (2017) test results, to validating a model and identifying the detail of the boiling mechanisms corresponding to different heat transfer rates. Hohne et al. (2017) used CFX and the RPI model as its base wall boiling model; however a large amount of development of the sub-models was carried out. Similar work is required for the evaporator boiling tube. Some of the modelling for the evaporator is actually more complicated. For example, the absolute pressure has to be modelled in detail to provide accurate material properties, while in the nuclear application the absolute pressure is so high relative to localised fluctuations that the material properties can be considered constant. The work of Hohne et al. (2017) provides good information to be utilised in future modelling of rising film tube evaporators (and calandria tubes in vacuum pans) for future investigations.

7. CONCLUSIONS

The investigations have determined that tubes S3 and M3 are preferable for use in Robert evaporators at the 1st to 3rd effects and would result in cost savings of ~20% for new installations. These tubes also provide the benefit at the 1st effect position (and also at the 2nd effect) in steam efficient configurations of having smaller juice volumes than the traditional M2 tube and so would result in reduced sucrose loss through hydrolysis. The replacement of a calandria in an existing evaporator comprising M2 tubes with S3 or M3 tubes may also be a very cost effective way to increase the heating surface area substantially (e.g., by up to 75% using S3 tubes). For the 4th and 5th effect positions the traditional tube (M2) is favoured.

8. PUBLICATIONS

The following conference papers have been presented:-

Thaval OP, Broadfoot, R (2014). Capital cost model for Robert evaporators. *Proceedings of the 36th Annual Conference of the Australian Society of Sugar Cane Technologists*, Gold Coast, Australia.

Thaval OP, Broadfoot, R, Kent GA & Rackemann, DW (2016). Determining optimum tube dimensions for Robert evaporators. *Proceedings of the XXIX International Society of Sugar Cane Technologists Congress*, Chiang Mai, Thailand.

Thaval OP, Broadfoot, R & Kent GA (2017). Boiling mechanism in rising film vertical tube evaproator. *Proceedings of the Annual Convention of Sugar Technologists Association of India*, Kochi, India.

Two papers for the International Journal of Heat and Mass Transfer are being prepared.

9. ACKNOWLEDGEMENTS

The investigations in this project were undertaken by Omkar Thaval for his PhD thesis "Investigating the effect of tube dimensions and operating conditions on heat transfer performance in a rising film vertical tube evaporator". This thesis was undertaken at the Queensland University of Technology, Brisbane. Omkar is thanked for his effort and commitment to undertaking this study and completing the onerous experimental program.

The management and staff at Rocky Point Mill are thanked for hosting Omkar and the evaporator rig for the experimental trials. Particular thanks are extended to Mr Bruce Tyson and Mr Terry Drury.

The funding for the project which was provided by Sugar Research Australia Limited and Sugar Research Limited is gratefully acknowledged.

QUT staff who assisted in the project include Dr Floren Plaza (for CFD modelling studies), Mr Neil McKenzie (installation of the instrumentation and control systems on the evaporator rig) and Mr David Moller (assistance with commissioning the evaporator rig).

10. REFERENCES

The PhD thesis of Omkar Thaval contains the full list of references cited during the project. This list is not repeated here. The references provided here are the ones cited in this document.

Broadfoot, R & Dunn, KG 2007, 'Assessing the effect of juice properties and operating conditions on the heat transfer in Robert evaporators', In *Proceedings of the Australian Society of Sugar Cane Technologists*, Vol. 29, pp. electronic media.

Guo, SY, White, ET & Wright, PG 1983, 'Heat transfer coefficients for natural circulation evaporators', In *Proceedings of the Australian Society of Sugar Cane Technologists*, Vol 5, pp. 237-244.

Hong Chae Kim, Won-Pil Baek & Soon Heung Chang 2000, 'Critical heat flux of water in vertical round tubes at low pressures and low flow conditions', *Nuclear Engineering and Design*, 199, pp. 49-73.

Hohne, T, Krepper, E, Montoya, G, Lucas, D 2017, 'CFD-simulation of boiling in a heated pipe including flow pattern transitions using the GENTOP concept', In *Nuclear Engineering and Design* 322, pp. 165-176.

Hugot, E, & Jenkins, GH 1986, '*Handbook of cane sugar engineering*', Vol. 7: Elsevier.

Kurul, N, & Podowski, MZ 1991, 'On the Modeling of Multidimensional Effects in Boiling Channels', In *Proceedings National Heat Transfer Conference*, Vol 27, pp. 30-40.

Moller, D, Wagner, S, Broadfoot, R & Stephens, D 2003, 'Modification to the evaporator station in preparation for a co-generation factory at Broadwater mill', In *Proceedings of the Australian Society of Sugar Cane Technologists*, Vol. 25, pp. electronic media.

Peacock, SD 2001, 'Mathematical modelling of climbing film evaporators', Master of Engineering thesis, University of Natal, South Africa.

Purchase, BS, Day-Lewis, CMJ & Schaffler, KJ 1987, 'A comparative study of sucrose degradation in different evaporators'. In *Proceedings of the South African Sugar Technologists' Association*, Vol. 61, pp. 8-13.

- Rackemann, DW & Broadfoot, R 2017, 'Effect of operating conditions on sucrose losses in evaporators in Australian sugar factories', In *Proceedings of the Australian Society of Sugar Cane Technologists*, Vol. 39, pp. 435-444.
- Rose, I, Scroope, P & Broadfoot, R 2009, 'Reducing factory steam consumption for cogeneration at Condong Mill'. In *Proceedings of the Australian Society of Sugar Cane Technologists*, Vol. 31, pp. 420-429.
- Schaffler, KJ, Muzzell, DJ & Schorn, PM 1985, 'An evaluation of sucrose inversion and monosaccharide degradation across evaporators at Darnall Mill'. In *Proceedings of the South African Sugar Technologists' Association*, Vol. 59, pp. 73-78.
- Shah, S & Peacock, SD 2013, 'Recirculation rate for Robert evaporators', In *Proceedings of the South African Sugar Technologists' Association*, Vol. 86, pp. 334-349.
- Stephens, DW 2001, 'Studies on modelling circulation in sugar vacuum pans', PhD Thesis, James Cook University, Townsville, Qld.
- Thaval, O. & Broadfoot, R 2014, 'Capital cost model for Robert evaporators'. In *Proceedings of the Australian Society of Sugar Cane Technologists*, Vol 36, pp. 331-342.
- Thaval, O 2017, 'Investigating the effect of tube dimensions and operating conditions on heat transfer performance in a rising film vertical tube evaporator', PhD thesis, Queensland University of Technology, Brisbane, Qld.
- Vukov, K 1965, 'Kinetic aspects of sucrose hydrolysis', In *International Sugar Journal*, Vol.67, pp. 172-175.
- Watson, LJ 1986, 'Performance of the new Fairymead evaporator'. In *Proceedings of the Australian Society of Sugar Cane Technologists*, Vol. 8, pp. 223-230.
- Wright, P, Silva, A & Pennisi, SN 2003, 'The SRI evaporator-a new Robert design'. In *Proceedings of the Australian Society of Sugar Cane Technologists*, Vol. 25, pp. electronic media.
- Wright, PG 2008, 'Heat transfer coefficient correlations for Robert juice evaporators'. In *Proceedings of the Australian Society of Sugar Cane Technologists*, Vol. 30, pp. 547-558.

11. APPENDIX

11.1. Appendix 1 METADATA DISCLOSURE

Table 31 Metadata disclosure 1

Data	Data from experimental trials on the pilot evaporator rig Results of data analyses
Stored Location	QUT server for CTCB
Access	Restricted to CTCB staff
Contact	Ross Broadfoot/David Moller/Darryn Rackemann

11.2. Appendix 2 Installation costs for Robert evaporators with the favoured tube dimensions

Design weight and design costs

The design weight was calculated when the entire juice side of the vessel is filled with juice (density – 1.2 kg/m³) and the steam side is entirely filled with condensate. This weight plus the weight of the empty vessel is the total weight on the foundations. The juice side volume includes all tubes, mini-downtakes, central downtake, vapour space and one-third of the top cone. These considerations are essential to ensure the support columns can withstand the weight of the vessel if the condensate pump or the juice valve fails and the vessel fills with juice and/or condensate. Figure 32 shows the design weights for the evaporators with the favoured tubes for the 1st, 3rd and 5th effect positions relative to the M2 evaporator at these effect positions.

The design costs include the project management costs and profit margin. The calculation methodology for determining the project management costs and profit margin were described in Thaval & Broadfoot (2014) and discussed in section 6.1. As shown in Table 25 and Table 26, there is a substantial reduction in fabrication costs for small and medium diameters and long tubes for the 3rd effect positions.

All of the costing calculations were based on 2014 prices.

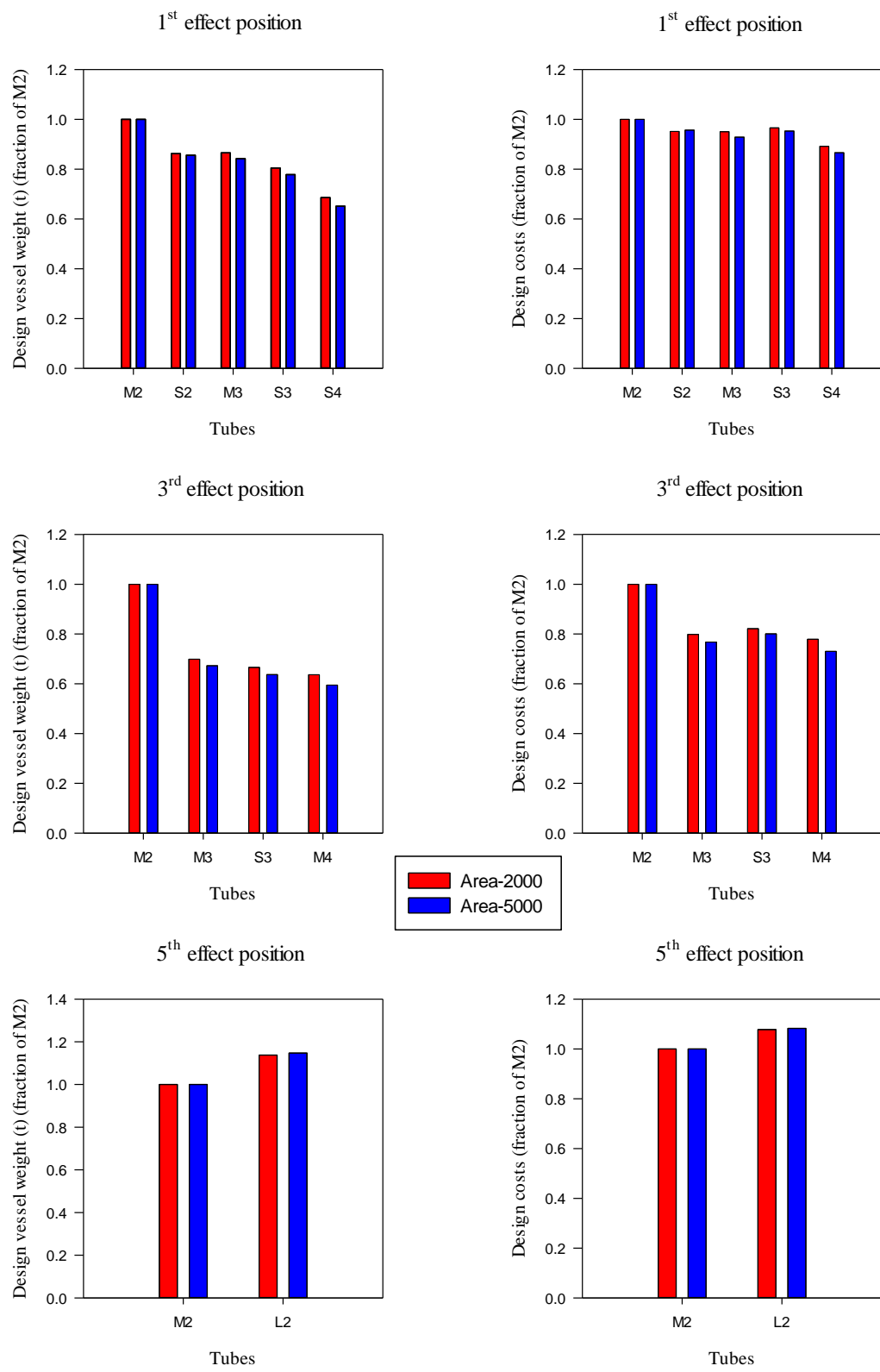


Figure 32 Design vessel weight and design costs for evaporators with the favoured tubes for 1st, 3rd and 5th effect positions

Foundation and structural costs

The foundations for the vessels were assumed to comprise a square pad of N32 concrete with sides equal in length to the diameter of the vessel plus one metre and a depth of 0.5 m. The reinforced steel mesh in the pad was assumed to be at three levels with spacing in each direction of 200 mm. The vessels are supported on universal beam pillars of dimensions 200 mm by 200 mm (weight 41 kg/m of length). The number of pillars required was based on each pillar being capable of supporting 96 t. The vessel weight used to calculate the number of supporting pillars was the mass on the foundations when the juice side is full of juice and the calandria is full of condensate. The minimum number of pillars used was six irrespective of weight of the vessel. For heavier vessels, the number of pillars was increased according to the calculation method above.

Table 32 shows the cost data for foundations and structure to support the evaporators. It was assumed that wastage of concrete, reinforced steel and pillars would be 6%. The labour requirement for preparation of the foundations, laying reinforced steel and filling with concrete was taken to be three man hours/tonne of steel.

Table 32 Cost data for foundations and structure to support the evaporator

Description of parameter	Value
N32 concrete for foundation	AUD 250 per m ³
Reinforced steel	AUD 4 per m
Universal beam pillar	AUD 240 per m
Wastage	6%
Labour requirement	3 man hours/tonne steel (preparation, laying reinforced steel and filling)
Labour cost	AUD 70 per man hour

Table 33 and Table 34 show the foundations and structural costs (materials and labour) for evaporators with the favoured tubes for the 1st, 3rd and 5th effect positions with equivalent evaporation performance to evaporators with M2 tubes for HSA of 2000 and 5000 m² respectively.

For 2000 m² HSA, there is a reduction in N32 concrete and reinforced steel costs of 20, 30 and 40% with M3, S3 and S4 tube dimensions respectively as compared to the evaporator with M2 tube dimensions. The cost savings are higher with 5000 m² HSA. For 2000 m² HSA, there is no reduction in the costs for the steel pillars when using tubes of smaller diameter or are longer as the number of pillars is at the minimum number of six. Vessels with longer tubes than M2 have the same number of pillars despite having smaller vessel diameter and less weight on the foundations. For the 5000 m² HSA the number of pillars varies among the vessels between 6 and 10, depending on the mass on the foundations.

Table 33 Foundations and structural costs for evaporators comprising the favoured tubes for 1st, 3rd and 5th effect positions (HSA of M2 evaporator of 2000 m²)

Effect number	Tubes	N32 concrete for foundation cost (AUD)	Reinforced steel cost (AUD)	Steel pillars cost (AUD)	Total foundation & structural costs (AUD)
1	M2	6043	5882	7560	19485
	S2	5275	5145	7560	17980
	M3	4757	4642	7560	16959
	S3	4423	4316	7560	16299
	S4	3481	3414	7560	14455
3	M2	6043	5882	7560	19485
	M3	3956	3873	7560	15389
	S3	3757	3680	7560	14997
	M4	3301	3235	7560	14096
5	M2	6043	5882	7560	19485
	L2	6804	6622	7560	20986

Table 34 Foundations and structural costs for evaporators comprising the favoured tubes for 1st, 3rd and 5th effect positions (HSA of M2 evaporator of 5000 m²)

Effect number	Tubes	N32 concrete for foundation cost (AUD)	Reinforced steel cost (AUD)	Steel pillars cost (AUD)	Total foundation & structural costs (AUD)
1	M2	12851	12468	10080	35399
	S2	11109	10780	10080	31969
	M3	9866	9592	10080	29538
	S3	9096	8833	10080	28009
	S4	7014	6834	7560	21408
3	M2	12851	12468	10080	35399
	M3	8088	7873	7560	23521
	S3	7621	7412	7560	22593
	M4	6551	6374	7560	20485
5	M2	12851	12468	10080	35399
	L2	14609	14171	12600	41380

Insulation and cladding costs

The vessel is insulated and clad at the top cone, the strake and the steam annulus. Table 35 shows the cost data for insulation and cladding of the evaporator. The scaffolding costs include the labour and materials and increase with the height of the vessel.

Table 35 Cost data for insulation and cladding of the evaporator

Description of parameter	Value
Insulation and cladding costs	AUD 340 per m ²
Scaffolding (including labour and materials)	AUD 30000 for 2 m calandria
	AUD 35000 for 3 m calandria
	AUD 40000 for 4 m calandria

Table 36 and Table 37 show the insulation and cladding costs of evaporators with the favoured tubes for the 1st, 3rd and 5th effect positions to equate to the M2 HSA of 2000 and 5000 m². It was observed that although there is a 15 – 20% reduction in the area for insulation with S3 and S4 tubes, the overall insulation and cladding cost savings are negligible. This result is due to the increased scaffolding costs for taller vessels.

Table 36 Insulation area and costs for the favoured tubes for 1st, 3rd and 5th effect positions (HSA of M2 evaporator of 2000 m²)

Effect number	Tubes	Area for insulation (m ²)	Insulation and cladding costs (AUD)
1	M2	189	100584
	S2	171	93774
	M3	176	100872
	S3	167	97450
	S4	155	98024
3	M2	189	100584
	M3	154	92535
	S3	148	90387
	M4	149	100584
5	M2	189	100584
	L2	206	107142

Table 37 Insulation area and costs for the favoured tubes for 1st, 3rd and 5th effect positions (HSA of M2 evaporators of 5000 m²)

Effect number	Tubes	Area for insulation (m ²)	Insulation and cladding costs (AUD)
1	M2	333	154602
	S2	298	141555
	M3	301	147454
	S3	283	140927
	S4	257	136143
3	M2	333	154602
	M3	260	132168
	S3	249	128021
	M4	245	154602
5	M2	333	154602
	L2	367	167411

11.3. Appendix 3 Details of the CFD modelling

Material properties

The material properties for each of the three cases are given in Table 38 for the juice, Table 39 for the juice vapour, and Table 40 for the low pressure steam. Table 40 also has a column for the steam condensation rates (or vapour flows out of the tubes) for the measured heat transfer rates.

Table 38Juice properties

Case	Headspace pressure	Headspace temp.	Boiling point elevation	Dynamic viscosity	Density	Specific heat capacity	Thermal cond	Surface tension
	(kPa)	(°C)	(°C)	(Pa.s)	(kg/m ³)	(kJ/kg.K)	(W/m.K)	(N/m)
Uniform boiling pattern	149	111.6	0.41	0.000437	1031.64	3.87	0.65	0.059
Low HTC at top	29	73.09	4.9	0.0211	1324.47	2.82	0.47	0.072
Low HTC at bottom	149	111.6	0.3	0.000394	1015.55	3.94	0.66	0.058

Table 39Juice vapour properties

Case	Pressure	Temperature	Dynamic viscosity	Thermal Conductivity	Density	Heat Capacity	Surface tension
	(kPa)	(°C)	(Pa.s)	(W/m.K)	(kg/m ³)	(kJ/kg.K)	(N/m)
Uniform boiling pattern	149	111.2	1.29E-05	0.0271	1.034	2.13	0.059
Low HTC at top	29	68.3	1.12E-05	0.0219	0.18528	1.98	0.064
Low HTC at bottom	149	111.2	1.29E-05	0.027	1.034	2.13	0.059

Table 40Low pressure steam properties

Case	Pressure	Temperature	Delta T	Latent heat	Steam condensation rate
	(kPa)	(°C)	(°C)	(kJ/kg)	(kg/s)
Uniform boiling pattern	182	117.25	5.65	2209.76	0.003934
Low HTC at top	89	96.38	23.29	2265.91	0.000973
Low HTC at bottom	182	117.25	5.79	2209.76	0.002461

Meshing

An inflation layer option was applied next to the tube wall, with five layers being obtained. The first inflation layer was a few mm deep while near the centre of the tube the tetrahedral mesh sides were about 10 mm long. The mesh obtained is shown in Figure 33. The mesh for the tank as shown in Figure 34 was coarser. A total of 104938 nodes and 280983 elements were modelled.

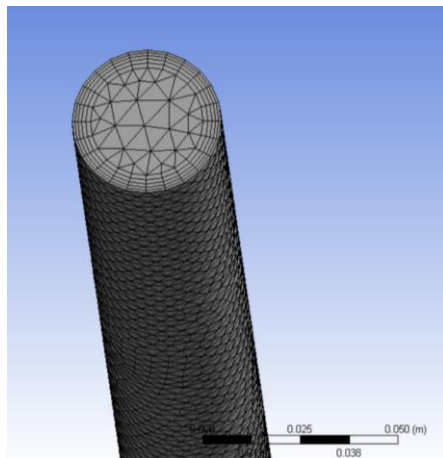


Figure 33 **Mesh achieved for tube volume**

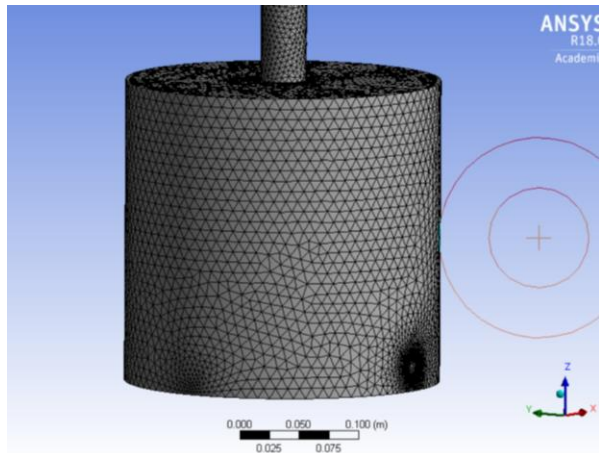


Figure 34 **Mesh achieved for tank volume**

Convergence

Figure 35, Figure 36 and Figure 37 show convergence response data for the simulations.

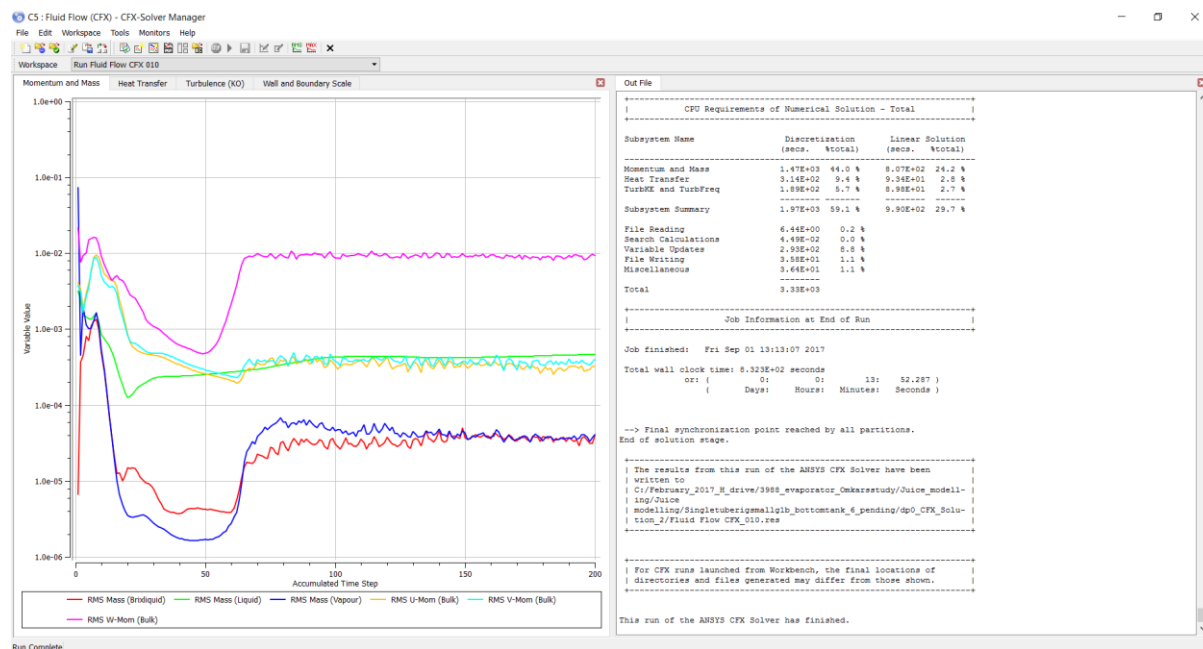


Figure 35 Momentum convergence

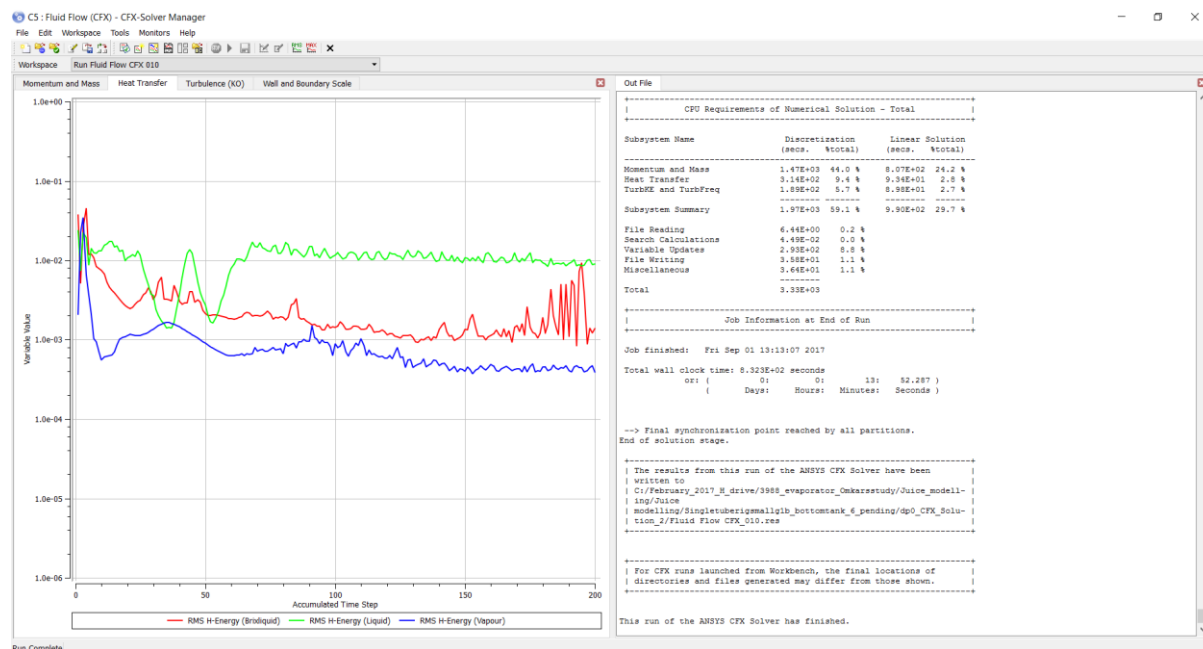


Figure 36 Energy convergence

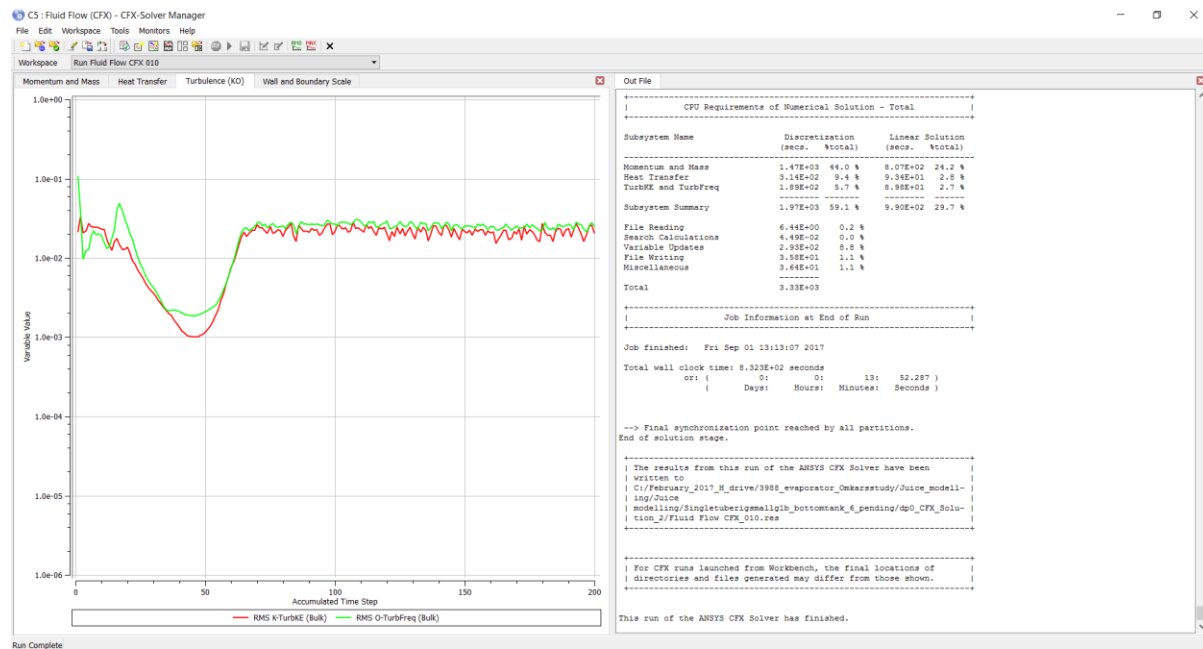


Figure 37 **Turbulence convergence**

11.4. Appendix 4 Summary of experimental results for three boiling cases used in CFD modelling

Table 41 Summary of experimental results for uniform boiling pattern adopted for CFD modelling (from Appendix L, Table L.1, Thaval (2017))

T _L (m)	T _D (mm)	Brix	JL (% tube height)	JL (mm)	HS (kPa abs)	ΔP (kPa)	ΔT (°C)	Section 1 (W/m ² /K)	Section 2 (W/m ² /K)	Section 3 (W/m ² /K)	Section 4 (W/m ² /K)	Overall (W/m ² /K)
2	44.45	20	40	800	149	33	5.65	5294	5909	5740	5093	5509

Table 42 Summary of experimental results for boiling pattern with low HTC at top of tube adopted for CFD modelling (from (Appendix M, Table M.1), Thaval (2017))

T _L (m)	T _D (mm)	Brix	JL (% tube height)	JL (mm)	HS (kPa abs)	ΔP (kPa)	ΔT (°C)	Section 1 (W/m ² /K)	Section 2 (W/m ² /K)	Section 3 (W/m ² /K)	Section 4 (W/m ² /K)	Overall (W/m ² /K)
3	44.45	70	30	900	29	60	23.29	0	0	422	482	226

Table 43 Summary of experimental results for boiling pattern with low HTC at bottom of tube adopted for CFD modelling (from Appendix N, Table N.1), Thaval (2017))

T _L (m)	T _D (mm)	Brix	JL (% tube height)	JL (mm)	HS (kPa abs)	ΔP (kPa)	ΔT (°C)	Section 1 (W/m ² /K)	Section 2 (W/m ² /K)	Section 3 (W/m ² /K)	Section 4 (W/m ² /K)	Overall (W/m ² /K)
3	38.1	16.3	50	1500	149	33	5.79	3155	3413	2475	1423	2616